

**STUDIES ON THE DEVELOPMENT OF TECHNOLOGY FOR
THE PRODUCTION, SEPARATION AND PURIFICATION OF
IODINE-131 FOR FORMULATION OF THERAPEUTIC
RADIOPHARMACEUTICALS**

By
RAJWARDHAN NANDRAM AMBADE
CHEM01201304009

Bhabha Atomic Research Centre, Mumbai

A thesis submitted to the
Board of Studies in Chemical Sciences
In partial fulfillment of requirements
for the Degree of
DOCTOR OF PHILOSOPHY
of
HOMI BHABHA NATIONAL INSTITUTE



December, 2019

Homi Bhabha National Institute¹

Recommendations of the Viva Voce Committee

As members of the Viva Voce Committee, we certify that we have read the dissertation prepared by Rajwardhan Nandram Ambade entitled "Studies On The Development Of Technology For The Production, Separation And Purification Of Iodine-131 For Formulation Of Therapeutic Radiopharmaceuticals" and recommend that it may be accepted as fulfilling the thesis requirement for the award of Degree of Doctor of Philosophy.

Chairman - Prof. Sharmila Banerjee

Sharmila Banerjee
1/10/2020

Guide / Convener - Prof. Ashutosh Dash

Ashutosh Dash

Co-guide - Prof. Sudipta Chakraborty

Sudipta Chakraborty
1/10/20

Examiner – Prof.(Dr.) P.K. Pradhan,

Dept. of Nuclear Medicine SGPGI, Lucknow

P.K. Pradhan

Member 1- Prof. Raghunath Acharya

Raghunath Acharya 1/10/2020

Member 2- Prof. Tapas Das

Tapas Das
01.10.2020

Final approval and acceptance of this thesis is contingent upon the candidate's submission of the final copies of the thesis to HBNI.

I/We hereby certify that I/we have read this thesis prepared under my/our direction and recommend that it may be accepted as fulfilling the thesis requirement.

Date: 1/10/20

Place: A. Nagar,
Mumbai

Signature

Sudipta Chakraborty

Co-guide (if any)

Signature

Ashutosh Dash

Guide

¹ This page is to be included only for final submission after successful completion of viva voce.

STATEMENT BY AUTHOR

This dissertation has been submitted in partial fulfillment of requirements for an advanced degree at Homi Bhabha National Institute (HBNI) and is deposited in the Library to be made available to borrowers under rules of the HBNI.

Brief quotations from this dissertation are allowable without special permission, provided that accurate acknowledgement of source is made. Requests for permission for extended quotation from or reproduction of this manuscript in whole or in part may be granted by the Competent Authority of HBNI when in his or her judgment the proposed use of the material is in the interests of scholarship. In all other instances, however, permission must be obtained from the author.



Rajwardhan Nandram Ambade

DECLARATION

I, hereby declare that the investigation presented in the thesis has been carried out by me. The work is original and has not been submitted earlier as a whole or in part for a degree / diploma at this or any other Institution / University.

A handwritten signature in black ink, appearing to read 'RA Ambade', with a long horizontal stroke extending to the right.

Rajwardhan Nandram Ambade

List of Publications arising from the thesis

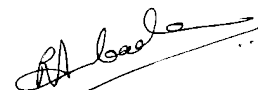
Journal

1. “Development of a dry distillation technology for the production of I-131 using medium flux reactor for radiopharmaceutical application”, **R. N. Ambade**, S. N. Shinde, M. S. A. Khan, S. P. Lohar, K. V. Vimalnath, P. V. Joshi, Sudipta chakraborty, M.R.A.Pillai, Ashutosh Dash., J. Radioanal. Nucl. Chem., 2015, 303, 451-467.
2. “Development of semiautomated module for preparation of ^{131}I labeled Lipiodol for liver cancer therapy”, Archana Mukherjee, Suresh Subramanian, **Rajwardhan Ambade**, Bhaurao Avhad, Ashutosh Dash, and Aruna Korde, Cancer Biother. and Radiophar., 2017,32, 33-37.
3. “Mechanochemically synthesized mesoporous alumina: An advanced sorbent for post-processing concentration of ^{131}I for cancer therapy”, **Rajwardhan Ambade**, Rubel Chakravarty, Jitendra Bahadur, Bharat Ganjave, Debasis Sen, Sudipta Chakraborty, and Ashutosh Dash, Journal of Chromatography A., 1612 (2020) 460614.

Conferences

1. “Reactor production and separation of ^{131}I for in vivo therapeutic applications” M.S.A. Khan, **R.N. Ambade**, S.N. Shinde, S.P. Lohar, S. Chakraborty, A. Dash; SESTEC 2014; 235 (RCS-8).
2. "Improvement of radioactive concentration of ^{131}I produced by dry distillation technique for use in high dose therapeutic capsules", **R.N. Ambade**, M.S.A. Khan, S.P. Lohar, S.N. Shinde, S. Chakraborty and A. Dash, NUCAR-2015, DAE-BARNS 12th National Symposium on Nuclear and Radiochemistry, 510 (F-29).

3. “Production of I-131 in high concentration suitable for I-131 MIBG therapy”; Mohammed Sahiralamkhan, **R. N. Ambade**, Lohar S. P. S. N. Shinde, S. Chakraborty, A. Dash; CHEMNUT-2015, 43.
4. “Preparation of ^{131}I -Lipiodol and fabrication of prototype semi-automated module”; Aruna Korde, Archana Mukherjee, **R. N. Ambade**, Ghanashyam Shirke, Rajendra Chavan, A Dash, Grace Samuel; Indian J. Nucl. Med., Vol. 28, Abstract Issue, S-44, Dec. 2013.
5. “Patient dose preparation of ^{131}I -Lipiodol using GMP compliant synthesis module and its biological evaluation”, Korde A, Subramanian S, **Ambade R N**, Avhad B G. Indian J. Nucl. Med. Vol. 30 Abstract Supplement issue (Dec. 2015), P-073, S60.
6. “Production of therapeutic doses of ^{131}I labeled lipiodol injection for the treatment of hepatocellular carcinoma” Archana Mukherjee, **Rajwardhan Ambade**, Barkha Karkhanis, Ashutosh Dash, Aruna Korde; Indian J. Nucl. Med., Volume 33, Abstract Supplement Issue, Dec. 2018; PV64, S104.



Rajwardhan Nandram Ambade

DEDICATIONS

To My Beloved Family

Especially to my Father

Late Nandram Bapurao Ambade 'Guruji'

& my Mother

Smt. Nirmalabai

for my education and intellectual development

ACKNOWLEDGEMENTS

Now, it is time to verbalize my gratitude to all those people without whom this work would not have been possible. First and foremost, I wish to express my deepest and sincere gratitude to my guide, **Prof. Ashutosh Dash**, Head, Radiopharmaceuticals Division for his invaluable guidance, constant encouragement and persistent motivation. His wide knowledge and logical way of thinking and reasoning on scientific problems greatly channeled me during the course of work. He nurtured my faculty of thinking and made me self-reliant.

I am thankful to my co-guide and immediate superior **Prof. Sudipta Chakraborty**, Head, Radiochemicals Section, for sharing with me his knowledge and scientific understanding during the fruitful discussions throughout the work and also during writing the thesis. I learned from him the art of writing manuscript and continue to learn.

I would like to express my sincere gratitude to **Prof. M. R. A. Pillai**, former Head, Radiopharmaceuticals Division. It was Dr. Pillai, who initially encouraged me to pursue the work for the thesis. Though my association with him was relatively short, this period in my career was the decisive moment and I will be indebted to him life-long.

I owe sincere thanks to **Prof. P. K. Pujari**, Associate Director, Radiochemistry and Isotope Group for providing me an opportunity to work in the Isotope Programme and for his administrative support during the course of the work.

I would take this opportunity to thank the respected members of my doctoral committee **Prof. Sharmila Banerjee** (Chairman), **Prof. Raghunath Acharya** (member) and **Prof. Tapas Das** (member) for their critical reviews of the work reported and for their accessibility, interest, academic support, insightful questions, valuable suggestions and helpful comments during the annual progress reviews and pre-synopsis presentation. I am grateful to **Prof. A.K. Tyagi**, Dean,

Academic, Chemical Sciences, HBNI for his support and encouragement during the course of the work.

I am grateful to **Shri V. Shivarudrappa**, **Shri. P.V. Joshi**, former Heads Radiochemicals Section, my senior colleagues **Shri S.N. Shinde**, and **Shri B.S. Kulloli** with whom I started my first scientific endeavor after joining BARC, for sharing their work experience and scientific knowledge with me.

I take this opportunity to express my sincere regards and deepest appreciation to **Dr. Rubel Chakravarty**, **Dr. Aruna Korade**, **Dr. Archana Mukherjee**, **Dr. Suresh Subramanian** and **Dr. Maithily Kameshwaran** for sharing their experimental expertise and scientific knowledge with me. I express my thanks to **Dr. S. V. Thakare**, **Shri. K. C. Jagadeesan** and **Shri A. R. Mathakar** for co-ordinating irradiations in Dhruva reactor.

I would also like to thank my colleagues of Radiochemicals Section, **Md. Sahiralam Khan**, **Shri. Sharad Lohar**, **Shri. Sachin Jadhav** and **Shri. Bharat Ganjave** for regularly helping in radiochemicals processing reported in this thesis and **Dr. K.V.V. Nair**, **Shri. Ramu Ram** for their help and support. I also thank **Dr. Manojkumar** and **Shri S.K. Saxena** for the support.

It gives me a great pleasure to acknowledge to **Dr. Haladhar D. Sarma**, Head, Experimental Animal Facility and Radioisotope Laboratory, Radiation Biology and Health Sciences Division for his kind help in carrying out biological evaluations of Lipiodol reported in this thesis.

I sincerely acknowledge for the engineering support from **Shri. B.G. Avhad**, Head, Engineering Services Section and his group for timely installation of various process gadgets and facility used for radiochemical processing. **Shri. Pritam Bansode** for help in making drawings used in the thesis and **Shri S. Moorthy** for fabrication of glasswares used in the processing, both are gratefully acknowledged.

It is my pleasant duty to acknowledge the help and technical assistance received from **Shri. R. G. Gawade, Shri. E. G. Mohite** and **Shri. B. D. Dodmani** throughout the course of work.

I also sincerely acknowledge all my colleagues from Radiopharmaceuticals Division for their help and support.

I am thankful to all my friends for their encouragement and support. I greatly value their friendship and deeply appreciate their belief in me. I wish to thank **Dr. Jeyakumar, RACD** for his moral support.

I cannot imagine my current position without the blessings of my teachers and will always be indebted to them.

Most importantly, I owe special gratitude to my beloved wife **Vaishali** for being there always supporting and encouraging me to complete the work. Last but not the least; I would like to acknowledge the presence of my daughters, **Cherisha** and **Rinzen**, the reason behind my every positivity in spite of all the odds.

Finally, I would like to thank all my well wisher which helped me in fulfilling this ambition of my life.



Rajwardhan Nandram Ambade

Trombay, Mumbai

December 2019

CONTENTS

	Page No
SUMMARY	x-xi
LIST OF FIGURES	xii-xvi
LIST OF TABLES	xvii-xviii
 Chapter 1	
Introduction	1
1.1 Application of radioisotopes in health care and introduction to radioiodine	3
1.2 Applications of radioisotopes for diagnostic and therapeutic purposes	9
1.2.1 Characteristics of diagnostic radiopharmaceuticals	9
1.2.2 Characteristics of therapeutic radiopharmaceuticals	10
1.2.3 Radioisotopes for theranostic applications	12
1.2.4 Applications of ^{131}I in nuclear medicine	13
1.2.4.1 Nuclear characteristics of ^{131}I	13
1.2.4.2 Decay scheme of ^{131}I	13
1.2.4.3 Gamma attenuation of ^{131}I	14
1.2.5 Diagnostic applications of ^{131}I	15
1.2.6 Therapeutic applications of ^{131}I	16
1.2.6.1 Dose of ^{131}I used in treatment	16
1.3 General method of production of radioisotopes	17

1.3.1	Reactor production of radioisotopes	17
1.3.2	Accelerator production of radioisotopes	19
1.3.3	Calculation of radioisotope yield	19
1.3.4	Correction of activation equation	21
1.3.5	Irradiation efficiency	21
1.4	General methods of production of ^{131}I	21
1.4.1	Production of ^{131}I using tellurium as target	21
1.4.2	Production of ^{131}I through fission	22
1.5	Separation of radioisotopes	22
1.5.1	Separation of radioiodine	22
1.5.1.1	Separation of ^{131}I by wet distillation method	22
1.5.1.1.1	Merits of wet distillation method	23
1.5.1.1.2	Demerits associated with wet distillation process	23
1.5.1.2	Separation of ^{131}I by dry distillation method	25
1.5.1.2.1	Advantages of dry distillation method	25
1.5.1.3	Separation of ^{131}I from fission products	26
1.6	Target selection	26
1.6.1	General rules for selecting target material	26
1.6.2	Precautions to be taken while irradiation	27
1.6.3	Safety investigation of target material	27
1.6.4	Enriched targets	28
1.6.5	Targets for producing ^{131}I and methods for radiochemical processing	28

1.6.6	Advantages of tellurium dioxide TeO ₂ target	30
1.6.7	Specifications for TeO ₂ target	30
1.7	Irradiation facility	31
1.8	Irradiation containers	32
1.8.1	Sealing method	33
1.8.2	Test for weld integrity	33
1.9	General terms used in the thesis	34
1.10	Motivation of the present work	38
1.11	Scope of the present thesis	39
CHAPTER-2	Dry Distillation Technology for Production and Radiochemical Separation of Iodine-131	41
2.1	Introduction	43
CHAPTER-2A	Development of Dry Distillation Technology for Radiochemical Separation and Purification of Iodine-131	47
2A.1	Selection of target material	49
2A.1.1	Feasibility of distillation of ¹³¹ I from tellurium metal powder	49
2A.1.1.1	Experimental procedure	49
a)	Material and equipments	49
b)	Neutron irradiation	50
c)	Separation of ¹³¹ I from irradiated tellurium metal powder	50

d)	Determination radionuclidic purity and separation yield of ^{131}I	51
e)	Determination of radiochemical purity	52
f)	Determination of tellurium content	52
2A.1.1.2	Results of the experiment and discussion	53
2A.1. 2	Feasibility of distillation of ^{131}I from irradiated TeO_2	56
2A.1. 2.1	Experimental procedure:	56
a)	Material and equipments	56
b)	Neutron irradiation	56
c)	Separation of ^{131}I from irradiated Tellurium dioxide	56
2A.1. 2.2	Results of the experiment and discussion	57
2A.1.3	Conclusion	60
2A.2	Design and Development of quarzwares, glasswares & equipments	60
2A.2.1	Quartz crucible	60
2A.2.2	Distillation flask	62
2A.2.3	Design and demonstration of glass coil as tellurium trap	63
2A.2.4	Iodine traps	64
2A.2.5	Resistance furnace (vertical type)	64
2A.2.6	Complete processing set-up	65
2A.3	Optimization of parameters for ^{131}I processing at pilot scale for	66

	Separation of ^{131}I from the neutron irradiated TeO_2	
2A.3.1	Materials and methods for Process optimization	66
2A.3.1.1	Target specifications	66
2A.3.1.2	Neutron irradiation	68
2A.3.1.3	Neutron irradiation conditions	69
2A.3.1.4	Cooling period	71
2A.3.2	Separation of ^{131}I from neutron irradiated TeO_2	72
2A.3.2.1	Optimization of distillation parameters	72
2A.3.2.2	Effect of temperature	73
2A.3.2.3	Rate of distillation	75
2A.3.2.4	Purification of ^{131}I from traces of TeO_2	76
2A.3.2.5	Trapping of ^{131}I	77
2A.4	Optimized protocol for radiochemical separation of ^{131}I from neutron irradiated TeO_2 target	78
CHAPTER-2B	Large Scale Production, Separation And Purification of Iodine-131 Using Dry Distillation Technique	81
2B.1	Materials and equipments	83
2B.2	Neutron irradiation	83
2B.3	Facility for large-scale radiochemical separation of ^{131}I	83
2B.4	Remotely operated custom made gadgets	85
2B.4.1	Irradiation container opening unit	85
2B.4.2	Semi-automated crucible holder	87

2B.4.3	Semi-automated flange lid holder	88
2B.4.4	Inconel cylinder	89
2B.4.5	Induction Furnace	90
2B.5	Complete processing set-up	91
2B.6	Radiochemical separation of ^{131}I by dry distillation method	92
2B.7	Quality control of separated ^{131}I	95
2B.7.1	Activity measurement	95
2B.7.2	Radionuclidic purity	96
2B.7.3	pH of ^{131}I solution	98
2B.7.4	Radiochemical purity	98
2B.7.5	Chemical purity	99
2B.8	^{131}I product specifications: Results	99
2B.9	Results of employment of the dry distillation technology for regular production and supply of ^{131}I -[NaI]	102
2B.10	Radiological safety	102
2B.11	Radioactive waste handling	103
2B.12	Discussion	104
2B.13	Conclusion	108
CHAPTER-3	Post Processing Concentration of I-131 for Therapeutic Applications	109
3.1	Introduction	111
3.2	Experimental	113

3.2.1	Materials	113
3.2.2	Methods	114
3.2.2.1	Structural characterization of mesoporous alumina	115
3.2.2.2	Determination of zeta-potential of mesoporous alumina	116
3.2.2.3	Determination of distribution coefficients (K_d) of I^- ions	116
3.2.2.4	Determination of time required to attain sorption equilibrium	117
3.2.2.5	Determination of $^{131}I^-$ sorption capacity of mesoporous alumina	117
a)	Static sorption capacity	117
b)	Breakthrough pattern under dynamic conditions	118
c)	Practical sorption capacity	119
3.2.2.6	$^{131}I^-$ ion desorption characteristics of mesoporous alumina	119
	(a) Optimization of desorption concentration	119
	(b) Optimization of flow rate of elution	119
	(c) Elution profile of the desorption of ^{131}I from the sorbent	120
3.2.2.7	Practical utility of the sorbent	120
3.2.2.8	Quality control of processed ^{131}I	120
	i) Radiochemical purity of ^{131}I	120
	ii) Chemical purity of ^{131}I	121
3.3.	Results and Discussion	121
3.3.1.	Synthesis and characterization of mesoporous alumina	122

3.3.2.	Zeta potential of mesoporous alumina	130
3.3.3.	Sorption characteristics of mesoporous alumina	131
3.3.4.	Desorption characteristics of mesoporous alumina	133
3.3.5.	Process demonstration for increasing radioactive concentration of ^{131}I	136
3.4.	Conclusions	139
CHAPTER-4	Formulation of Patient Dose of ^{131}I-Lipiodol and its Clinical Utilization for The Treatment of Hepatocellular Carcinoma	141
4.1	Introduction	143
4.2	Characteristics of ^{131}I -Lipiodol	147
4.3	Radiolabeling process optimization for ^{131}I -Lipiodol formulation	148
4.3.1	Materials and methods	148
4.3.1.1	Design and fabrication of semi-automated module	149
4.3.2	Preparation of ^{131}I -Lipiodol using module	150
4.3.3	Quality control tests of ^{131}I -Lipiodol	152
4.3.3.1	Tests of radionuclide identification and radionuclidic purity	152
4.3.3.2	Assay of radioactivity	152
4.3.3.3	Test of radiochemical purity	152
4.3.3.4	Stability	153
4.3.3.5	Sterility and bacterial endotoxin test (BET)	153

4.3.3.6	Biological evaluation	154
4.4	Formulation of actual patient dose of ^{131}I -Lipiodol for clinical utilization	154
4.5	Results and discussion	155
4.5.1	Design and fabrication of semi-automated module	155
4.5.2	Preparation of ^{131}I -Lipiodol using module	157
4.5.3	Quality control tests of ^{131}I -Lipiodol	157
4.5.3.1	Test for radionuclide purity	157
4.5.3.2	Test for radiochemical purity	158
4.5.3.3	Stability	160
4.5.3.4	Sterility and bacterial endotoxin testing (BET)	160
4.5.3.5	Biological evaluation	161
4.5.3.6	Radiochemical yield of ^{131}I -Lipiodol and its specification	162
4.6	Formulation of actual patient dose of ^{131}I -Lipiodol for clinical utilization	165
4.7	Clinical evaluation	166
4.8	Safety features during processing of patient dose ^{131}I -Lipiodol	168
4.9	Discussion	169
4.10	Conclusions	170
	References	171-178

Homi Bhabha National Institute

Ph. D. PROGRAMME

Name of Candidate:	Rajwardhan N. Ambade
Name of the Constituent Institution:	Bhabha Atomic Research centre, Mumbai
Enrollment Number:	CHEM01201304009
Title of the Thesis:	Studies on the Development Of Technology for the Production, Separation and Purification of Iodine-131 for Formulation of Therapeutic Radiopharmaceuticals

ABSTRACT

To meet growing demands for ^{131}I and iodinated medicinal products, its production, separation and purification for therapeutic applications is very much needed. In the current work, ^{131}I production methodology and development of new method and technology from lab-scale to large-scale and its purification has been discussed. Dry distillation method for ^{131}I production has been developed indigenously and its technology employed for large-scale regular production and supply. About 180 g of TeO_2 was irradiated at the Dhruva reactor and ^{131}I was radiochemically separated by employing the dry distillation technology. A maximum recovery of $\sim 85\%$ of ^{131}I was achieved. The final product was subjected to QC analysis which showed that radionuclidic and radiochemical purities of $>99.9\%$ and $>97\%$ were obtained, respectively. The developed method provides ^{131}I radioactive concentration of $130\text{--}148\text{ GBq mL}^{-1}$ which is suffice to carry out the formulations of ^{131}I -MIBG and ^{131}I -Lipiodol. To meet the increasing requirements of higher radioactive concentration of I-131 for preparation of therapeutic capsules for treatment of

thyroid cancer, a column chromatographic radiochemical concentration method has been developed. For this purpose, mesoporous alumina was synthesized by solid state mechanochemical approach and used as chromatographic sorbent. The higher radioactive concentration of [^{131}I]NaI achieved using the developed protocol could be used for preparation of high dose therapeutic capsules (7.4 GBq) for the treatment of thyroid cancer. A technology was developed for safe formulation of ^{131}I -Lipiodol as a cost-effective therapeutic radiopharmaceutical for treatment of hepatocellular carcinoma. The developed protocol was demonstrated successfully for the formulation of several patient doses of the radiopharmaceutical for the first time in India and used for clinical treatment of HCC and PVT.

In brief in the present studies ^{131}I production, separation and purification method was developed, demonstrated at pilot-scale and employed for plant-scale regular production and supply of ^{131}I . Post processing concentration of ^{131}I was increased by column chromatography. Finally intended applications of produced ^{131}I for formulation of ^{131}I -Lipiodol for clinical dose preparation were demonstrated and ^{131}I -Lipiodol was used first time in India for the treatment of patients with liver cancer and successful results were achieved.

SUMMARY

Production, separation and purification of ^{131}I for therapeutic applications involve various steps. Target selection and preparations before neutron irradiation is a key step on which separation and purification steps are depend upon. In the current work, ^{131}I production methodology and development of new method and technology from lab-scale to large-scale and its purification has been discussed. Dry distillation method for ^{131}I production has been developed indigenously and its technology employed for large-scale regular production and supply. About 180 g of TeO_2 was irradiated at the Dhruva reactor and ^{131}I was radiochemically separated by employing the dry distillation technology. A maximum recovery of $\sim 85\%$ of ^{131}I was achieved. The final product was subjected to QC analysis which showed that radionuclidic and radiochemical purities of $>99.9\%$ and $>97\%$ were obtained, respectively. The developed method provides ^{131}I radioactive concentration of $130\text{--}148\text{ GBq mL}^{-1}$ which is suffice to carry out the formulations of ^{131}I -MIBG and ^{131}I -Lipiodol. Quality of produced ^{131}I complies with the specifications in pharmacopeia. I-131 having β , γ radiation emission finds applications as therapeutic and diagnostic radioisotope. To meet on demand specific requirements of higher radioactive concentration of ^{131}I , new material and method has been developed. Mesoporous alumina was synthesized mechanochemically and was used in column chromatography to increase 5-10 times post processing radioactive concentration of ^{131}I . As a result, irrespective of initial volume of feed, final eluted ^{131}I activity was concentrated in 2 mL. In this process adequately high radioactive concentration of ^{131}I (upto 1.7 TBq mL^{-1}) could be achieved. Moreover, it meets all the specifications for its clinical use. The higher radioactive concentrated ^{131}I can be used for preparation of high dose therapeutic capsules (7.4 GBq) for the treatment of thyroid cancer. Formulation of ^{131}I radiopharmaceutical for therapeutic application has been carried out. A

technology was developed for safe processing of single and two patient doses ^{131}I -Lipiodol for treatment of hepatocellular carcinoma. Semi-automation gadget and module was developed and demonstrated its utilization for clinical dose preparation and formulation of ^{131}I -Lipiodol. Thirteen batches processed, complied with specified quality criteria of RCP > 99 %, radioassay $0.74\text{ GBq} - 1.5\text{ GBq mL}^{-1}$ ($20 - 40\text{ mCi mL}^{-1}$), BET < 25 EU mL^{-1} and sterility as per the Indian pharmacopeia standards. Decay corrected quantities of therapeutic doses of ^{131}I -Lipiodol injection were supplied to nuclear medicine center for clinical studies in liver cancer patients. Single photon emission computed tomography images at 24 and 72 h post injection revealed desired retention of ^{131}I activity in the liver. Among agents for Trans Arterial Radio Embolization (TARE), ^{131}I -Lipiodol could be prepared in multiple patient doses at relatively low cost compared to other agents. A successful patient dose formulation of ^{131}I -Lipiodol injection was demonstrated and made available first time in India and used for clinical treatment of HCC and PVT.

In brief in the present studies ^{131}I production, separation and purification method was developed, demonstrated at pilot scale and employed for plant scale regular production and supply of ^{131}I . Post processing concentration of ^{131}I was increased by column chromatography. Finally intended applications of produced ^{131}I for formulation of ^{131}I -Lipiodol for clinical dose preparation were demonstrated and ^{131}I -Lipiodol was used first time in India for the treatment of patients with liver cancer and successful results were achieved.

LIST OF FUGURES

<i>Sr. No.</i>	<i>Figure Caption</i>	<i>Page No</i>
<i>Fig. 1.1:</i>	<i>Simplified decay scheme of ^{131}I</i>	<i>14</i>
<i>Fig. 1.2:</i>	<i>Irradiation containers</i>	<i>33</i>
<i>Fig. 2A.1:</i>	<i>Apparatus for dry distillation of ^{131}I from irradiated Te metal powder</i>	<i>51</i>
<i>Fig. 2A.2:</i>	<i>Gamma ray Spectrum of irradiated tellurium powder before experiment</i>	<i>54</i>
<i>Fig. 2A.3:</i>	<i>Gamma ray Spectrum of irradiated tellurium after distillation</i>	<i>54</i>
<i>Fig. 2A.4:</i>	<i>Gamma ray spectrum of ^{131}I trapped.</i>	<i>55</i>
<i>Fig. 2A.5:</i>	<i>Paper chromatography pattern of ^{131}I produced using metallic Te as target</i>	<i>55</i>
<i>Fig. 2A.6:</i>	<i>Gamma ray spectrum of irradiated tellurium dioxide before experiment</i>	<i>58</i>
<i>Fig. 2A.7:</i>	<i>Gamma ray spectrum of irradiated tellurium dioxide after distillation</i>	<i>58</i>
<i>Fig. 2A.8:</i>	<i>Gamma ray spectrum of ^{131}I trapped</i>	<i>59</i>
<i>Fig. 2A.9:</i>	<i>Paper chromatographic pattern of ^{131}I produced using TeO_2 as target</i>	<i>59</i>
<i>Fig. 2A.10:</i>	<i>Schematic diagram of quartz crucible</i>	<i>61</i>
<i>Fig. 2A.11:</i>	<i>Schematic diagram of ^{131}I distillation flask</i>	<i>62</i>

Fig. 2A.12:	<i>Schematic diagram of tellurium trap (dimensions in mm)</i>	63
Fig. 2A.13:	<i>Schematic diagram of ^{131}I traps (dimensions in mm)</i>	64
Fig. 2A.14:	<i>Schematic diagram of resistance furnace</i>	65
Fig. 2A.15:	<i>Distillation assembly for ^{131}I dry distillation</i>	66
Fig. 2A.16:	<i>Activation reactions and decay mode of (a) ^{126}Te and (b) ^{128}Te formed during neutron irradiation of natural Tellurium</i>	69
Fig. 2A.17:	<i>Calculated production yields of ^{131}I at EOI by neutron irradiation of 1 g TeO_2 target as a function of irradiation time at various thermal neutron flux values</i>	70
Fig. 2A.18:	<i>^{131}I activity produced as a function of the irradiation time</i>	71
Fig. 2A.19:	<i>Radioactivity concentration of ^{131}I, $^{131\text{m}}\text{Te}$ and ^{131}Te per g of TeO_2 as a function of cooling time from EOI</i>	72
Fig. 2A.20:	<i>Decay scheme of neutron irradiated ^{130}Te for production of ^{131}I</i>	72
Fig. 2A.21:	<i>Effect of distillation temperature on the yield ^{131}I</i>	74
Fig. 2A.22:	<i>Rate of distillation of ^{131}I</i>	75
Fig. 2A.23:	<i>Flow sheet of protocol for radiochemical processing of ^{131}I</i>	79
Fig. 2B.1:	<i>150 mm lead shielded Radiochemical processing plant</i>	85
Fig. 2B.2:	<i>Semi-automatic irradiation container opening unit</i>	86
	<i>(a) photographic image of actual unit (b) schematic diagram</i>	
Fig. 2B.3:	<i>Semi-automatic crucible holder (photographic image of actual unit)</i>	87
Fig. 2B.4:	<i>Semi-automated flange lid holder (photographic image of</i>	89

	<i>actual unit)</i>	
Fig. 2B.5:	<i>Schematic diagram of inconel cylinder for induction furnace</i>	90
Fig. 2B.6:	<i>Induction heating system (a) block diagram; (b) induction coil around the quartz cylinder containing inconel cylinder; (c) side view of induction coil</i>	91
Fig. 2B.7:	<i>Schematic diagram of ^{131}I dry distillation complete processing set up</i>	91
Fig. 2B.8:	<i>(a) Gamma ray spectrum of ^{131}I</i>	97
	<i>(b) Decay curve for ^{131}I</i>	97
Fig. 2B.9:	<i>Paper electrophoresis pattern of ^{131}I</i>	99
Fig. 2B.10:	<i>Typical report on analysis of ^{131}I-[NaI]</i>	101
Fig. 3.1:	<i>Schematic diagram showing synthesis of mesoporous alumina by solid state mechanochemical approach and its utilization as a sorbent in concentration of ^{131}I.</i>	121
Fig. 3.2:	<i>Particle size distribution of the reaction mixture after grinding</i>	123
Fig. 3.3:	<i>Particle size distribution of the product after calcination</i>	123
Fig. 3.4:	<i>XRD pattern of mesoporous alumina.</i>	125
Fig. 3.5:	<i>SEM image of mesoporous alumina.</i>	125
Fig. 3.6:	<i>EDS spectrum of mesoporous alumina</i>	126
Fig. 3.7:	<i>TEM image of mesoporous alumina.</i>	126
Fig. 3.8 (i)	<i>Combined SANS and SAXS profile of mesoporous alumina plotted on a double logarithmic scale.</i>	128
Fig. 3.8 (ii)	<i>Pore size distribution as obtained from the scattering profile.</i>	128

Fig. 3.9 (i)	<i>Nitrogen adsorption/desorption isotherms for mesoporous alumina.</i>	129
Fig. 3.9 (ii)	<i>Pore size distribution as obtained from nitrogen absorption-desorption study.</i>	129
Fig. 3.10:	<i>Zeta potential of mesoporous alumina at different pH.</i>	131
Fig. 3.11:	<i>K_d values for I⁻ ions in mesoporous alumina sorbent at different pH.</i>	132
Fig. 3.12:	<i>Kinetics of I⁻ sorption in mesoporous alumina.</i>	132
Fig. 3.13:	<i>Breakthrough profile of ¹³¹I in a column packed with 200 mg of mesoporous alumina sorbent. The radioactive solution was passed through the column at a flow rate of 0.5 mL min⁻¹.</i>	133
Fig. 3.14:	<i>Optimization of the concentration of NaOH solution for elution of ¹³¹I adsorbed in the column.</i>	134
Fig. 3.15:	<i>Optimization of flow rate of elution.</i>	135
Fig. 3.16:	<i>Elution profile of ¹³¹I.</i>	135
Fig. 3.17:	<i>Paper electrophoresis pattern of ¹³¹I solution obtained after the concentration procedure.</i>	137
Fig. 4.1:	<i>Schematic of injection of therapeutic agent via hepatic artery to liver cancer</i>	143
Fig. 4.2:	<i>Ethyl 9, 10 di-iodostearate, iodinated ethyl ester</i>	145
Fig. 4.3:	<i>Schematic of semi-automated module for ¹³¹I-Lipiodol processing</i>	149
Fig. 4.4:	<i>Schematics of the process system for production of ¹³¹I-</i>	151

Lipiodol

Fig. 4.5:	<i>Flow sheet of ^{131}I-Lipiodol formulation</i>	<i>155</i>
Fig. 4.6 (a)	<i>Photograph of internal set up for ^{131}I-Lipiodol processing</i>	<i>156</i>
Fig. 4.6 (b)	<i>Photograph of control panel for remote operations in ^{131}I-Lipiodol processing</i>	<i>156</i>
Fig. 4.7:	<i>Radionuclidic identification and purity of ^{131}I-Lipiodol</i>	<i>158</i>
Fig. 4.8 (a):	<i>Radiochemical purity of ^{131}I-Lipiodol (Methanol Solvent)</i>	<i>159</i>
Fig. 4.8 (b)	<i>Radiochemical purity of ^{131}I-Lipiodol (ethyl ether/petroleum ether solvent)</i>	<i>159</i>
Fig. 4.9:	<i>Whole body scan of patient treated with ^{131}I-Lipiodol</i>	<i>167</i>
Fig. 4.9 (a)	<i>24 h post-administration (anterior and posterior view),</i>	<i>167</i>
Fig. 4.9 (b)	<i>48 h post-administration (anterior and posterior view),</i>	<i>167</i>
Fig. 4.9 (c)	<i>72 h post-administration (anterior and posterior view)</i>	<i>168</i>

LIST OF TABLES

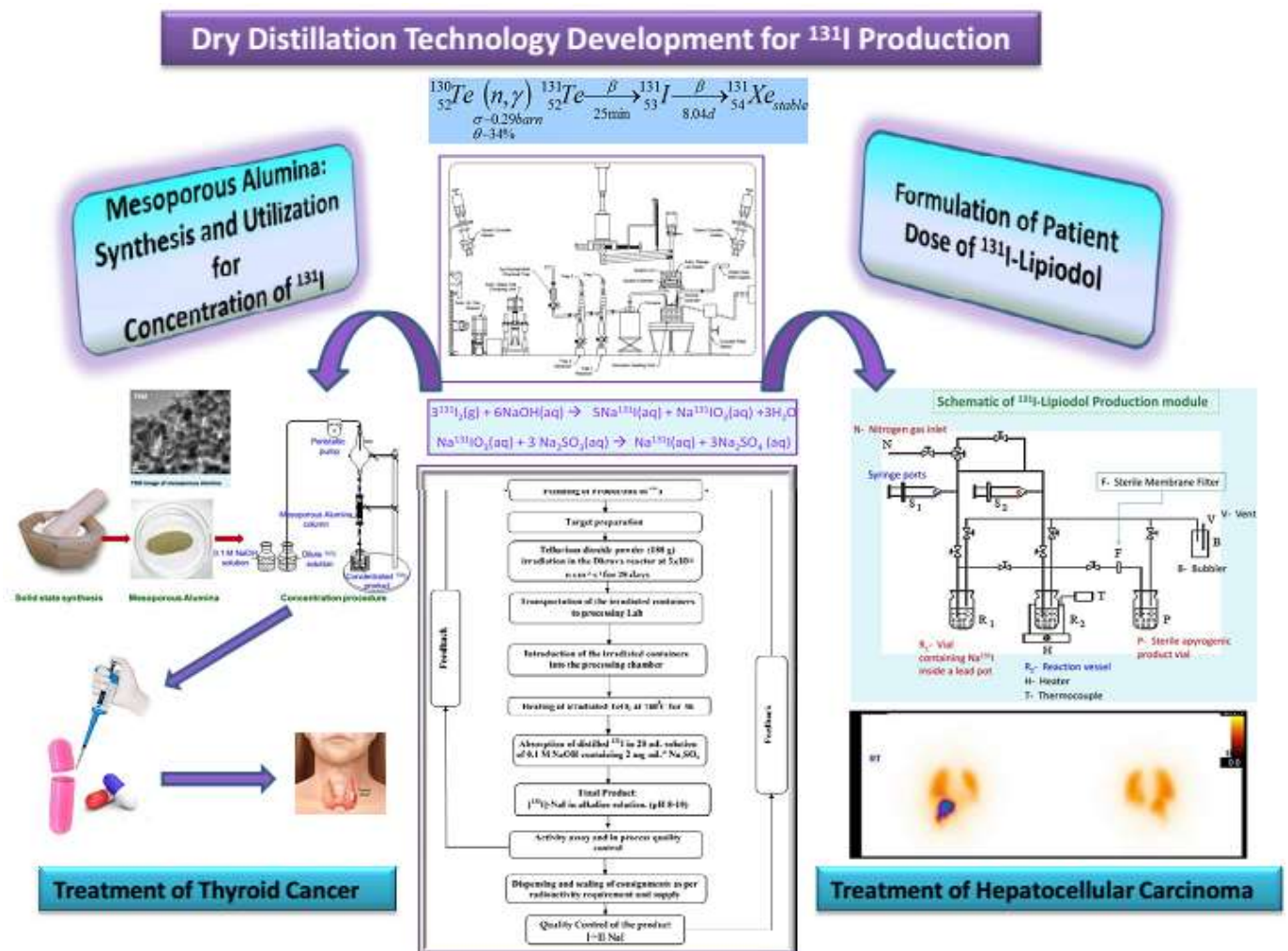
<i>Sr. No.</i>	<i>Table Caption</i>	<i>Page No</i>
<i>Table 1.1:</i>	<i>Radioisotopes of iodine and their nuclear characteristics</i>	<i>5</i>
<i>Table 1.2:</i>	<i>Principal radiation emission data of ^{131}I</i>	<i>13</i>
<i>Table 1.3:</i>	<i>Attenuation of lead shielding for gamma emitted from ^{131}I</i>	<i>15</i>
<i>Table 1.4:</i>	<i>Target materials and ^{131}I processing methods</i>	<i>29</i>
<i>Table 1.5:</i>	<i>Properties of Te, Iodine and TeO_2</i>	<i>30</i>
<i>Table 1.6:</i>	<i>Concentration range of the impurities in the TeO_2 target (typical)</i>	<i>31</i>
<i>Table 1.7:</i>	<i>Typical isotopic composition of natural tellurium</i>	<i>31</i>
<i>Table 2A.1:</i>	<i>Isotopic abundance of natural tellurium and corresponding cross section of (n,γ) reactions.</i>	<i>67</i>
<i>Table 2A.2:</i>	<i>Other isotopes produced during the neutron irradiation of natural tellurium</i>	<i>68</i>
<i>Table 2B.1.</i>	<i>^{131}I activities collected in different batches</i>	<i>94</i>
<i>Table 2B.2:</i>	<i>Production of ^{131}I using natural TeO_2 target at Dhruva reactor</i>	<i>94</i>
<i>Table 2B.3:</i>	<i>Report on analysis of Sodium Iodide (I-131) solution</i>	<i>100</i>
<i>Table 2B.4:</i>	<i>Results of Production of ^{131}I by dry distillation technology</i>	<i>102</i>
<i>Table 3.1:</i>	<i>Concentration of ^{131}I by solid phase extraction procedure in several batches</i>	<i>138</i>
<i>Table 4.1:</i>	<i>Therapeutic agents used in treatment of hepatocellular carcinoma</i>	<i>146</i>

(HCC)

<i>Table 4.2:</i>	<i>Radiochemical Purity of ^{131}I-Lipiodol</i>	<i>160</i>
<i>Table 4.3:</i>	<i>In-vivo distribution data (% ID/Organ) of ^{131}I-Lipiodol in normal Wistar rats ($n = 4$)</i>	<i>162</i>
<i>Table 4.4:</i>	<i>Scaling-up of radiosynthesis of ^{131}I-Lipiodol under optimized conditions with semi-automated module</i>	<i>163</i>
<i>Table 4.5:</i>	<i>Specifications/Acceptance criteria of ^{131}I-Lipiodol injection</i>	<i>164</i>
<i>Table 4.6:</i>	<i>Data of actual patient dose preparation of ^{131}I-Lipiodol</i>	<i>166</i>

Highlights

- Development of a robust method for production, separation and purification of I-131 in pilot-scale from irradiated tellurium dioxide target by dry distillation method.
- The developed technology of dry distillation was employed for large-scale production, separation, purification and supply of multi-curie amount of ^{131}I on regular basis for societal benefit.
- Post processing concentration of ^{131}I using column chromatography for high dose therapeutic capsule preparation is reported.
- Application of ^{131}I produced by the developed method is demonstrated by development of formulation methodology and technology for clinical patient dose preparation of ^{131}I -Lipiodol for the treatment of hepatocellular carcinoma.



CHAPTER-1

INTRODUCTION

“yogā ve jāyatī bhūri”

“Wisdom is the outcome of patience.”

25/52. Khuddakanikāya, Dhammapadapāḷi

1.1 Application of radioisotopes in health care and introduction to radioiodine

The application of radioisotopes in medicine and healthcare is an important peaceful application of atomic energy. In 1896, Henri Becquerel discovered natural radioactivity. In 1898, Madam Curie discovered two radioactive elements polonium and radium [1]. Subsequently in 1901, the radioactivity of radium was used for treating cancer. Thereafter, there was a tremendous growth in the field of applications of radioisotopes in health care. The early history of the application of radioisotopes in healthcare paved the way to the development of a new area of medical research, nuclear medicine. The Hungarian scientist, George de Hevesy, father of nuclear medicine, invented the tracer principle / technique for which he was awarded noble prize in medicine in 1944 [2]. In fact the fundamental principle of nuclear medicine is based on the tracer principle.

Emilio Segre and Glenn Seaborg discovered the artificial element ^{99m}Tc in 1938 [2]. Subsequently, in 1957, ^{99}Mo - ^{99m}Tc generator was developed [3]. Hal O. Anchor designed and demonstrated the scintillation camera in 1950. These two events are very important to the growth of nuclear medicine. The progress of nuclear medicine became rapid after the launch of commercially available gamma cameras. This enabled *in-vivo* imaging of brain, gall bladder, heart, kidney, liver, lung, pancreas, stomach, thyroid, etc. using radiopharmaceuticals. After ^{99m}Tc , which is diagnostic radioisotope, ^{131}I and ^{60}Co found major role particularly as therapeutic radionuclides. Even now, iodine radioisotopes find extensive applications in the field of healthcare due to various advantages associated with them.

Iodine therapy (as iodide) was used in 1911 by David Marine for Graves' disease. Graves' disease is a common thyroid problem leading to hyperthyroidism which was reported by Sir Robert Graves in the early 19th century [4]. After the invention of artificial radioactivity and production of artificial radioisotopes by Irene and Joliot Curie in 1934, E. Fermi produced

^{138}I in the same year [5]. This event laid the basis for its many uses in medicine. In 1938, Glenn T. Seaborg and John Livingood discovered radioactive isotopes of iodine ^{131}I and ^{130}I at the Berkeley radiation laboratory. These were produced by using ^{128}Te as target in cyclotron [6].

By the time the iodine radioisotopes were discovered it was well known that iodine deficiency leads to thyroid related disorders in human being [7]. Later in 1940, Berkeley demonstrated radioiodine accumulation by the normal human thyroid gland using external detectors [8]. Later radioactive iodine was used in Graves' disease in 1943 by Hertz and Roberts [4]. Radioiodine therapy is a part of nuclear medicine for treating thyroid disorders including thyroid cancer. A small dose of radioactive iodine ^{131}I gets absorbed into the bloodstream after its intake by the patient and gets concentrated in the thyroid gland. The absorbed and concentrated ^{131}I destroys the gland's cells.

A list of radioisotopes of iodine and the nuclear decay characteristics of the radioisotopes are given in Table 1.1.

Table 1.1: Radioisotopes of iodine and their nuclear characteristics

Isotope	Half-life	Mode of Decay, %; Major Energies keV, %; Intensity of γ -ray;	Daughter product	Reference
^{108}I	36 ms	α 91%; EC, β^+ 100; p <1	-	-
^{109}I	92.8 μs	p 99.996%; α 0.014%	-	NDS 137, 1 (2016)
^{110}I	0.664 s	α 3444, 17 %	^{106}Sb	NDS 109, 943 (2008)
^{111}I	2.5 s	α 3152, 0.088 %	^{107}Sb	NDS 109, 1383 (2008)
^{112}I	3.34 s	EC, β^+ 100; γ 688.9, 786.9	^{112}Te	NDS 124, 157 (2015)
^{113}I	6.6 s	EC, β^+ 100; γ 896.0, 774	^{113}Te	NDS 111, 1471 (2010)
^{114}I	2.1 s	EC, β^+ 100; γ 708.8, 46.8, 682.5, 8	^{114}Te	NDS 113, 515 (2012)
$^{114\text{m}}\text{I}$	6.2 s	EC, β^+ 91	^{114}Te	
$^{114\text{m}}\text{I}$	6.2 s	IT 9 %	^{114}I	
^{115}I	1.3 m	EC, β^+ 100; γ 284, 460	^{115}Te	NDS 113,2391 (2012)
$^{115\text{m}}\text{I}$	0.5 ns	IT 100, γ	^{115}I	
^{116}I	2.91 s	EC, β^+ 100; 3144, 70.8, 2816, 18.7; γ 1022.0, 193.4, 678.92, 8.55	^{116}Te	NDS 111, 717 (2010)
$^{116\text{m}}\text{I}$	3.27 μs	IT 100; γ	^{116}I	
^{117}I	2.22 m	β^+ 77; 1505, 70, 1519, 8; γ 1022, 166, 325, 75	^{117}Te	-
^{118}I	13.7 m	EC, β^+ 100; 2504, 32.8; 2769, 16.7; γ 1022.0, 185; 605.6, 77.6	^{118}Te	NDS 75, 99 (1995)
$^{118\text{m}}\text{I}$	8.5 m	EC; β^+ 100; γ	^{118}Te	
^{119}I	19.1 m	EC; β^+ 100; 1005, 50.4; 958, 1.6;	^{119}Te	NDS 110, 2945 (2009)

		γ 1022, 115; 257.52, 86.3		
^{120}I	81.2 m	EC; β^+ 100; 1845.0, 29.3; 2099.3, 19.0; γ 1022, 137; 560, 69.6	^{120}Te	NDS 96, 241 (2002)
$^{120\text{m}}\text{I}$	53 m	EC; β^+ 100; γ	^{120}Te	
^{121}I	2.12 h	EC; β^+ 100; 475, 10.3; 334, 0.26; γ 212.3, 84.3; 27.465, 38.8	^{121}Te	NDS 111, 1619 (2010)
^{122}I	3.63 m	EC; β^+ 100; 1458.1, 67; 1195.3, 10; γ 1022, 156, 564.119, 18	^{122}Te	NDS 108, 455 (2007)
^{123}I	13.223 h	EC; β^+ 100; γ 158.97, 83.3, 27.465, 45.9, 528.96, 1.28	^{123}Te	NDS 102, 547 (2004)
^{124}I	4.1760 d	EC; β^+ 100; 687.04, 11.7; 674.74, 10.7; γ 602.73, 62.9, 1022.0, 45	^{124}Te	NDS 109, 1655 (2008)
^{125}I	59.407 d	EC; 100; γ 27.465, 73.4; 27.187, 39.4; 35.4922, 6.63	^{125}Te	NDS 112, 495 (2011)
^{126}I	12.93 d	EC; β^+ 100; 530, 0.81; 216.8, 0.198; β^- 292.5, 33.4, 461.5, 10.3; γ 388.63, 35.6, 666.331, 32.9 27.465, 20.5, 491.243, 2.88	^{126}Te	NDS 97, 765 (2002)
^{126}I	12.93 d	EC; β^- 100	^{126}Xe	
^{127}I	stable	100 % abundance	-	-
^{128}I	24.99 m	β^- 93.1 (8%); 833.4, 80.0; 635.1,	^{128}Xe	NDS 129, 191 (2015)

		11.56; γ 442.901, 12.61; 27.465, 2.7; 526.557, 1.203		
^{128}I	24.99 m	EC; β^+ 6.9%; 113.7, 0.0026,		
^{129}I	1.57×10^7 Y	β^- 100; 40.03, 100; 37, 99.5; γ 29.781, 36.1; 39.578, 7.42	^{129}Xe	NDS 121, 143 (2014)
^{130}I	12.36 h	β^- 100; 347.1, 48; 184.5, 46.7; γ 536.066, 99.0; 668.536, 96	^{130}Xe	NDS 93, 33 (2001)
$^{130\text{m}}\text{I}$	8.84 m	IT 84%;	^{130}I	NDS 93, 33 (2001)
$^{130\text{m}}\text{I}$	8.84 m	β^- 16%;	^{130}Xe	NDS 93, 33 (2001)
^{131}I	8.0252 d	β^- 100; 191.58, 89.6; 96.62, 7.23; γ 364.489, 81.5; 636.989, 7.16;	^{131}Xe	NDS 107, 2715 (2006)
^{132}I	2.295 h	β^- 100; 841.8, 19.0; 422.1, 19.0; γ 667.714, 98.7; 772.6; 75.6	^{132}Xe	NDS 104, , 497 (2005)
$^{132\text{m}}\text{I}$	1.387 h	IT 86%;	^{132}I	
$^{132\text{m}}\text{I}$	1.387 h	β^- 14%;	^{132}Xe	
^{133}I	20.83 h	β^- 100; 439.4, 83.42, 297.4, 4.18; γ 529.872, 87.0; 875.329, 4.51;	^{133}Xe	NDS 97, 765 (2002)
$^{133\text{m}}\text{I}$	9 s	IT 100;	^{133}I	
^{134}I	52.5 m	β^- 100; 473.5, 30.4; 594.3, 16.2; γ 847.025, 96; 884.09, 65;	^{134}Xe	NDS 103, 1 (2004)
$^{134\text{m}}\text{I}$	3.52 m	IT 97.7%;	^{134}I	
$^{134\text{m}}\text{I}$	3.52 m	β^- 2.3%;	^{134}Xe	
^{135}I	6.58 h	β^- 100; 498.8, 23.6; 324.3, 21.8;	^{135}Xe	NDS 109, 517 (2008)

		γ 1260.409, 28.7; 1131.511, 22.6		
^{136}I	83.4 s	β^- 100; 1843, 34; 2465, 28.8; γ 1313.02, 66.7; 1321.08, 24.8;	^{136}Xe	NDS 95, 837 (2002)
$^{136\text{m}}\text{I}$	46.9 s	β^- 100;	^{136}Xe	
^{137}I	24.5 s	β^- 100; 2589, 45.2; 2015, 8.9; 548, 0.61; 458, 0.31; γ 1218, 12.8; 601.05, 4.8; 4379.7, 0.036; 4880.5, 0.014;	^{137}Xe	NDS 108, 2173 (2007)
$^{137\text{m}}\text{I}$	24.5 s	β^- 7.14%;	^{137}Xe	
^{138}I	6.26 s	β^- 100; 3487, 32; 3225, 27; γ 588.825, 56; 875.23, 9.2; 601.0, 1.14; 385.2, 0.0612;	^{138}Xe	NDS 146, 1 (2017)
$^{138\text{m}}\text{I}$	6.26 s	β^- 5.44%; n	^{137}Xe	
^{139}I	2.28 s	β^- 100; 3188, 22; 3193, 21; γ 527.7, 8.3; 571.2, 8.1; 588.8, 5.67; 483.6, 1.71;	^{139}Xe	NDS 138, 1 (2016)
^{139}I	2.28 s	β^- 10%; n;	^{138}Xe	
^{140}I	0.84 s	β^- 100; 3532, 39; 3.74E3, 27; γ 376.657, 97.99; 457.63, 68;	^{140}Xe	NDS 108, 1287 (2007)
^{140}I	0.84 s	β^- 9.3%; n;	^{139}Xe	
^{141}I	0.43 s	β^- 100; β^- ; n 21.2;	^{141}Xe	NDS 122, 1 (2014)
^{142}I	222 ms	-	-	NDS 112, 1949 (2011)
^{143}I	130 ms	β^- , ?	-	NDS 113, 715 (2012)
^{144}I	300 ns	-	-	NDS 93, 599 (2001)
^{145}I	407 ns	β^- ?, β^- n	-	-

1.2 Applications of radioisotopes for diagnostic and therapeutic purposes

Radioisotopes are used for human healthcare for detection or for therapy or for both the purposes. Depending upon the desired application, suitable radioisotope is selected for the formulation of radiopharmaceutical. Radiopharmaceuticals are special class of radiochemical formulations having high purity and safety for human administration and used for either diagnosis or therapy.

1.2.1 Characteristics of diagnostic radiopharmaceuticals

The radioisotopes are used to formulate diagnostic radiopharmaceuticals. They are used *in-vivo* to monitor both physiological and biochemical functions of a diseased organ/tissues. The characteristic features of an ideal diagnostic radiopharmaceutical are listed below.

- i. No particulate emission: Diagnostic radionuclide should be pure γ emitter and should not emit any particulate radiation (α , β^- particles, Auger electrons). Particulate emissions are responsible for high radiation dose burden to the patients undergoing diagnosis because of their high linear energy transfer (LET).
 - ii. Suitable γ photon energy and high yield: High yield γ photon in the energy range of 80-300 keV is used in nuclear medicine for imaging. Also a radionuclide decaying by emission of positrons is used for imaging studies in positron emission tomography (PET).
 - iii. Suitable physical half-life ($T_{1/2}$) of radionuclide: The chosen radioisotope should have moderate half-life for completing both preparation of radiopharmaceuticals, quality control studies and diagnostic processes. At the same time, too long half-life is not desirable as it remains in the body for long duration and thereby increasing radiation dose burden to the patient.
-

- iv. High specific activity and radionuclide purity: The radionuclide with high specific activity is used in the radiopharmaceutical with a view to administer a small mass of the radiopharmaceutical into the patient. High radionuclidic purity is necessary to reduce the unwanted radiation dose to the non-target organs and tissues.
- v. Simple preparation of the radiopharmaceutical: Tagging of the radionuclide to the carrier molecule should be simple and easily achievable.
- vi. High stability: The radiopharmaceuticals prepared should have high *in vitro* and *in-vivo* stability. The radioisotope should not separate from radiopharmaceuticals *in-vivo*.
- vii. Short effective half-life: The radionuclide must have short effective half-life, so that the radiopharmaceutical disappears from the biological system rapidly after completion of the diagnostic study.
- viii. Specific *in-vivo* localization and high target/non-target ratio: An ideal diagnostic radiopharmaceutical should accumulate only in the organ/tissue of interest and exhibit no uptake in any other non-target organ/tissue. For any diagnostic study, it is desirable that the radiopharmaceutical be localized preferentially in the organ of interest and wash out rapidly from all other organs/tissue. This helps in providing maximum efficacy in diagnosis and at the same time minimum radiation dose to the patient.

1.2.2 Characteristics of therapeutic radiopharmaceuticals

The radioisotopes to be used in the preparation of therapeutic radiopharmaceuticals have to fulfill the following conditions,

- (i) Particulate emission: The radioisotope should emit either α , β^- or Auger electron which gives cytotoxic doses of ionizing radiation to proliferating the cancer cells. The type and energy of particle emission required for a particular application will depend on many factors, such as nature of the disease to be treated, the area and accessibility
-

of the diseased site, size of the tumor, intratumor distribution and pharmacokinetics of the tracer.

- (ii) Emission of imagable γ photons with low abundances: Emission of γ photons with suitable energy, with low abundance is always advantageous for monitoring the pharmacokinetics as well as *in-vivo* localization of the radiopharmaceuticals as a function of time also for carrying out simultaneous dosimetry studies in patients. The γ photon do not contributes to therapeutic effectiveness but increases radiation burden to the patients. Low abundance of γ radiation will give less radiation to the patient.
 - (iii) Suitable half-life: The therapeutic efficacy of radiopharmaceuticals can be achieved well when the physical half-life of the radionuclide is suitable to the treatment. The rate of decay must be suitable with the rate of localization of the agent in the target tissue along with the clearance of radioactivity from the normal tissue.
 - (iv) High specific activity and radionuclidic purity of the radionuclide: High specific activity of the radioisotope will be advantageous in administering the desired therapeutic dose using minimum amount of carrier molecule. High radionuclidic purity radioisotope will minimize the unwanted dose burden to the patient from other radionuclide impurities.
 - (v) High stability: The radionuclide should have high chemical affinity to the carrier molecule that results in highly stable radiopharmaceutical preparation. When a radiopharmaceutical is injected in human body the loss of radionuclide from the radiolabeled molecule results in the increase of radiation dose burden to non-target organs (poor target to non-target ratio). Hence a strong bonding between the radionuclide and the carrier moiety is essential to prevent gradual *in-vivo* release of the radionuclide from the carrier moiety.
-

- (vi) Specific *in-vivo* localization and high target to non-target ratio: An ideal therapeutic radioisotope/ radiopharmaceutical must demonstrate high specific localization in the diseased organ/tissue with a rapid excretion from the non-target organs and should exhibit a high target to non-target ratio. This will ensure maximum therapeutic efficacy of the radiopharmaceuticals.

1.2.3 Radioisotopes for theranostic applications

Theranostics is a new field of medicine which combines specific targeted therapy based on specific targeted diagnostic tests. In radiopharmaceuticals, substituting a radionuclide with therapeutic potential, usually a beta emitter (alpha and Auger electron emitters have been used less often), for a gamma emitting diagnostic radionuclide makes it a theranostic radiopharmaceutical. Theranostic agent combines diagnostic and therapeutic capabilities into a single agent. Theranostics involves the administration of a diagnostic agent for the applications listed as (i) To determine localization in the site or disease state under study as a surrogate for a potential therapeutic agent with similar chemical properties; (ii) To examine its bio-distribution as predictive of off-target (adverse) effects of the potential therapeutic agent; (iii) As an aid in determining the optimal therapeutic dosage or activity to be administered, based on the anticipated tumoricidal doses measured in the tumor site and (iv) To monitor the response to this treatment.

The first theranostic radiopharmaceutical in nuclear medicine history was radioiodine, which was used for therapy and imaging in thyroid diseases. A diagnostic scan with ^{123}I -, ^{124}I -, or a low activity of ^{131}I -iodide is followed by therapy with high activity ^{131}I -iodide. Other examples of theranostic radiopharmaceuticals are ^{68}Ga -DOTATATE (^{68}Ga : $T_{1/2}$: 68 min, β^+) and ^{177}Lu -DOTATATE (^{177}Lu : $T_{1/2}$: 6.7 d, β^- : 497 keV) used for diagnosis and treatment of neuroendocrine tumours, respectively [9]. Cu-64 ($T_{1/2}$: 12.7 h, EC, β^+ : 653 keV, β^- : 579 keV, γ :

1346 keV) has positron particles which are used in diagnosis and beta particles and Auger electrons both of which find use in therapy. Hence it is also a theranostic radionuclide used for diagnostic and therapeutic purpose in nuclear medicine [9].

1.2.4 Applications of ^{131}I in nuclear medicine

As it has been seen in the previous sections that ^{131}I plays a major role in the diagnostic and therapeutic applications.

1.2.4.1 Nuclear characteristics of ^{131}I

It is a β^- emitting radionuclide with a physical half-life of 8.02 days. Its principal γ -ray has an energy of 364 keV whereas the principal β -particle has a maximum energy of 0.61 MeV. The other relevant data have been listed in table 1.2.

Table 1.2: Principal radiation emission data of ^{131}I

Main Radiations	Branching	E
β^-	0.896	0.606 MeV
γ	0.815	364 keV
β^-	0.0039	0.807 MeV
γ	0.00021	164 keV
β^-	0.0723	0.334 MeV
γ	0.0716	637 keV

1.2.4.2 Decay Scheme of ^{131}I

Beta decay of ^{131}I to ^{131}Xe is illustrated in the simplified decay scheme [10] in Fig. 1.1.

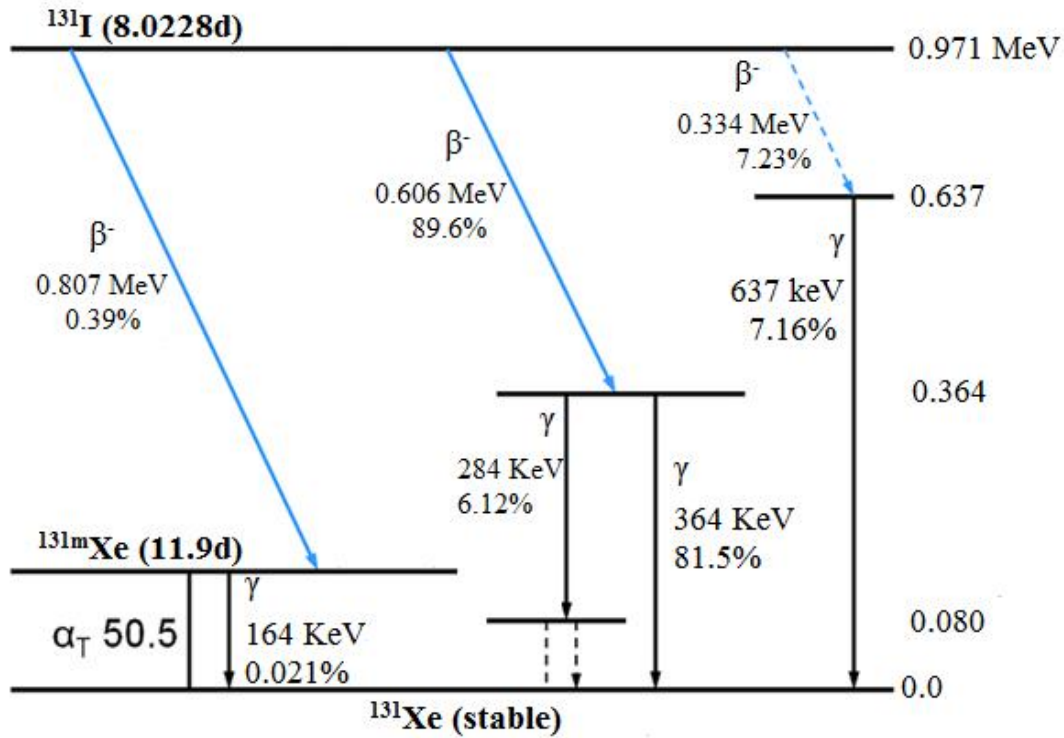


Fig. 1.1: Simplified decay scheme of ^{131}I

1.2.4.3 Gamma attenuation of ^{131}I

The specific gamma ray constant for ^{131}I is $15.8 \mu\text{C kg}^{-1} \text{MBq}^{-1} \text{h}^{-1}$ (2.27 R/mCi-hr) at 1 cm. This necessitates the handling of ^{131}I with adequate radiation protection. For this purpose, lead sheets or Pb castles of required thickness are used. The first half-value layer is 0.24 cm of lead. Further attenuation details are provided in Table 1.3. It may be noted from the table that the use of 2.55 cm of lead will attenuate the radiation emitted by a factor of about 1000.

Table 1.3: Attenuation of lead shielding for gamma emitted from ^{131}I

Shield thickness (Pb) cm	Coefficient of attenuation
0.24	0.50
0.89	10^{-01}
1.60	10^{-02}
2.55	10^{-03}
3.73	10^{-04}

1.2.5 Diagnostic applications of ^{131}I

The thyroid gland absorbs iodine. For this reason, a radioactive iodine uptake test is a useful diagnostic imaging procedure for thyroid related disorders. Nuclear medicine is a division of diagnostic imaging that uses small amounts of radioactive isotopes, such as radioactive ^{131}I , to diagnose a variety of diseases and abnormalities in the body. The isotope or radiotracer is injected into a vein, swallowed or inhaled as a gas. After a brief rest period, the radiotracer accumulates in the body and gives off energy in the form of gamma rays. The energy is detected with a PET scanner, gamma camera or a probe. Together with a computer, the amount of radiotracer that is absorbed is measured and images of the thyroid are produced. The radiotracer breaks down naturally and is eliminated from the body through urine and feces within the first few hours or days after the procedure.

Because of the carcinogenicity of its beta radiation in the thyroid in small doses, ^{131}I is rarely used primarily or solely for diagnosis (although in the past this was more common due to this isotope's relative ease of production and low expense). Instead the more purely gamma-emitting radioiodine ^{123}I is used in diagnostic testing (nuclear medicine scan of the thyroid). The longer half-lived ^{125}I is also occasionally used when a longer half-life radioiodine is

needed for diagnosis, and in brachytherapy treatment (isotope confined in small seed-like metal capsules). The other radioisotopes of iodine are never used in brachytherapy.

1.2.6 Therapeutic applications of ^{131}I

One of the major therapeutic applications of ^{131}I is the treatment of thyrotoxicosis (hyperthyroidism) and some types of thyroid cancers that absorb iodine. It is also used for some non-cancerous hyperactive thyroid nodules (abnormally active thyroid tissue that is not malignant). When a small dose of ^{131}I is swallowed, it is absorbed into the bloodstream and concentrated from the blood by the thyroid gland, where it begins destroying the gland's cells. Rapidly dividing cells, including cancer cells, are highly sensitive to radiation exposure. In all of these therapeutic uses, ^{131}I destroys tissue by short-range beta radiation. About 90% of its radiation damage to tissue is via beta radiation, and the rest occurs via its gamma radiation (at a longer distance from the radioisotope). It can be seen in diagnostic scans after its use as therapy, because ^{131}I is also a gamma-emitter. The ^{131}I isotope is also used as a radioactive label for certain radiopharmaceuticals that can be used for therapy, e.g. ^{131}I -metaiodobenzylguanidine (^{131}I -MIBG) for imaging and treating pheochromocytoma and neuroblastoma.

1.2.6.1 Dose of ^{131}I used in treatment

The dose used in treatment can be calculated by using a formula:

$$D = (C.W)/U$$

Where D: is the dose (in Ci) used

C: the radioactivity of ^{131}I necessary for 1 gram of the thyroid tissue.

This value is often determined from 80 μCi to 120 μCi (that is from 2.96 to 4.44 MBq) depending on the characteristics of goiter, concentration of thyroid related hormones in plasma and the over physical status of the patient.

W: the weight (in gram) of thyroid gland. Its value is determined by palpation. It is cross checked with scintigram and with ultrasonic pictures of the thyroid gland later.

U: 24-hour thyroid uptake after dose administration (in %).

1.3 General methods of production of radioisotopes

In the past the artificial production of radioisotopes was envisaged by transforming a stable nuclide into a radioisotope by some nuclear reaction. Later the cyclotrons and nuclear reactors opened the floodgate for producing a large number of artificial radioisotopes. The nuclear reactions based on the bombardment of target nuclei with either neutrons or charged particles turned to be an alternate to the production of radioisotopes.

1.3.1 Reactor production of radioisotopes

Nuclear reactors are the important and main sources of producing radioisotopes. The important nuclear reactions in which the radioisotopes are formed in the reactor are briefly described below,

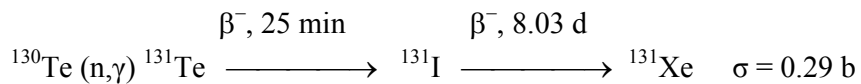
i) Neutron capture followed by gamma emission (n, γ)

In this reaction, a thermal neutron is absorbed by an atomic nucleus which gets excited energetically and de-excites by emitting gamma rays. In this process the resulting nucleus will have one more neutron without changing the number of protons leading to the formation of an isotope of the same element. Examples,

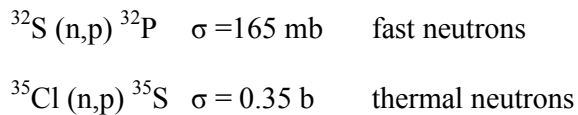


ii) Neutron capture followed by β^- emission

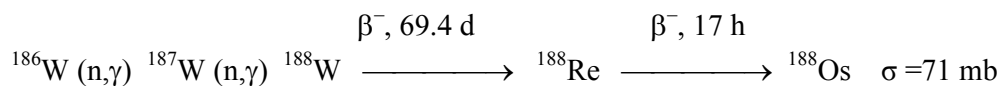
Some of the neutrons capture reactions (n,γ) produce short-lived radioisotope which decays into another radioisotope of long half-life. Here the target nucleus and the product nucleus are of different elements (i.e. chemically different) and thus can be separated by using suitable chemical separation technique. Example,

**iii) Neutron capture followed by charged particle emission**

Absorption of fast neutrons (sometimes thermal neutrons) leads to the emission of charged particle (p or α). Example,

**iv) Multistage neutron capture process**

In this reaction, the target radionuclide absorbs the neutron and its successive products will also follow similar neutron capture and form a radioisotope. This process has poor yield due to formation of very small quantity of intermediate isotope, thus reducing the probability of successive neutron capture. For example

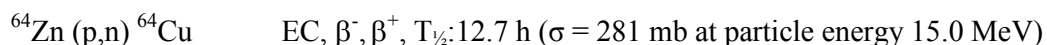
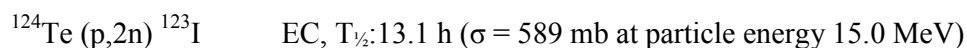
**v) Neutron capture followed by fission**

The fissile isotopes such as ^{235}U and ^{239}Pu undergo nuclear fission upon absorption of thermal neutrons producing a wide variety of radioisotopes known as fission products. The formed

fission products include stable isotopes, long- and short-lived radioisotopes. Some of the important radioisotopes formed during fission are ^{85}Kr , ^{89}Sr , ^{90}Sr , ^{99}Mo , ^{131}I , ^{133}Xe , ^{137}Cs , ^{140}Ba , ^{147}Pm , etc. Generally for the production of radioisotopes by this method, either natural or enriched uranium is subjected to fission. ^{131}I , a radioisotope found substantial applications in nuclear medicine, is produced with a fission yield of 2.9 % during nuclear fission of ^{235}U .

1.3.2 Accelerator production of radioisotopes

Cyclotrons are used for accelerating charged particles like p, ^2D and α particle as projectile to enter the target nucleus for producing radioisotopes. In accelerator bombardment the product is normally an element different from the target. This necessitates radiochemical separation of the desired radioisotope element to obtain high specific activity. The target material is deposited on a metal foil as thin layer and used in accelerators to avoid decrease in projectile energy through the target. A few examples of cyclotron produced radionuclides are:



1.3.3 Calculation of radioisotope yield

In the production of radioisotopes, it is necessary to know how much of the radioisotopes have formed while irradiating the target either with neutrons or charged particles. In order to understand the yield calculations, it is necessary to know the rate of formation of the radioisotope in the given method of production. For instance, when a radioisotope is produced in a nuclear reactor by bombarding the target with neutrons, the rate of production of radioisotope is given as

$$\frac{dN_2}{dt} = N_T \sigma \phi \dots\dots\dots (1)$$

Where,

N_1 is the number of product atoms at anytime, t

N_T is the total number of target atoms

ϕ is the neutron flux ($n\text{ cm}^{-2}\text{ s}^{-1}$)

σ is the reaction cross-section (cm^2)

Equation (1) considers the neutron flux to be isotropic.

Since the product radioisotope also decays with its own half-life, the net growth rate of product atoms can be obtained by subtracting the rate of decay from the rate of formation of the product atoms and the same can be expressed as

$$\frac{dN_1}{dt} = N_T \sigma \phi - \lambda N_1 \dots \dots \dots (2)$$

Where λ is the decay constant of the product nucleus

If the activity of the product atoms is A_1 then the number of atoms of the product atoms can be calculated by using the relation

$$A_1 = N_1 \lambda_1 = N_T \sigma \phi (1 - e^{-\lambda_1 t}) \dots \dots \dots (3)$$

Since the activity is exponentially related to the irradiation time (t_1), the activity depends on two conditions.

Condition 1: when $t \ll t_{1/2}$, the exponential term $((1 - e^{-\lambda t})$ known as growth factor) $\cong \lambda$

$$A_1 = N_T \sigma \phi \lambda \dots \dots \dots (4)$$

Condition 2: when $t \gg t_{1/2}$, the exponential term (known as growth factor) $\cong 1$

$$A_1 = N_T \sigma \phi \dots \dots \dots (5)$$

The activity in this condition is the maximum and is called as saturation activity.

The above conditions clearly indicate that the irradiation time is important in achieving the required activity. In view of this, in general, irradiation is not being done for a period greater than 3-4 half-lives of the product radioisotope.

1.3.4 Corrections to the activation equation

In practice, the activity induced in the target under irradiation will be less than the activity calculated using the above equation due to several factors. They are (i) self-shielding effect in the target, (ii) power variation in the reactor, (iii) flux depression due to adjacent samples in the reactor especially when such samples are high neutron absorbers, (iv) burn-up of the target material with time and (v) destruction of the product nucleus due to subsequent neutron capture.

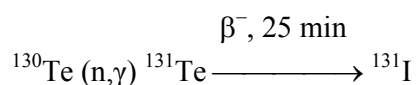
1.3.5 Irradiation efficiency

Irradiation efficiency is the ratio of the activity actually produced in the target to the activity calculated using the basic growth equation. It depends on the cumulative effects of all the aforementioned factors. Practically the irradiation efficiency is determined by trial irradiation.

1.4 General methods of production of ^{131}I

1.4.1 Production of ^{131}I using Tellurium as target

Radioisotope ^{131}I produced by exposing tellurium (generally natural tellurium) target material to the neutron flux in a nuclear reactor for an appropriate time. Thermal neutrons of energy 0.025 eV at 20 °C used in nuclear reactor for bombardment. The nuclear reaction is given below

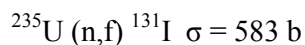


Cross section (σ) = 0.2 b

Natural abundance (θ) = 34.48 %

1.4.2 Production of ^{131}I through fission

Nuclear fission of ^{235}U (Low Enriched Uranium < 20 % ^{235}U) caused by neutron capture process of energy 0.025 eV. Iodine-131 is one of the important fission products formed during the fission of ^{235}U with overall fission yield of 2.9 % [11].



1.5 Separation of radioisotopes

After the completion of irradiation process the product radioisotope needs to be separated from the target as well as from other elements, if any. The separation of radioisotope of a particular element is imperative to achieve the required specific activity and radionuclide purity. Although a number of methods have been reported, the prominent methods of radiochemical separation involve solvent extraction, ion exchange, distillation, precipitation and chromatography.

1.5.1 Separation of radioiodine

The method which is most widely used for the separation of radioiodine from the target matrices such as U, Te etc., is distillation. This method is based on the vaporization of elemental iodine from the matrix. The iodine present in the sample or matrix is vaporized at a particular temperature and it is transported through a carrier gas. The separated fraction of iodine is trapped in a suitable solution, which is usually a solution of sodium sulphite. The distillation method involves the initial dissolution of the matrix followed by distillation of iodine.

1.5.1.1 Separation of ^{131}I by wet distillation method

Iodine-131 is produced by the neutron irradiation of tellurium (^{130}Te) according to the nuclear reaction $^{130}\text{Te} (n,\gamma) ^{131}\text{Te}$ wherein the ^{131}Te gives ^{131}I by β^- decay. The irradiated tellurium

powder is transferred into dissolution flask. The oxidation mixture containing 15 N chromic acid solution and 50 % H_2SO_4 is loaded into the dissolution flask [12]. The mixture is subsequently refluxed for two and half hours. After dissolution, the mixture is cooled for 3 hours. During the process of dissolution the iodine is oxidized to iodic acid. Sufficiently excess oxalic acid dihydrate is added to reduce the excess of chromic acid as well as the iodic acid into iodide. After the completion of reduction reaction, the distillation of ^{131}I is carried out for half an hour or till no more ^{131}I distils into the receiver flask containing 0.01 M Na_2SO_3 . The pH of the distillate is adjusted to approx. 8 by adding necessary quantity of 1 N NaOH solution. Finally the radioactive ^{131}I solution is transferred into a storage bottle. Although this method has many advantages over the conventional chemical methods of separation, it has certain demerits as furnished below,

1.5.1.1.1 Merits of wet distillation method

The wet distillation process has operationally simple in handling highly volatile ^{131}I in solution form. In India it served more than 40 years in processing ^{131}I because it is well established process.

1.5.1.1.2 Demerits associated with wet distillation process

- If tellurium metal of fine particle size (>100 mesh) is used for irradiation, it leads to ardent reaction, at times leading to explosion, during the dissolution stage.
- It generates a significant volume of radioactive liquid waste with high dose rate. For instance, in our lab around 12 liters of radioactive liquid waste (Dose rate >10 R/Hr) generated per month for producing ^{131}I activity of 3.7 TBq – 4.07 TBq (100-110 Ci). Moreover the liquid active waste generated poses waste management problem.

- It uses a solution of chromic acid and sulphuric acid, which is corrosive in nature. This causes corrosion of the facility and equipments.
- It is laborious and time consuming process
- Limits the radioactive concentration in the distillate
- Increased MEN-REM (Roentgen Equivalent Man) expenditure of the occupational workers

Wet distillation process is a well established process serving for 4 decades for ^{131}I processing and uninterrupted production of ^{131}I in our facility. There is a need to scale up the process to meet the increasing demand of ^{131}I . However, there are some inherent difficulties for scaling-up the process such as (i) restricted volume of dissolution flask, (ii) economic viability of using enriched target (iii) generation of large volumes of active liquid waste and (iv) inconvenient in the operation due to requirement of increasing lead shielding.

The following data enable us to understand the problems associated with the scale-up of ^{131}I production. Irradiation of 81 g of natural tellurium for 28 days at a total irradiation of 1100 MWD resulted in 740 GBq (20 Ci) of ^{131}I which also generated around 2.5 litres of highly acidic liquid waste. During the process the average occupational dose received by the operators was $\sim 123 \mu\text{Sv}$ per week.

Another alternative route of producing ^{131}I is through nuclear fission. The irradiated target (^{235}U) is associated with very high radioactivity due to the presence of a large number of fission products. Therefore, processing of such target material requires specially designed hot-cell for handling high active materials. Obviously, the process requires additional safety measures for the facility as well as for the occupational workers. Therefore, this demands a modified distillation method which can address some of the major issues posed by the wet distillation method.

1.5.1.2 Separation of ^{131}I by dry distillation method

Dry distillation method is a modified distillation method having many advantages over the existing wet distillation method. The main advantage is that it enables the direct distillation of the irradiated solid target material and hence, the cumbersome dissolution procedure is avoided. The dry distillation of iodine from the irradiated target material (TeO_2) is carried out at a temperature of 733°C or above. Unlike the wet distillation process, the direct solid distillation does not produce any active liquid waste, thereby overcoming the problem of radioactive waste management to a great extent.

1.5.1.2.1 Advantages of dry distillation method

- (i) In dry distillation method of ^{131}I processing, there is no radioactive liquid waste generation.
 - (ii) It yields high chemically pure ^{131}I (which responds well for iodination of even sensitive biological molecules) as it does not involve handling of other added chemicals during ^{131}I separation process.
 - (iii) High radioactive concentration of ^{131}I is possible which shows greater compatibility for formulation of radiopharmaceuticals.
 - (iv) As this method is rapid and convenient in processing ^{131}I , it exhibits less radiation dose to the operators.
 - (v) The design of the apparatus can be accommodative to up-scaling of ^{131}I production to meet future needs.
-

1.5.1.3 Separation of ^{131}I from fission products

Iodine-131 is one of the important fission products formed during the fission of ^{235}U [13]. Difficulty associated with this scheme of production is that ^{131}I is formed along with other fission products and therefore, it is associated with very high activity and thereby, very high radiation dose. The ^{131}I or iodine needs to be separated from other fission products as well as the target uranium so as to obtain the required radiochemical purity. Irradiated target plates are dissolved in concentrated NaOH. Methods known for separating iodine from uranium and fission products were developed with a view to separate both iodine and fission molybdenum. Typically the method involves the initial separation of uranium and some of the fission products as a solid residue and the supernatant that contains I and Mo is subjected independently to two different schemes of separation for separating Mo and I. The separated fraction of iodine is further purified by separating it on an anion exchange resin followed by a distillation step.

1.6.1 Target selection

1.6.1 General rules for selecting target material

The selection of target element or material or isotope [13] is very important while producing the radioisotopes by irradiation method. Ideally a target material should meet the following conditions.

- (a) Target material should be readily available and economically viable
 - (b) Target material should be physically and chemically stable while irradiation.
 - (c) The metallic or elemental form, oxides and carbonates are generally preferred as they exhibit adequate stability while irradiation.
 - (d) High density material is preferred as it will have large number of atoms per unit volume of the target material.
-

- (e) Easy handling of the material and it should associate with less number of other nuclides.
- (f) Target material should be chemically as pure as possible.

1.6.2 Precautions to be taken while irradiation

The following points should be kept in mind while selecting a target material for irradiation in a reactor.

Substances which are explosive, pyrophoric, or volatile, are not suitable for irradiation in the reactor. As a policy, in many reactors, Hg in elemental form is not permitted for irradiation since it forms amalgam with the reactor components. Target should not decompose under irradiation to form any gaseous products. Since targets in metallic form like cobalt do contain certain amount of adsorbed gases like hydrogen, nitrogen, etc. such targets should be degassed in an inert atmosphere before encapsulation. Targets like cobalt are normally plated with nickel, to avoid oxide formation leading to contamination during post-irradiation handling.

1.6.3 Safety investigation of target material

Safety of the target material and its product is ensured by choosing suitable encapsulation. For example, when the irradiation of telluric acid is performed to produce ^{131}I , there is a possibility of leak out of the container. This demands encapsulation of the target in air-tight container to prevent the escape of radioactive iodine vapor. Moreover, such release of iodine vapor or any other gas leads to pressure built-up in the encapsulation causing rupture or failure.

1.6.4 Enriched targets

When a radioisotope with high yield and specific activity from a target element with more than one isotope is required, enriched isotope is selected. The introduction of an enriched isotope will permit production of a radioisotope in high radiochemical purity when the naturally available element inevitably produces a long lived by-product.

1.6.5 Targets for producing ^{131}I and methods for radiochemical processing

Literature survey revealed that for the production of ^{131}I the targets used are (a) Elemental tellurium (b) Tellurium dioxide (c) Tellurium compounds that are soluble in water and (d) Uranium.

Elemental tellurium: Elemental Te in the form of powder is used. The use of powder form is essentially to facilitate the dissolution of the target after irradiation. It is necessary to ensure that the target should not contain significant amount of iodine as it would lead to decrease in specific activity of the product, ^{131}I . Therefore, iodine content should be controlled in the target prior to its irradiation.

Although elemental tellurium has been employed for reactor irradiation, the most obvious disadvantage is its tendency to blow up upon heating. Additionally, elemental tellurium cannot be heated in presence of oxygen without changing its chemical state. In view of the perceived danger of irradiation container bursts during neutron irradiation owing to the internal pressure increase by the generation of gases as a result of thermal decomposition of target, the scope of using telluric acid which decomposes at about 110 °C is precluded.

Tellurium dioxide: This oxide is also one of the targets for producing ^{131}I . However, the presence of selenium impurity is not desirable as it gets along with iodine in its volatile oxide form while distilling the irradiated target.

Tellurium compounds: Tellurium compounds like telluric, meta and ortho telluric acids are also considered as targets for producing ^{131}I . The choice of these materials is dependant upon certain conditions. For instance, telluric acid (H_6TeO_6) is selected where the irradiation facility has neutron flux in the order of $10^{12} \text{ n cm}^{-2}\text{s}^{-1}$ and the irradiation temperature is below 90°C . Similarly, the meta telluric acid (H_2TeO_4) is used when the irradiation temperature is around 160°C . Further the compounds of Te such as potassium and ammonium tellurates are also found to be suitable targets for producing ^{131}I

Uranium: Enriched uranium is considered to be a better target than the natural uranium owing to the fact that it provides high yield of ^{131}I . LEU (low enriched uranium) in the form of metallic, alloys and oxide forms are preferred for irradiation.

Processing methods: After the irradiation, depending upon the chemical nature of the target material the processing or separation method is chosen. The selection of the method basically depends mainly on the recovery of ^{131}I from the irradiated target material. Table 1.4 lists the nature of the target material and its relevant processing method.

Table 1.4: Target materials and ^{131}I processing methods

Target Material	Processing method
Tellurium metal powder	Wet distillation method
Tellurium dioxide powder	Dry distillation method or Wet distillation method
Uranium-235	Wet distillation method
Telluric acid	Wet distillation method
Polymetatelluric acid	Wet distillation method

1.6.6 Advantages of tellurium dioxide (TeO_2) target

Among all the probable targets of tellurium, TeO_2 is found to be most promising. The decisive advantage of using TeO_2 is derived from its good melting and solidification properties. Tellurium dioxide does not substantially change chemically at a temperature lower than 400 °C. It has sufficient stability under irradiation conditions of nuclear reactors. In view of these attributes, our selection of target resides on TeO_2 . Table 1.5 provides some important physical parameters for Te metal in comparison with TeO_2 as well as the product, iodine.

Table 1.5: Properties of Te, Iodine and TeO_2

Property / Material	Tellurium	Iodine	TeO_2
MP	449.5 °C	113.7 °C	733.0 °C
BP	989.8 °C	184.5 °C	1245.0 °C
Density at RT	6.27 g/cc	4.93 g/cc	6.67 g/cc
Vapor pressure	53 mbar at 727 °C	0.413 mbar at 25°C	Negligible at 727 °C

MP: Melting point; BP: Boiling point, RT: Room Temperature

1.6.7 Specifications for TeO_2 target

In order to achieve better yield and to obtain maximum recovery of the product during separation, the target tellurium dioxide has to meet certain specifications. The important specifications are TeO_2 should have a purity of 99.99 %, and particulate form with 100 mesh size and it should be free flowing. In addition, the concentrations of some elements present as impurities have also been restricted to certain specified values. This restriction is mainly to avoid unwanted production of activation products that would give significant radiation dose. Therefore, the target material should be highly pure and it should accompany with a

certificate of analysis. Else the target should be pre-analyzed for its purity prior to its irradiation. Table 1.6 shows typical concentration range of the impurities present in the target material.

Table 1.6: Concentration range of the impurities in the TeO_2 target (typical)

Element	Ag	Al	Ca	Cu	Fe	Mg	Na	Ni	Pb	Sb	Se	Se	Si	Ti
Conc. (ppm)	< 5	<10	<10	<10	<10	<10	< 1	< 5	<20	<20	<2.5	< 5	<10	<10

Since the production of ^{131}I depends on the isotopic abundance of ^{130}Te , the isotopic composition of the target (Te) is also important. The natural abundance of ^{130}Te is 34.48 % and hence, the target is expected to have this natural abundance or more. Table 1.7 gives the natural isotopes of tellurium and their isotopic abundances.

Table 1.7: Typical isotopic composition of natural tellurium

Te	120	122	123	124	125	126	128	130
%	0.09	2.46	0.87	4.61	6.99	18.71	31.79	34.48

1.7 Irradiation facility

For the present work, all the irradiation studies have been carried out in Dhruva Reactor at BARC, India. Dhruva is a tank type, heavy water moderated and cooled thermal research reactor available for isotope production with a maximum neutron flux of $1.8 \times 10^{14} \text{ n.cm}^{-2}.\text{s}^{-1}$ [14]. It uses metallic uranium as fuel encapsulated in aluminum clad. Fuel assemblies, experimental and irradiation assemblies and shut off rods are arranged in a square lattice totally acquiring 146 positions. Special assemblies called tray rods, made of aluminum houses in which many irradiation containers are placed in the reactor, are used for irradiation of the target materials. A single tray rod can hold 90 irradiation containers. The tray rods are

handled by the lead shielded refueling machines and delivered into a shielded cell equipped with master-slave manipulators, where the sample changes were carried out. The irradiated capsules are then loaded into lead shielded flasks of appropriate thickness and transported to radioisotope processing laboratory for further processing. In Dhruva, at 100 MWD power, the neutron flux levels at tray rod locations of sample irradiation from $0.05 \times 10^{14} \text{ n cm}^{-2} \text{ s}^{-1}$ to maximum $1 \times 10^{14} \text{ n cm}^{-2} \text{ s}^{-1}$ with neutron energy $< 0.625 \text{ eV}$.

1.8 Irradiation containers

The irradiation container consists of a cylinder and a lid. They are made up of 1S aluminum having dimension of 22 mm (l) x 44.5 mm (h). An accurately weighed amount of TeO_2 was transferred into the irradiation container (Fig. 1.2), encapsulated by cold-pressure-weld and irradiated in the Dhruva research reactor of our institution at a neutron flux of $\sim 5\text{-}9 \times 10^{13} \text{ n cm}^{-2} \text{ s}^{-1}$. After neutron irradiation of the TeO_2 target in the reactor, the irradiation containers were kept in a lead-shielded flask and transported into the radiochemical processing laboratory.

Irradiation containers are usually made of aluminum and preferably should have a low content of sodium, manganese and copper. The functions of the container may be summarized as follows

- (a) It must isolate the target material from external disturbances.
 - (b) It must reduce any hazard attendant upon the use of the target materials.
 - (c) It must be easy to locate in the irradiation, loading and unloading positions.
-

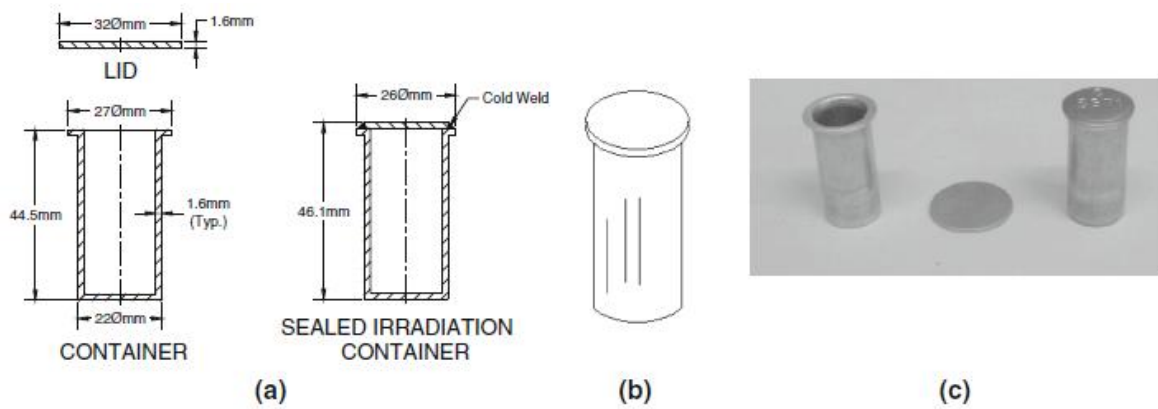


Fig. 1.2: Irradiation containers

1.8.1 Sealing method

Cold-welding is readily achieved with an ordinary laboratory press and mould, and will produce containers capable of withstanding internal pressures of up to $40\text{-}50 \text{ kg cm}^{-2}$. The loaded capsule is placed in the sealing die and the buffed lid is placed on the buffed capsule flange. The die lid is carefully fitted. The assembled die is placed in a standard laboratory hydraulic press and is pressed to 10000 lb in^{-2} . It is held at this pressure for 10 sec. The pressure is slowly released.

1.8.2 Test for weld integrity

The cold-welded irradiation container is placed in a glass cylinder containing water. The glass cylinder is sealed and evacuated rapidly. A leaking weld is identified by the appearance of a stream of air bubbles rising to the surface from the flaw in the weld.

1.9 General terms used in the thesis

Radiopharmaceuticals: Radiopharmaceuticals are defined as a special class of radiochemical formulations having high purity and safety for human administration and used for either diagnosis or therapy.

Diagnostic Radiopharmaceuticals: Diagnostic radiopharmaceuticals are defined as the radiolabeled molecules designed to produce images of the morphology or physiological functions of specific organs/tissue.

Therapeutic Radiopharmaceuticals: Therapeutic radiopharmaceuticals are defined as radiolabeled molecules designed to deliver therapeutic dose of ionizing radiation to the diseased sites (most often cancerous tumors) with high specificity in the body.

Radiochemical Purity is the fraction of the radionuclide of interest in the stated chemical form.

Radioactive Concentration is the activity per unit volume of the product.

Radionuclidic Purity is the percentage of radioactivity of the radionuclide of interest in a given sample in relation to the total radioactivity.

Specific Activity is defined as the activity per unit mass of the substance.

Radiotherapy: This technique is used to cure cancers or at least to alleviate the most distressing symptoms, by killing the cancerous cells. A beam of high energy X rays, gamma rays or electrons is directed towards the diseased tissue so as to give it a high dose while sparing the surrounding healthy tissue.

Effective Half-life (T_e), which is defined as

$$1/T_e = 1/T_p + 1/T_b$$

$$\text{or, } T_e = T_p \times T_b / (T_p + T_b)$$

Where T_p is the physical half-life and T_b is the biological half-life.

Linear Energy Transfer (LET): Energy transferred per unit length of track (kilo electron volt per micron; keV/ μm)

Absorbed dose: It is the energy imparted by radiation to unit mass of matter (tissue) expressed in Gray (Gy). Practically it is calculated from the activity expressed in mCi or MBq using the following equation.

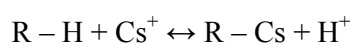
$$\text{Gy} = (\text{activity/volume}) \times \text{residence time (t)} \times \text{S (mGy/MBq/sec)}$$

Where S is the specific value for a radionuclide which refers to linear energy transfer of it's radiation and relative biological weighting factors. As residence time can be derived from effective half-life using, Residence time, $t = T_{1/2\text{eff}} / \ln 2$.

Equivalent Dose: It is the absorbed dose weighted for the hazard of different types of radiation.

Effective Dose: It is the 'Equivalent dose' weighted for the harm to different cells / tissues. In others it is the doubly weighted absorbed dose, weighted for type of radiation and weighted for the radiation risk for the cells / tissues.

Ion Exchange: Ion exchange specifically refers to the process of reversible exchange of ions having charges of the same sign between an electrolyte solution and the ion exchanger



Thus, an essential pre-requisite for ion exchange is that the elemental ion (radio-nuclide) of interest should be present as ions.

Distribution Coefficient (K_d): Ion exchange equilibrium can be conveniently expressed in terms of distribution coefficient. Distribution coefficient is defined as a ratio of concentration of the counter ion in the exchanger and the solution at equilibrium. K_d may be stated as

$$K_d (\text{mL/gm}) = \frac{\text{Sorbed radio-isotope / gm of ion exchanger}}{\text{Dissolved radio-isotope / ml of solution}}$$

TACE: Transcatheter Arterial Chemoembolization is an invasive procedure performed in interventional radiology to block a tumor's blood supply. Small embolic particles coated with chemotherapeutic drugs are injected selectively through a catheter into an artery directly supplying the tumor. These particles both block the blood supply and induce cytotoxicity, attacking the tumor.

TARE: Trans-Arterial Radioembolization is a technique of embolization in conjunction with a radiotherapy agent.

PVT: Portal Vein Thrombosis is a form of venous thrombosis affecting the hepatic portal vein, which can lead to portal hypertension and reduction in the blood supply to the liver.

XRD: X-ray Diffraction is a rapid analytical technique used to study crystal structures and material characterization. It is based on the Bragg's law and the elastic scattering of X-ray photons by atoms in a periodic lattice. For electromagnetic radiation (X-ray) to be diffracted the spacing in the grating should be of the same order as the wavelength.

FESEM: Field Emission Scanning Electron Microscopy (FESEM) provides topographical and elemental information at magnifications of 10x to 300,000x, with virtually unlimited depth of field. FESEM based studies suggested significant advantages like: focusing with higher resolution, ability to measure structural and micromechanical properties and the potential of imaging in well accuracy manner.

TEM: Transmission Electron Microscopy is a microscopy technique in which a beam of electrons is transmitted through a specimen to form an image. TEM can be used to study the growth of layers, their composition and defects in semiconductors. High resolution can be used to analyze the quality, shape, size and density of quantum wells, wires and dots.

SAXS: Small Angle X-ray Scattering is primarily used for investigating long range periodicity or order in the materials. The length scale probed by SAXS is 10-1000 Å

corresponding to an angle range of 0° - 0.5° . The inverse relationship between scattering angle and particle size is utilized to glean information on the structure of solids and liquids.

SANS: Small-Angle Neutron Scattering is used to study the structure of various substances on a length scale of 10 - 5000 Å based on elastic neutron scattering at small scattering angles. It gathers the information on particle size and thickness of surfactant coating, number density & volume fraction, composition, shape & size distribution, and interaction & ordering of the material.

MSANS: Moderate Resolution Small Angle Neutron Scattering is used to study micro-structural characterization of material like pore morphology and pore size distribution. MSANS instrument are with a pair of single-bounce flat crystals as monochromator and analyzer, able to analyze and characterize various materials such as ceramics, alloys and rocks.

BET: Brunauer-Emmett-Teller (BET) theory aims to explain the physical adsorption of gas (generally Nitrogen) molecules on a solid surface and serves as the basis for an important analysis technique for the measurement of the specific surface area of materials. Large specific surface area corresponds to high porosity of the material.

SEM: Scanning Electron Microscopy is a method of producing an image of a surface by scanning an electron beam over the sample and measuring the electronic interactions with the interface. It is used for materials evaluation like Grain size, Surface roughness, Porosity, Particle size distributions, Material homogeneity, Intermetallic distribution and diffusion.

ICP-AES: Inductively Coupled Plasma-Atomic Emission Spectroscopy is an emission spectrophotometric technique, exploiting the fact that excited electrons emit energy at a given wavelength as they return to ground state after excitation by high temperature Argon Plasma. It is used for the detection of chemical elements.

EDS: Energy Dispersive Spectroscopy (EDS) identifies the elemental composition of materials imaged in a scanning electron microscope for all elements with an atomic number greater than boron. Most elements are detected at concentrations on the order of 0.1 percent. As the electron beam of the SEM is scanned across the sample surface, it generates X-ray fluorescence from the atoms in its path. The energy of each X-ray photon is characteristic of the element that produced it. The EDS microanalysis system collects the X-rays, sorts and plots them by energy, and automatically identifies and labels the elements responsible for the peaks in this energy distribution.

1.10 Motivation of the present work

Iodine-131 is being produced using different target materials and various radiochemical separation techniques are employed in different countries as per the availability of technology for several decades. In India, wet chemical separation method was in practice since last 50 years. Due to the disadvantages like generation of highly acidic liquid waste which poses problems in waste management and difficulty in scaling-up of the processing capacity, there was a need to look for an alternative methodology to produce ^{131}I in bulk quantities with safe practices to cater the futuristic demand. There was a need to develop a new indigenous technology for ^{131}I production and purification for formulation of ^{131}I radiopharmaceuticals. The work reported in this thesis is aimed towards development of indigenous dry distillation technology for production and separation of ^{131}I which is easy in operation, robust in scaling-up, safe in handling, has no liquid radioactive waste generation and obtaining purified ^{131}I and demonstration of utility of produced ^{131}I in formulation of a therapeutic radiopharmaceutical.

1.11 Scope of the present thesis

The work carried out in this thesis pertains to the development of technology for the production, separation and purification of ^{131}I using novel approaches. The ^{131}I produced by newly developed technology was used for formulation of therapeutic radiopharmaceuticals. First two chapters describes the development of dry distillation technology for ^{131}I production and the third chapter describe the solid state synthesis of mesoporous alumina for increasing the post-processing radioactive concentration of ^{131}I for therapeutic capsule preparation. The forth chapter focuses on the development of therapeutic radiopharmaceutical ^{131}I -Lipiodol and its clinical utilization using ^{131}I produced by above methodology.

CHAPTER-2

Dry Distillation Technology for Production and Radiochemical Separation of Iodine-131

“Distillation, King in separations, will remain as the workhorse separation device of the process industries. Even though it is old in the art, with a relatively mature technology support base, it attracts research and professional interest. Without question, distillation will sail into the future with clear skies and a strong wind. It will remain the key separation method against which alternate methods must be judged.”

Dr. James R. Fair, 1990

This chapter consists of two parts, viz. Part 2A and 2B. Part 2A deals with the development of dry distillation technology for ^{131}I processing and purification whereas part 2B describes the application of developed dry distillation technology for large scale production, separation and purification of ^{131}I .

2.1. Introduction

Iodine-131 is one of the radionuclides most widely used for the preparation of a host of *in-vivo* radiopharmaceuticals for a variety of nuclear medicine procedures [15-22]. Widespread applications of ^{131}I have not only stimulated the progress in nuclear medicine procedures, but also have driven the field significantly forward. By virtue of its favorable nuclear characteristics, ^{131}I occupies an important place at the forefront of nuclear medicine. The utility of ^{131}I therapy for treatment of benign and malignant thyroid disorders is well known. It will continue to remain as a mainstay of therapy for the treatment of toxic thyroid nodules, Graves' disease, volume reduction of long-standing goiters and differentiated thyroid cancer [15-22]. In order to determine the size, location, and function of the thyroid gland, ^{131}I in much smaller doses is also regularly used for imaging. In addition to the management of thyroid cancer, utility of ^{131}I had virtually pervaded all areas of *in-vivo* radionuclide therapy. Metaiodobenzylguanidine (MIBG) labeled with ^{131}I has been used not only for the management of chromaffin tumors (neuroblastoma, pheochromocytoma, and paraganglioma), but also emerged as the most widespread agent for the functional imaging of pheochromocytoma and paragangliomas for detection of these tumors [23-27]. The past decade has witnessed a remarkable interest in the use of ^{131}I -labeled tositumomab (Bexar), a radiolabeled CD20-directed antibody, in the treatment of patients with CD20 antigen-expressing relapsed or refractory, low-grade, follicular, or transformed non-Hodgkin lymphoma (NHL), including patients with rituximab refractory NHL [28–33]. While the utility of ^{131}I has made significant inroads into the field of nuclear medicine and undergone

phenomenal expansion and growth, cost effective availability of ^{131}I of desired quantity and quality represents the key determinant that underpin its survival, strength and success in nuclear medicine. With expanding areas of applications and growing interest in the use of ^{131}I labeled radiopharmaceuticals, the domestic demands of ^{131}I has increased several folds over the years. In this context, acquiring local production capability of clinical grade ^{131}I is extremely important to meet the growing regional demands to reap the proven benefit of ^{131}I -labeled radiopharmaceuticals. In view of this, it is imperative to consider all possible ^{131}I production options conscientiously and select the most economically and technologically viable option that will provide clinical grade ^{131}I on a regular basis.

The general ^{131}I production route is either from $^{130}\text{Te} (n,\gamma) ^{131}\text{Te} \xrightarrow{\beta^-} ^{131}\text{I}$ nuclear reactions [34–40] or from $^{235}\text{U} (n,f) ^{131}\text{I}$ [41–49]. While the production of ^{131}I through fission route obviously hold promise as a viable approach and is followed by some institutions, the implicit need of an elaborate complex radiochemical separation and purification procedure to isolate ^{131}I of requisite purity as well as generation of significant amount of radioactive wastes emerged as the major issues that needs to be addressed satisfactorily in ensuring successful implementation of this strategy. Even though there is no scientific barrier for its adaption, there are concerns about technical and economic implications that continue to thwart efforts for its widespread adoption. In this context, the scope of accessing ^{131}I through neutron activation of ^{130}Te merits attention. With a view to separate ^{131}I from the neutron irradiated Te target, two neutron irradiated target processing strategies are widely followed. The first concerns dissolution of the irradiated target in mineral acid followed by distillation referred to as wet distillation technique, while the second entails dry-distillation of the irradiated target. Although the scope of using wet chemical thermal distillation concept is relatively more appealing in term of operational simplicity in handling highly volatile ^{131}I in solution, the inherent need of concentrated acid to dissolve the irradiated Te target and

requirement of an elaborate radiochemical separation procedure emerged as the major impediments that limits its applicability to a small batch size. Nevertheless, the process has an additional disadvantage of inadvertent introduction of chemical impurities into the ^{131}I during chemical treatments of neutron irradiated Te target.

In order to circumvent such limitations, the scope of using dry-distillation technique, which relies primarily on the differences in the volatilization properties of iodine and tellurium target is a promising pathway as it not only precludes the chemical dissolution of irradiated target, but also offers the flexibility to scale-up or -down to its level of operation in response to requirements.

To be self reliant and make easy technology for adoption in regular production and supply of ^{131}I , development of dry distillation route of ^{131}I processing was taken up. Practical realization of a dry distillation technique requires introspection of process technology, conscious development of process equipments; challenges in addressing handling of volatile radioactive iodine at elevated temperature; in depth analysis of the quality of ^{131}I and adherence to regulatory compliance. This sequential step in the development of indigenous technology includes selection of target, optimization of irradiation parameters, design and development of process equipment, careful optimization of the process and in depth analysis of radiological safety. The quality of ^{131}I for radiopharmaceutical applications was also evaluated to ensure that it is within the stipulated limit of the pharmacopeia.

CHAPTER-2A

Development of Dry Distillation Technology for Radiochemical Separation and Purification of Iodine-131

“kayirā ce kayirāthenaṃ”

“Try your best in whatever task you have set yourself”

25/156. Saṃyuttanikāya, Dhammapadapāḷi

In the current chapter, optimization of various parameters essential for development of dry distillation technology for radiochemical processing and separation of ^{131}I are described in detail.

2A.1 Selection of target material

For the process of dry distillation and wet distillation of ^{131}I , tellurium target material in different chemical forms has been used worldwide [13]. In India, tellurium metal powder was used as target in wet method. Tellurium metal (melting point of 449.5°C) was easily available in large quantity [12]. The utility of the same material was also explored to study feasibility of ^{131}I separation using dry distillation method. Tellurium dioxide (melting point of 733.0°C) has stability at higher temperature. Hence both the targets were used independently to study the feasibility of ^{131}I separation using dry distillation method.

2A.1.1 Feasibility of distillation of ^{131}I from tellurium metal powder

2A.1.1.1 Experimental Procedure

(a) Materials and equipments

Natural tellurium metal powder (40-60 mesh size) purity $> 99.99\%$ was used as a target procured from Nuclear Fuel Complex, Hyderabad, India. Sodium Hydroxide and Sodium Sulfite (AR grade) were procured from Merck, India. Argon gas (purity $\sim 99.99\%$) was procured from Tripti Gases Pvt. Ltd. Mumbai, India. High resolution γ -ray spectrometer consisting of an HPGe detector coupled to a Computer-based 4 k multi-channel analyzer (MCA) of Eurysis Measures, France, was used for γ -ray spectroscopic measurements. A locally procured chromatography unit was used for the determination of radiochemical purity of ^{131}I produced. A well-type NaI(Tl) scintillation counter of Electronic Enterprises Pvt. Ltd, Hyderabad, India was used to measure the activity of chromatography paper strip during

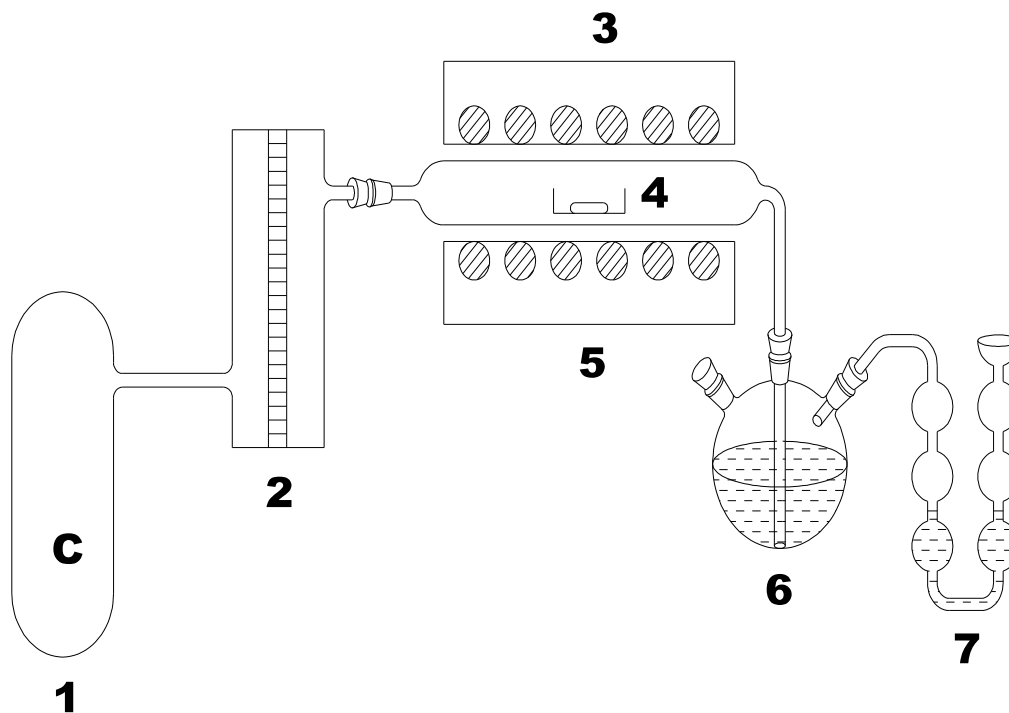
radiochemical purity assay. A horizontal furnace was locally fabricated (Model No.:BARC3 from Agnee Engineering, Mumbai) for heating irradiated target material. Radionuclidic purity was determined by recording the γ -ray spectrum of the appropriately diluted solution of the activity in a high resolution gamma spectrometry system.

(b) Neutron irradiation

About 50-100 mg tellurium metal powder was weighed, transferred into 1S aluminum irradiation container and subsequently the container was sealed by cold welding. The container was irradiated in the Dhruva reactor at a neutron flux of $\sim 1.4 \times 10^{13} \text{ n cm}^{-2} \text{ s}^{-1}$. After irradiation the containers (containing Te metal powder) were kept in a lead shielded flask and transported into radiochemical processing laboratory.

(c) Separation of ^{131}I from irradiated tellurium metal powder

Irradiated tellurium powder recovered from irradiation container and a few milligram of the irradiated target was taken out to measure the activity of ^{131}I produced. Subsequently, the irradiated target Te metal powder transferred to a quartz boat which was then introduced at the center of quartz tube into the furnace as shown in Fig. 2A.1. The quartz tube was then connected at one end to argon gas and another to ^{131}I trapping system after closing the quartz tube. Argon gas was used as non-reactive carrier gas with a flow rate of $40\text{-}50 \text{ mL min}^{-1}$. Furnace temperature was increased to $450\text{-}460^\circ\text{C}$ at the rate of $15^\circ\text{C per min.}$ and continuous bubbling was observed in the ^{131}I trap containing 40 mL solution of 0.1 M NaOH and $0.2 \text{ mg mL}^{-1} \text{ Na}_2\text{SO}_3$. The distillation process was continued for 6 h. After distillation and cooling few milligram tellurium metal remnants was dissolved in chromic acid and sulfuric acid mixture. It was adequately diluted and ^{131}I activity was measured. A small amount of ^{131}I trapped in the solution of 0.1 M NaOH containing $0.2 \text{ mg mL}^{-1} \text{ Na}_2\text{SO}_3$ was also adequately diluted (so that to keep the dead time of the detector within 2 %) and counted by pre-calibrated HPGe detector (Fig. 2A.2, Fig. 2A.3 and Fig. 2A.4).



1. Argon gas cylinder 2. Rotameter 3. Furnace 4. Quartz boat containing irradiated Target (Te/ TeO₂) 5. Quartz Tube 6. ¹³¹I receiver flask (0.1M NaOH containing 0.2 mg mL⁻¹ Na₂SO₃) 7. NaOH Trap (0.5 M)

Fig. 2A.1: Apparatus for dry distillation of ¹³¹I from irradiated Te metal powder

Another set of experiments were carried out to study tellurium carryover in the final product. 80 g of inactive tellurium metal powder which was required to one batch of wet distillation for processing ~ 20 Ci ¹³¹I, was taken into the quartz boat and subsequently heated to 450-460 °C using the same trapping solutions, parameters and conditions as mentioned above and the results are described in section 2A.1.1.2.

(d) Determination radionuclidic purity and separation yield of ¹³¹I

Radionuclidic purity was ascertained by γ -ray spectrometry. A small aliquot of appropriately diluted activity was withdrawn and placed on a HPGe detector such that the dead time of the

detector was < 2 %. The gamma-ray spectrum was recorded for 30 min. Table of Isotopes [50] and Gamma Ray Catalogue [51] were used for confirmation of the measured gamma energies.

(e) Determination of radiochemical purity

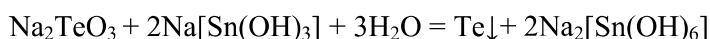
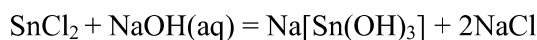
Radiochemical purity was determined by paper chromatography, using iodide and iodate carrier and a solvent mixture of 75 % methanol and 25 % water adjusted to pH 7-8 with potassium carbonate. In order to saturate the chromatography papers with the solvent vapors, it was kept hanging above the solvent into the chromatography jar for 15-20 min. At the point of spotting, the carrier (5 μ L each of 1.5 % w/v KI and 1.5 % w/v KIO₃ solutions) and ~ 5 μ L activity was spotted and dried. The paper strip dipped into the solvent for ascending chromatography and run to develop the chromatogram. The chromatography paper was dried and the movement of iodide ion was spotted by spraying palladous chloride and the movement of iodate ion by mixture of starch, acetic acid and potassium iodide onto the strip. The strips were counted by cutting it into 1 cm pieces. Percent activity in the iodide zone was calculated which gives % radiochemical purity.

(f) Determination of tellurium content

One drop of standard tellurium (Standard tellurium solution 10.0 ppm: Stock solution of 1000 ppm tellurium was prepared by dissolving 125.1 mg of tellurium dioxide in 100 ml of distilled water. The stock solution was diluted with distilled water to prepare the standard solution with concentration of 10 ppm.), water (blank) and sodium iodide (sample) solution was placed into each hole of a spot plate. One drop each of stannous chloride [Stannous chloride solution 5.0% (fresh preparation): Stannous Chloride dihydrate (SnCl₂.2H₂O) 0.25 g was dissolved in 0.25 ml of conc. HCl, heated to make it a clear solution and diluted to 5.0 ml with distilled water], saturated sodium carbonate and 25 % of sodium hydroxide solution

were added respectively into each hole of the spot plate. The black precipitation of Te metal from the sample was compared with standard Te and blank. (Te^{4+} was reduced by Sn^{2+} to give the black tellurium metal). If there was preservative such as sodium thiosulfate ($\text{Na}_2\text{S}_2\text{O}_3$) in the sample solution, it will give the dark brown precipitation together with Te metal [52].

Chemical reaction:



2A.1.1.2 Results of the experiment and discussion

Gamma ray spectra of irradiated tellurium metal powder before and after distillation of ^{131}I were illustrated in Fig. 2A.2 and 2A.3, respectively. On the other hand, γ -ray spectrum of distilled ^{131}I was shown in Fig. 2A.4. Gamma ray spectrum of the separated ^{131}I sample was identical to that of specimen of ^{131}I of known purity that exhibits a major photo peak having energy of 364 keV. There was no extraneous gamma emitting radionuclide was present in the active samples apart from ^{131}I (Fig. 2A.4). Hence radionuclidic purity of separated ^{131}I was ~100 %.

Radiochemical purity of the product ^{131}I was checked with paper chromatography method and found to be 98.5 ± 0.9 % as iodide as shown in Fig. 2A.5. Tellurium content in the ^{131}I trapping solution as chemical impurity was tested by spot test method and found to be $< 5 \mu\text{g mL}^{-1}$ when upto 100 mg Te metal powder was used for distillation. But when a batch size of 80 g Te was used for distillation it was found to be $> 40 \mu\text{g mL}^{-1}$ while the limit is $< 5 \mu\text{g mL}^{-1}$ of active ^{131}I solution. Hence it may be concluded that the use of metallic tellurium as the target material for large-scale production of ^{131}I by dry distillation technique may not be suitable proposition as it led to Te impurity in the final product beyond permissible limit.

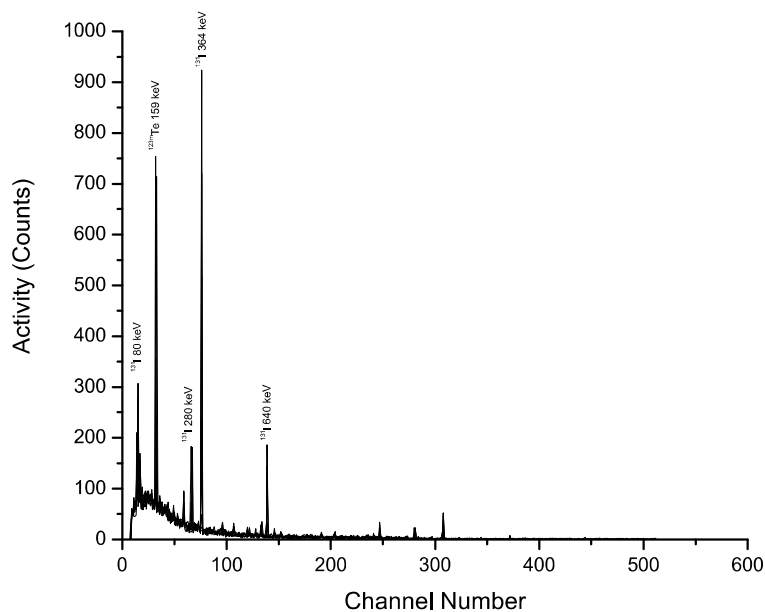


Fig. 2A.2: Gamma ray spectrum of irradiated tellurium powder before experiment

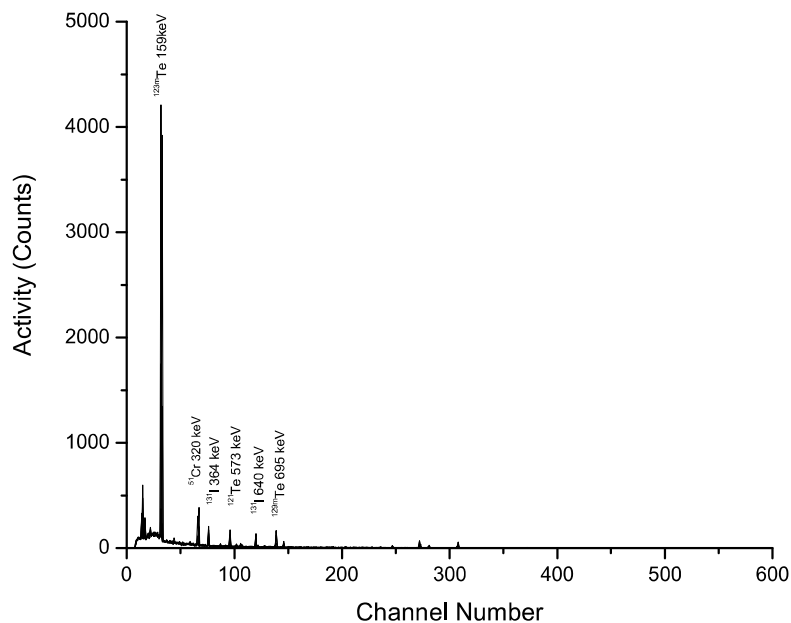


Fig. 2A.3: Gamma ray spectrum of irradiated tellurium after distillation

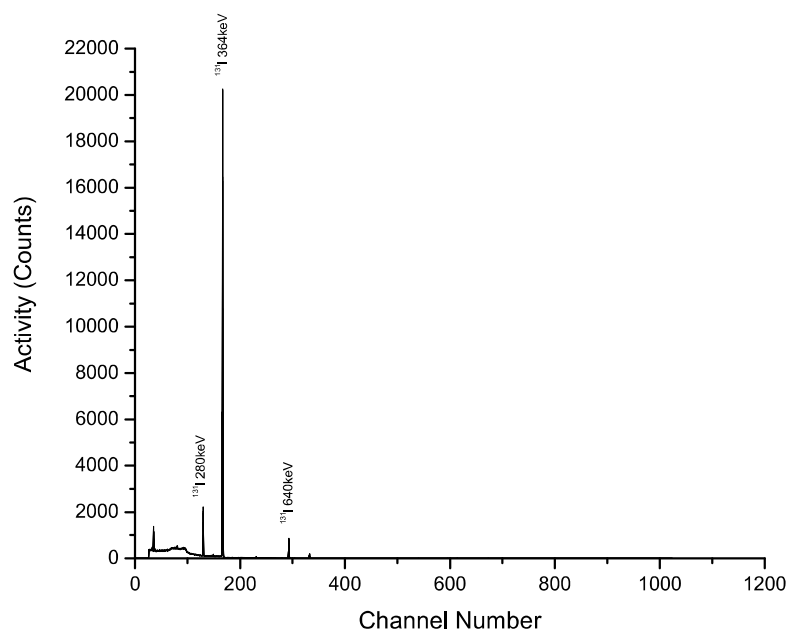


Fig. 2A.4: Gamma ray spectrum of ^{131}I trapped.

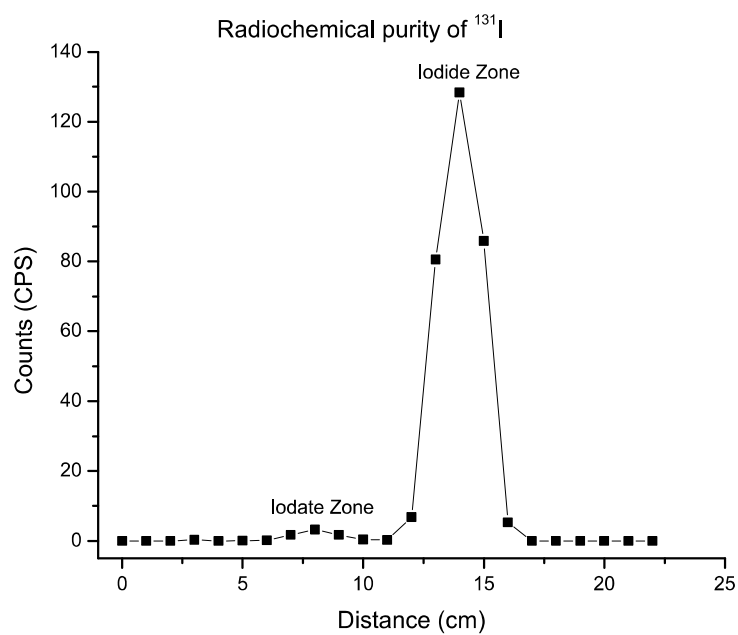


Fig. 2A.5: Paper chromatography pattern of ^{131}I produced using metallic Te as target

2A.1. 2 Feasibility of distillation of ^{131}I from irradiated TeO_2

2A.1.2.1 Experimental Procedure

(a) Materials and equipments

Natural tellurium dioxide (TeO_2), Purity > 99.999 %, procured from Alfa Aeser, Mumbai, India, was used as a target. All other chemicals and equipments used in the studies were same as specified in the section 2A.1.1.1 (a).

(b) Neutron irradiation

About 50-300 mg tellurium dioxide powder was weighed, transferred into 1S aluminum irradiation container and subsequently the container was sealed by cold welding. The container was irradiated in the Dhruva reactor at a neutron flux of $\sim 4 \times 10^{13} \text{ n cm}^{-2} \text{ s}^{-1}$. After irradiation the container was kept in a lead shielded flask and transported into radiochemical processing laboratory.

(c) Separation of ^{131}I from irradiated tellurium dioxide

To measure total ^{131}I into irradiated tellurium dioxide, few milligram of it was taken out before the distillation, dissolved in conc. NaOH, adequately diluted and γ -ray spectrum were recorded. Subsequently, the irradiated target material was transferred to a quartz boat which was introduced at the center of quartz tube into the furnace as shown in Fig. 2A.1. Furnace temperature was increased to 740-750 °C. The experimental set up and the distillation process remains same as described in the section 2A.1.1.1 (c). After distillation and cooling of the furnace, few milligrams tellurium dioxide remnants was dissolved in conc. NaOH solution, adequately diluted. A small amount of active ^{131}I trapped solution was also adequately diluted and both were counted by using a pre-calibrated HPGe-MCA for ^{131}I .

Another set of similar experiments were carried out to study tellurium carryover in the final product. For this 100 g inactive TeO_2 which was equivalent to $\sim 20 \text{ Ci}$ of ^{131}I batch size was taken for experiment. It was transferred to the quartz boat and subsequently heated to 740-

750 °C using the similar trapping solutions, parameters and conditions as mentioned above (2A.1.1.1(c)). Radionuclide identification and purity was checked as described in 2A.1.1.1(d). Radiochemical purity of ^{131}I was checked in the trapped solution (as described in 2A.1.1.1(e)). Final ^{131}I trap solution was taken out and tested for tellurium carryover into it (as described in 2A.1.1.1(f)).

2A.1.2.2 Results of the experiment and discussion

Gamma ray spectra of irradiated tellurium dioxide before and after distillation of ^{131}I were illustrated in Fig. 2A.6 and Fig. 2A.7, respectively while γ -ray spectrum of distilled ^{131}I was shown in Fig. 2A.8. There was no extraneous gamma emitting radionuclide was present in the active samples apart from ^{131}I . The amount of ^{131}I distillation from irradiated TeO_2 was found to be $98.7 \pm 1.1 \%$. Radionuclidic purity and radiochemical purity was found to be $> 99.9 \%$ and $98.8 \pm 0.9 \%$, respectively (Fig. 2A.8 and 2A.9). Tellurium content in the ^{131}I trapping solution was tested by spot test method and was found to be $< 5\mu\text{g mL}^{-1}$ (when only 50-300 mg TeO_2 was handled). Tellurium content in the trap solutions of batch size distillation of inactive TeO_2 shows tellurium content $20\text{-}40\mu\text{g mL}^{-1}$ (experimental TeO_2 was 100 g) while the limit is $< 5\mu\text{g mL}^{-1}$ of active ^{131}I solution. Hence it was concluded that tellurium carryover was quite high when high amount of tellurium dioxide (100 g) was handled. Te carryover was unacceptable as it was a chemical impurity as well as it may add radionuclidic impurity in the product ^{131}I . In this case Te carryover in the final product could be minimized by using tellurium trap in between the distillation unit and ^{131}I traps.

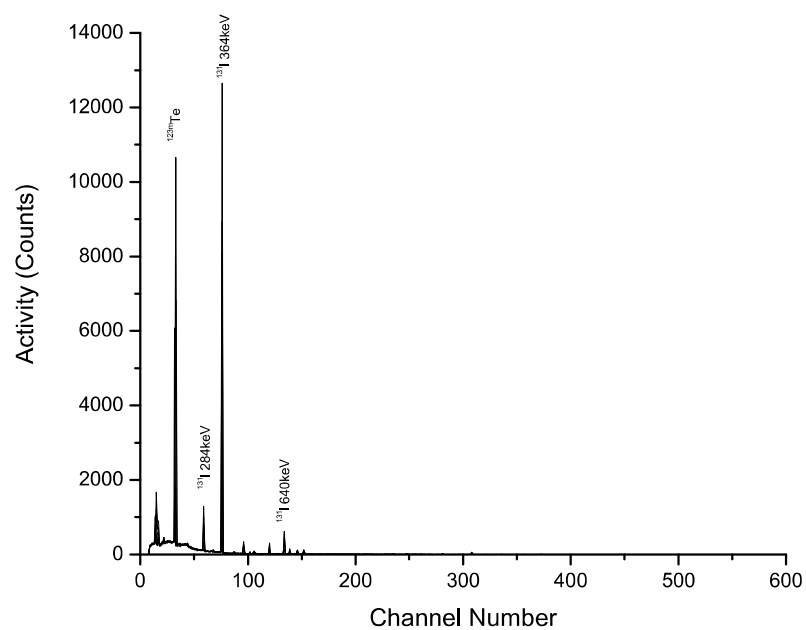


Fig. 2A.6: Gamma ray spectrum of irradiated tellurium dioxide before experiment

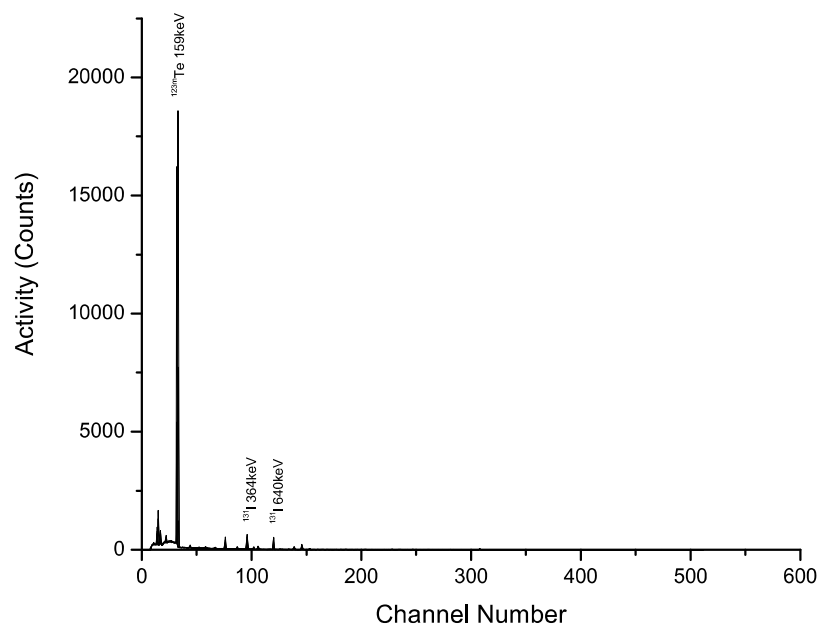


Fig. 2A.7: Gamma ray spectrum of irradiated tellurium dioxide after distillation

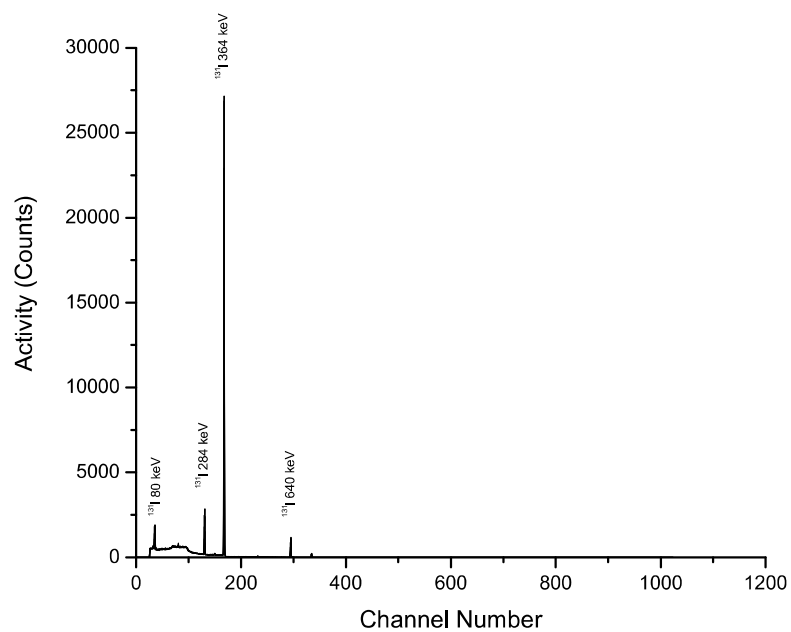


Fig. 2A.8: Gamma ray spectrum of ^{131}I trapped

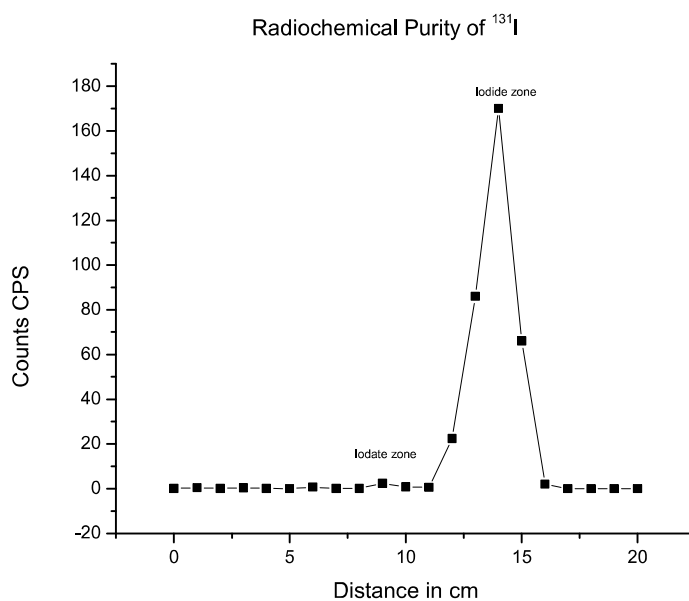


Fig. 2A.9: Paper chromatographic pattern of ^{131}I produced using TeO_2 as target

2A.1.3 Conclusion

Based on the experiments on feasibility of distillation of ^{131}I from irradiated metallic tellurium and tellurium dioxide powder, it was concluded that metallic tellurium was not suitable because it blows-up upon heating to melting temperature and both the ends of quartz tube becomes black (due to deposition of Te carryover on the inner surface of the quartz tube) in each batch. While in case of tellurium dioxide which has an advantage of stability at higher temperature, both the ends of quartz tube was clear and no blackening was observed in it. It was observed that very delicate and fragile glasswares were very difficult to handle in the horizontal furnace. Hence, glassware and experimental set-up modification needs to be done in future to handle higher amount of ^{131}I activity.

Based on these feasibility studies, it was finally concluded that tellurium dioxide would be used as the target material for the development of dry distillation technology for large-scale production of ^{131}I . In all the experiments carried out further, tellurium dioxide powder was used as the target material.

2A.2. Design and development of quartzwares, glasswares and furnace

In order to develop an indigenous technology for large scale production and radiochemical processing of ^{131}I , the required glasswares, quartzwares and furnace were designed, developed and fabricated in house after thorough investigation and experimentation. Keeping in mind that the entire chemical operation needed to be carried out remotely inside the lead shielded glove box facility glasswares were designed accordingly.

2A.2.1 Quartz crucible

The quartz crucible was designed in such a way that the irradiated TeO_2 powder could be added to quartz crucible using a funnel which later on could be transferred to the furnace

vertically inside the distillation flask for distillation. It prevents the spillage of irradiated target and confines it in a safe manner while facilitating the release of distilled ^{131}I through opening at the top. In order to reduce radiation dose level in the distillation flask and from waste management point of view, neutron irradiated TeO_2 was collected in a ~ 425 mL quartz crucible. After distillation, the un-distilled ^{131}I and other nonvolatile long lived radioactive impurities remained within the quartz crucible which was removed, stored underneath the cell for radioactive decay and then processed as radioactive solid waste. Such an arrangement not only offered the scope of reducing the radiation dose inside the processing facility but also simplified the radioactive waste management process. Schematic diagram of the quartz crucible is depicted in Fig. 2A.10. In order to protect the distillation flask from the glassification action of molten tellurium dioxide, irradiated TeO_2 were collected in a quartz crucible.

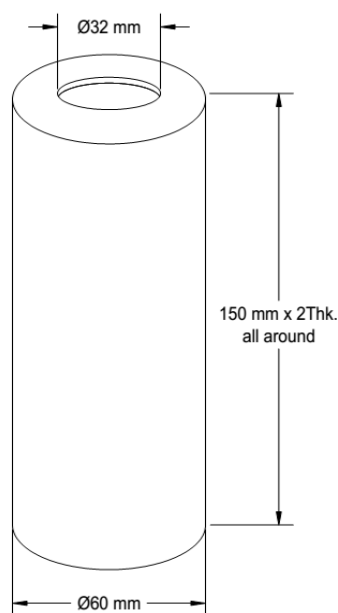


Fig. 2A.10: Schematic diagram of quartz crucible

2A.2.2 Distillation flask

A custom made distillation flask was designed and fabricated for the dry distillation of ^{131}I from irradiated TeO_2 powder. The distillation flask used in this investigation was made of quartz (outer diameter = 70 mm; height = 160 mm). A schematic diagram of the quartz distillation apparatus is shown in Fig. 2A.11. The distillation flask consists of a quartz container, gasket and lid. It has a circumferential flange opening having a seat for receiving the gasket. The lid has a circumferential wall configured to surround the circumferential flange and rests on the container along an engagement mechanism such that the gasket was compressed inwards by the circumferential wall of the lid to enable airtight locking by means of a flange. The lid can be removed when needed. It has an opening at the bottom portion to purge carrier gas through it and outlet opening near the flange at the top. The ends of the quartz tubes are composed of ground joints for leak-tight fitting with other quartz wares. The outlet can be connected to the coil trap.

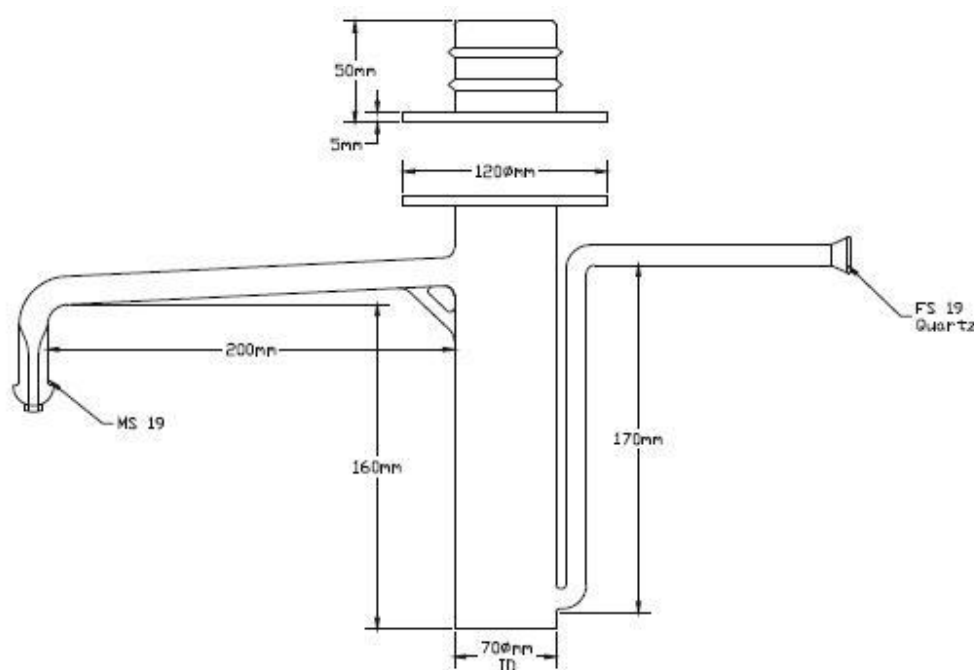


Fig. 2A.11: Schematic diagram of ^{131}I distillation flask

2A.2.3 Design and demonstration of glass coil as Tellurium trap

Feasibility study of using TeO_2 (2A.1.2.2) showed that, batch size utilization of 100 g of TeO_2 for distillation resulted in tellurium carryover in ^{131}I traps. It necessitates effectively trapping of tellurium before the ^{131}I trap to get tellurium free ^{131}I . Hence it should be located just before ^{131}I trap.

Tellurium trap was essentially a coil condenser and consists of a glass spiral coil (Fig. 2A.12) running along the length of the trap. Radioiodine (^{131}I) from the outlet of the distillation flask containing traces of TeO_2 was allowed to flow through a given size orifice of the coiled tube in which TeO_2 got trapped. The coiled tube provides additional surface area as well as path length for efficient trapping of TeO_2 .

The chemical form of ^{131}I , which distills from irradiated TeO_2 , in Te matrix was not known while it was trapped in reducing environment. ^{131}I gets reduced to I^- form in a Na_2SO_3 solution. To solve the problem of Te carryover in ^{131}I trap, various traps were tried. The glass coil trap, designed for the present work with an aim to increase path length for ^{131}I carryover so that the surface area for Te trapping becomes more.

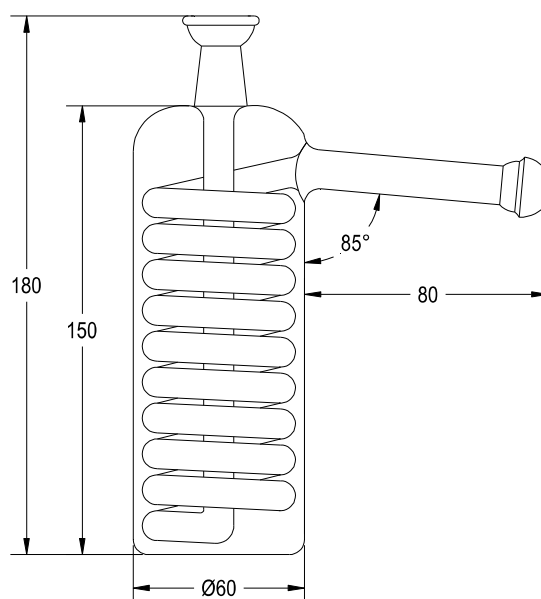


Fig. 2A.12: Schematic diagram of tellurium trap (dimensions in mm)

2A.2.4 Iodine traps

Two vertical traps, made up of corning glass [Fig. 2A.13 (a), (b) and (c)] connected in series were designed in order to trap ^{131}I efficiently. It contained the ^{131}I trapping solution (8-20 mL solution of 0.1 M NaOH containing $0.2 \text{ mg mL}^{-1} \text{ Na}_2\text{SO}_3$) and has a provision to remove the solution by applying suction trap to the adjacent side at temporary storage of ^{131}I . Visual observation of carrier gas bubbling through the trapping solution in the traps was possible.

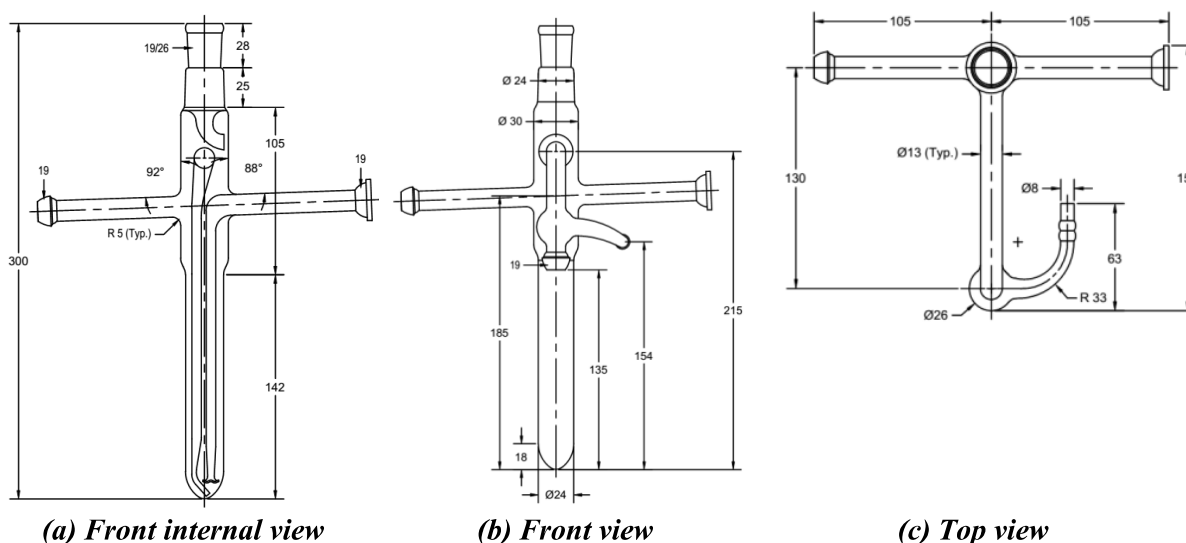


Fig. 2A.13: Schematic diagram of ^{131}I traps (dimensions in mm)

2A.2.5 Resistance furnace (vertical type)

A special resistance furnace is designed to heat the designed quartzware so as to distill ^{131}I from irradiated TeO_2 as shown in the Fig. 2A.14. It contains a proportional-integral-derivative (PID) based temperature controller with single set point, digital indicators, control panel with solid state relay and has control accuracy of $\pm 3^\circ\text{C}$. Control panel is placed at 6 meter away from the furnace in such a way that it needed to handle remotely inside the glove box. Vertical resistance type furnace sealed at bottom with muffle inner lining of 95 mm (ID), 100 mm (H) and 250 mm (OD) has detachable thermocouple at the base of furnace. The furnace is designed for maximum temperature capacity of 1000°C and operating at 740°C .

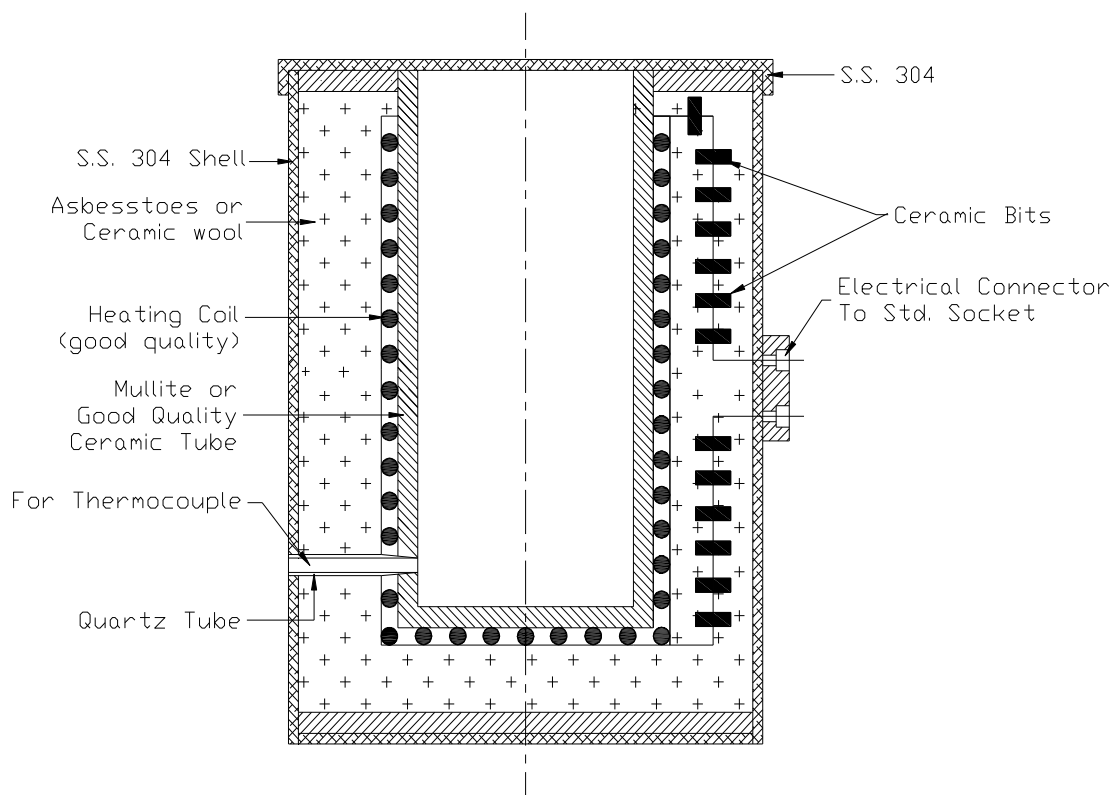


Fig. 2A.14: Schematic diagram of resistance furnace

2A.2.6 Complete processing set-up

Combining the indigenously designed and fabricated units as described in the previous sections, the complete distillation assembly was made as shown schematically in Fig. 2A.15. In this set-up the distillation flask containing quartz crucible which holds the irradiated target goes into the furnace. The side arm of the distillation flask was connected to tellurium coil trap and was maintained at 100 °C along with coil trap. These are subsequently connected to ^{131}I traps. A silver impregnated charcoal trap was connected to the outlet of ^{131}I trap.

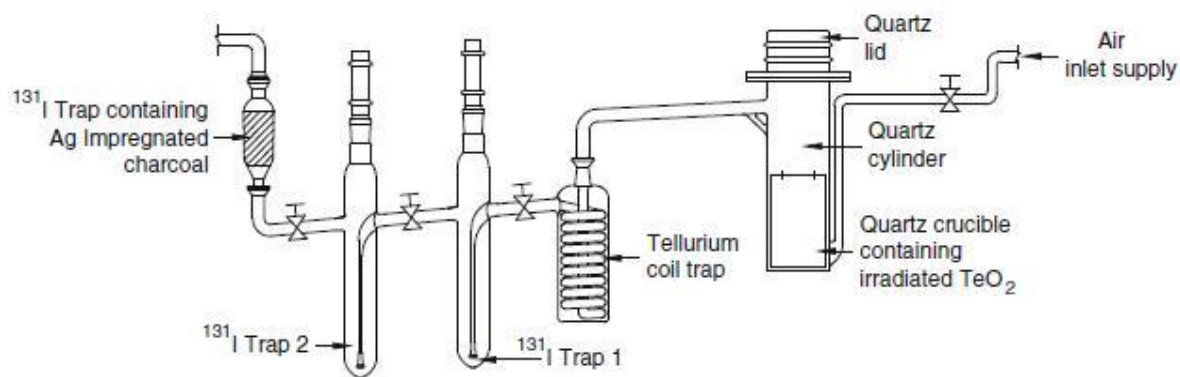


Fig. 2A.15: Distillation assembly for ^{131}I dry distillation

2A.3 Optimization of parameters for ^{131}I processing at pilot scale for separation of ^{131}I from the neutron irradiated TeO_2

2A.3.1 Materials and methods for process optimization

A resistance furnace was used for heating the irradiated target material during processing. Radioactivity assay was carried out by measuring the ionization current obtained when an aliquot of the batch was placed inside a pre-calibrated well-type ion-chamber. All other chemicals and equipments used in the studies were same as specified in the section 2A.1.2.1 (a).

2A.3.1.1 Target specifications

Tellurium dioxide powder of either natural isotopic composition or enriched in ^{130}Te could be used for production of ^{131}I through $^{130}\text{Te} (n,\gamma) ^{131}\text{Te} \xrightarrow{\beta^-} ^{131}\text{I}$ route. The natural isotopic composition of Te and the thermal neutron capture cross-sections are shown in Table 2A.1. Since, natural Te contains 33.8 % of ^{130}Te and ^{131}I is radiochemically isolated, use of Te target enriched in ^{130}Te would not enhance the specific activity of ^{131}I to any significant extent. Further radionuclidic purity > 99.9 %. Hence, TeO_2 target of natural isotopic composition was selected as the target for providing ^{131}I at an affordable cost.

Table 2A.1: Isotopic abundance of natural tellurium and corresponding cross section of (n,γ) reactions.

Tellurium isotope	% Abundance	Nuclear reaction	Thermal neutron cross-sections (σ) in barn(b)
^{120}Te	0.09	$^{120}\text{Te}(n,\gamma)^{121}\text{Te}$	2.00
		$^{120}\text{Te}(n,\gamma)^{121\text{m}}\text{Te}$	0.34
^{122}Te	2.46	$^{122}\text{Te}(n,\gamma)^{123\text{m}}\text{Te}$	1.10
^{124}Te	4.61	$^{124}\text{Te}(n,\gamma)^{125\text{m}}\text{Te}$	0.04
^{126}Te	18.71	$^{126}\text{Te}(n,\gamma)^{127}\text{Te}$	0.90
		$^{126}\text{Te}(n,\gamma)^{127\text{m}}\text{Te}$	0.135
^{128}Te	31.7	$^{128}\text{Te}(n,\gamma)^{129}\text{Te}$	0.14
		$^{128}\text{Te}(n,\gamma)^{129\text{m}}\text{Te}$	0.015
^{130}Te	33.8	$^{130}\text{Te}(n,\gamma)^{131}\text{Te}$	0.20
		$^{130}\text{Te}(n,\gamma)^{131\text{m}}\text{Te}$	0.04

Selection of an appropriate target for the reactor production of ^{131}I represents not only the first step but also the cornerstone for its success. With a view to select an appropriate target for the reactor production of ^{131}I , it was essential to examine the prospect of using natural tellurium target as it represents the least expensive target to produce ^{131}I .

Other isotopes produced either directly or resulting from the decay of activated radionuclides after the neutron irradiation of natural tellurium was shown in Table 2A.2.

The production of ^{121}Sb (stable), ^{123}Te (stable), and ^{125}Te (stable) during neutron irradiation is not a major problem as these isotopes will neither reduce the specific activity of ^{131}I , nor get distilled during the separation of ^{131}I . The presence of ^{126}Te in 18.71 % and ^{128}Te in 31.7 %

abundances in natural tellurium leads to the concomitant production of ^{127}I (stable) and ^{129}I , respectively as described in the Table 2A.2. The sequence of activation reactions and decay mode is depicted in Fig. 2A.16. ^{127}I is inactive whereas ^{129}I is long-lived with a half-life of 1.7×10^7 years. The amount of ^{129}I activity formed was very low due to its long half-life. However, the presence ^{127}I decreases the specific activity of ^{131}I . The specific activity of ^{131}I obtained using natural tellurium was adequate for meeting clinical requirements.

Table 2A.2: Other isotopes produced during the neutron irradiation of natural tellurium

Tellurium isotope in target	% Abundance	Isotope produced	Half-life ($T_{1/2}$)	Disintegration products
^{120}Te	0.09	^{121}Te	16.8 days	$^{121}\text{Te} \rightarrow ^{121}\text{Sb}$ (stable)
		$^{121\text{m}}\text{Te}$	154 days	
^{122}Te	2.46	$^{123\text{m}}\text{Te}$	119.7 days	^{123}Te (stable)
^{124}Te	4.61	$^{125\text{m}}\text{Te}$	57.4 days	^{125}Te (stable)
^{126}Te	18.71	^{127}Te	9.35 h	$^{127}\text{Te} \rightarrow ^{127}\text{I}$ (stable)
		$^{127\text{m}}\text{Te}$	109 days	
^{128}Te	31.7	^{129}Te	69.6 min.	$^{129}\text{Te} \rightarrow ^{129}\text{I}$ (1.7×10^7 Y)
		$^{129\text{m}}\text{Te}$	33.6 days	

2A.3.1.2 Neutron irradiation

20 g Tellurium dioxide placed in a 1S aluminum container was encapsulated and irradiated in the Dhruva reactor at a neutron flux of $\sim 5 \times 10^{13} \text{ n cm}^{-2} \text{ s}^{-1}$ for different time period of irradiation. After irradiation, the container were kept in a lead-shielded flask and transported into radiochemical processing laboratory.

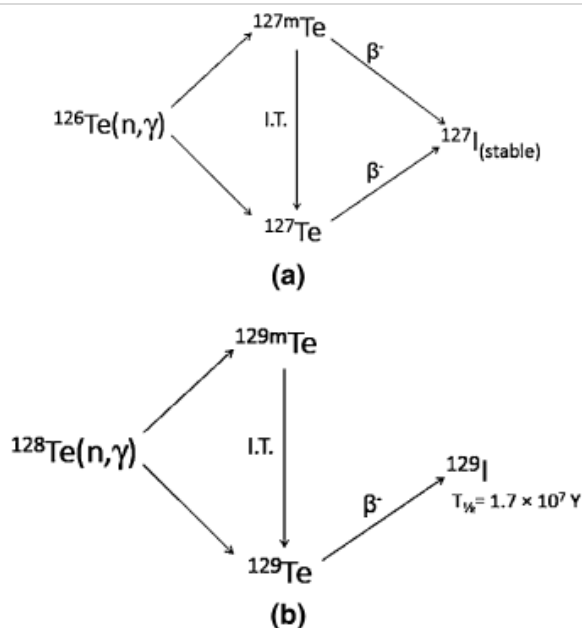


Fig. 2A.16: Activation reactions and decay mode of (a) ^{126}Te and (b) ^{128}Te formed during neutron irradiation of natural tellurium

2A.3.1.3 Neutron irradiation conditions

Among the main factors contributing to the production of ^{131}I in a nuclear reactor, the irradiation time and neutron flux are the ones. In order to produce ^{131}I of acceptable specific activity and required quantity, judicious optimization of irradiation parameters was viewed as a necessity and pursued.

The ^{131}I activity produced at the end of neutron irradiation (EOI) of TeO_2 as a function of irradiation time at different thermal neutron fluxes has been calculated and the results are shown in Fig. 2A.17. It was evident from the figure that higher the thermal neutron flux, the shorter will be the irradiation period required for attaining the desired activity. The available thermal neutron flux in the Dhruva reactor of our institute for irradiation of TeO_2 target was $\sim 5 \times 10^{13} \text{ n cm}^{-2} \text{ s}^{-1}$.

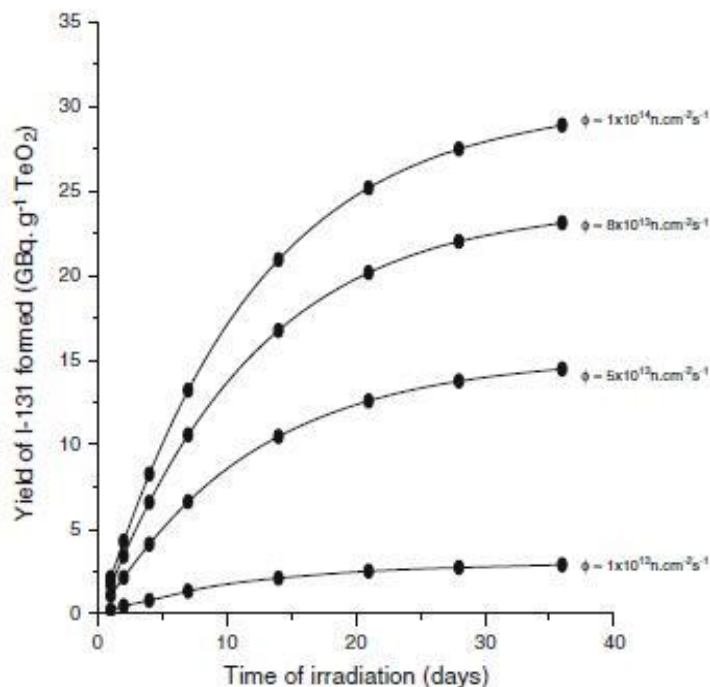


Fig. 2A.17: Calculated production yields of ^{131}I at EOI by neutron irradiation of 1 g TeO $_2$ target as a function of irradiation time at various thermal neutron flux values

The typical calculated yields of ^{131}I from 1 g natural TeO $_2$ for different durations of irradiation in the Dhruva reactor at a neutron flux of $\sim 5 \times 10^{13} \text{ n cm}^{-2} \text{ s}^{-1}$ is shown in Fig. 2A.18. As expected, the production of ^{131}I activity increases with increasing irradiation time and attains almost saturation after 30 days ($\sim 4T_{1/2}$). While ^{131}I production was carried out in research reactors, no reactor is solely dedicated to radioisotope production. Therefore, continuous irradiation of the target in the reactor was plausibly a challenging task. As the ‘Dhruva’ reactor of our institution is a multi-purpose research reactor, numbers of planned closures due to regular maintenance or for other programs, are likely to be expected during operational cycle of 4 weeks. Taking into account the planned closures of ‘Dhruva’ reactor, an irradiation period of 21 days was selected as the duration of irradiation.

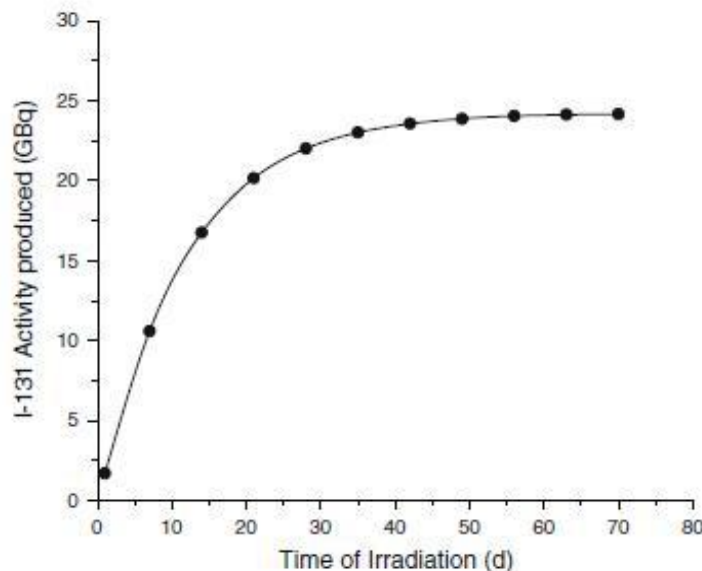


Fig. 2A.18: ^{131}I activity produced as a function of the irradiation time

2A.3.1.4 Cooling period

As ^{131}Te decays more rapidly than the ^{131}I activity, complete decay of ^{131}Te to ^{131}I can be achieved through the effective use of cooling time. The relative activity decay of ^{131}Te and ^{131}I as a function of the cooling time is shown in Fig. 2A.19. The amount of $^{131\text{m}}\text{Te}$ in the irradiated target was significantly less than ^{131}Te although it decays at a much lower rate compared to ^{131}Te . Overall, it was evident from the result that in order to achieve an optimum yield of ^{131}I at the time of processing, a post irradiation cooling of irradiated target for ~2 days was required. In this method, ^{131}I can be produced from ^{130}Te via two nuclear reactions: $^{130}\text{Te} (n,\gamma) ^{131}\text{Te}$ ($T_{1/2} = 25$ min) and $^{130}\text{Te} (n,\gamma) ^{131\text{m}}\text{Te}$ ($T_{1/2} = 30$ h) with thermal-neutron cross sections of 0.2 and 0.04 b, respectively, from three decay branches as per the details illustrated in Fig. 2A.20.

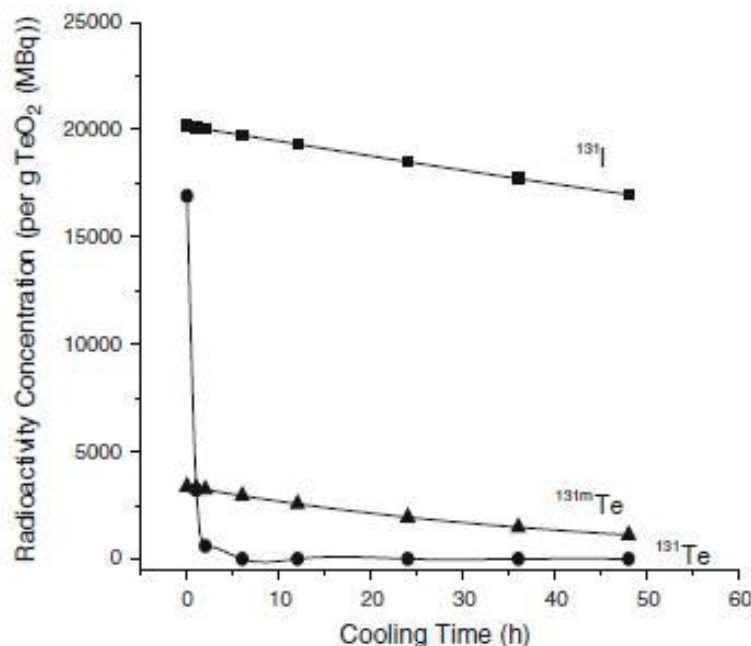


Fig. 2A.19: Radioactivity concentration of ^{131}I , $^{131\text{m}}\text{Te}$ and ^{131}Te per g of TeO_2 as a function of cooling time from EOI

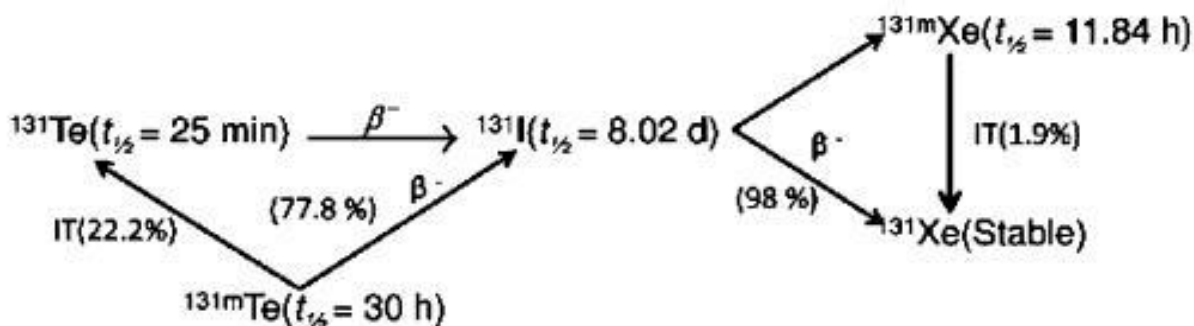


Fig. 2A.20: Decay scheme of neutron irradiated ^{130}Te for production of ^{131}I

2A.3.2 Separation of ^{131}I from neutron irradiated TeO_2

2A.3.2.1 Optimization of distillation parameters

Aluminum containers containing irradiated TeO_2 cut opened and TeO_2 was transferred to distillation flask kept inside the resistance furnace. Flange lid of the distillation flask was closed leak tight. ^{131}I trapping solutions 20 mL (solution of 0.1 M NaOH containing 0.2 mg

mL⁻¹ Na₂SO₃) were added to trap 1 and 2. Before starting the furnace heating, distillation system connected to the inflow of carrier gas (Argon) which was used for the study with the flow rate of 20-30 mL min⁻¹. Temperature was allowed to reach to 750 °C and ¹³¹I distillation was studied.

In order to perform the separation of ¹³¹I from the TeO₂ target, a distillation set up was designed and fabricated to suit operational requirements as described in Section 2A.2.6 (Fig. 2A.15). The design was based on the containment of ¹³¹I gas, compatibility with molten tellurium dioxide, handling conditions, and economic indices. The capacity of the flask was suitable to handle 500 g of irradiated target (in order to scale up ¹³¹I production). The designed distillation assembly was found to be simple, safe and amenable for remote-control operation. One of the enduring attempts to increase the collection efficiency of ¹³¹I vapor was the use of a carrier gas stream as it helps in sweeping the ¹³¹I vapor released from the irradiated tellurium dioxide. Use of carrier gas is also attractive owing to its ability to discourage the condensation of ¹³¹I vapor in the connecting tube. The action of the carrier gas stream was studied using different gas such as nitrogen, argon, oxygen and air with the distillation system and procedures described above. In our studies argon gas was selected as a carrier gas for further studies.

2A.3.2.2 Effect of temperature

20 g tellurium dioxide placed in an aluminum container, was encapsulated and irradiated in the Dhruva reactor at a neutron flux of $\sim 5 \times 10^{13}$ n cm⁻² s⁻¹ for 28 days. Irradiation container was cut opened and irradiated TeO₂ was transferred to quartz crucible. It was then transferred to distillation flask inside the furnace. Flange lid was closed and the system checked for leak-tightness. Trapping solutions added into each ¹³¹I trap. Distilled ¹³¹I activity was carried away

to the trap solution by a flow of argon gas (with flow rate of 20-30 mL min⁻¹). ¹³¹I trapped in the trap solution was measured using pre-calibrated ion chamber.

To determine the effect of distillation temperature, several experiments were carried out by increasing the distillation temperature from 200 °C to 850 °C. In each case distillation was carried out for 3 h. The influence of distillation temperature on the removal of ¹³¹I vapor from the irradiated TeO₂ was investigated and the result is depicted in Fig. 2A.21. It was observed from the result that, distillation temperatures below 500 °C were ineffective for releasing ¹³¹I vapor from the neutron irradiated TeO₂. The iodine release starts when the distillation temperature reaches to 600 °C and at temperature > 700 °C, ¹³¹I release was more efficient. When the temperature reaches to 740 °C, the activity of ¹³¹I released became constant and further rise in temperature did not show any appreciable increase ¹³¹I release. From the aforementioned results, the recommended working distillation temperature for the optimum recovery of ¹³¹I from neutron irradiated TeO₂ target was deduced to be 740 °C.

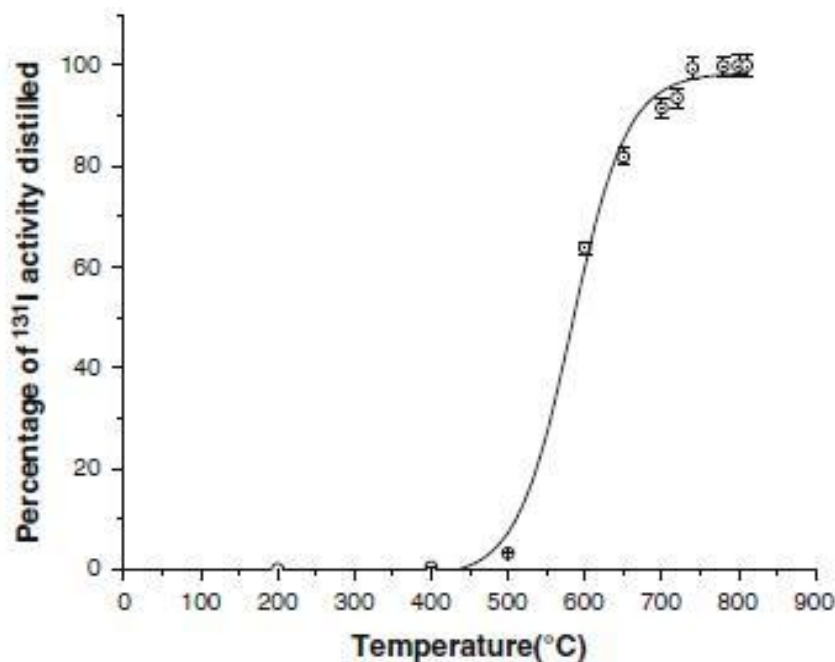


Fig. 2A.21: Effect of distillation temperature on the yield ¹³¹I

2A.3.2.3 Rate of distillation

After optimization of distillation temperature, the time required for the quantitative release of ^{131}I from neutron irradiated TeO_2 was the other critical parameter. In order to optimize the distillation time, distillation experiments were carried out using irradiated TeO_2 target (as described in the previous section) and ^{131}I activity in the trap solution was measured at regular intervals of 10 min. starting from 10 min. to 150 min. Distillation was carried out at optimized temperature of 740°C .

The fractional yields of ^{131}I at different time were determined and the result is shown in Fig. 2A.22. Our analysis of result revealed a progressive increase in yields of ^{131}I . As inferred from the curves, a distillation period of 90 min. was required to attain optimum ^{131}I production yields. While longer heating periods have no adverse effect upon the ^{131}I production yield, no beneficial results were obtained thereby.

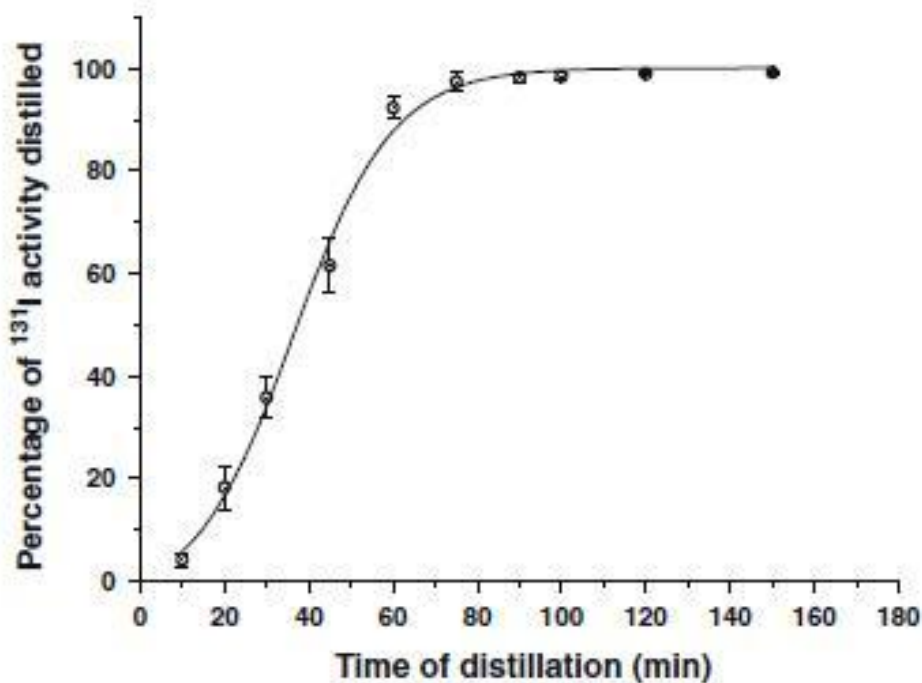


Fig. 2A.22: Rate of distillation of ^{131}I

2A.3.2.4 Purification of ^{131}I from traces of TeO_2

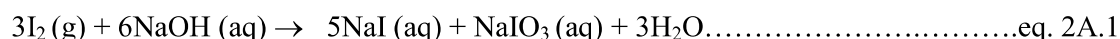
In order to restrict the Te carryover in product ^{131}I , tellurium coil trap was used and the other experimental parameters were same as described in earlier sections. Tellurium content in each trap was tested as per the procedure illustrated in 2A.1.1.1. (f).

While the use of argon as the carrier gas at temperatures above the melting point of tellurium dioxide (735 °C) was an effective strategy to achieve near quantitative release of ^{131}I vapor from the neutron irradiated target, the concomitant sublimation of TeO_2 was a major impediment that needs to be addressed suitably. The presence of trace amount of TeO_2 in the distilled ^{131}I vapor constitutes a chemical impurity that limits its utility in nuclear medicine procedures. In this context, the prospect of adopting physical separation strategies seemed reasonable as it not only precludes the inadvertent introduction of extraneous chemical impurities but also minimize the generation of radioactive, chemical, or mixed wastes. In the quest for an innovative approach away from the existing paradigm, the scope of circulating the ^{131}I vapor containing trace amount of TeO_2 in circular coiled tubing maintained at a temperature below the sublimation temperature of TeO_2 and above the volatilization temperature of elemental iodine seemed to be a trustworthy option. This concept has been simplified in our work and led to the development of specially designed circular coil glass tubing positioned between distillation assembly and $^{131}\text{I}_2$ trap through which ^{131}I vapor containing trace amount of TeO_2 was allowed to circulate. This in flow action causes TeO_2 to make numerous collisions with the interior surface of the tubing, gets deposited and offers a viable mean of getting separated from the $^{131}\text{I}_2$ vapor stream. The scope of using circular coil glass tubing seemed attractive as it increases the path length and at the same time maintained compactness. While the temperature of the circular coil glass tubing was conducive for trapping the TeO_2 carryover satisfactorily, it was sufficiently high to retain ^{131}I in volatilized state. In an attempt to preclude the premature condensation of the distilled $^{131}\text{I}_2$ in the glass

coil trap and for ensuring efficient ^{131}I vapor transport, this region was heated to 100 °C with the help of a resistance furnace. Our present study has demonstrated that by a judicious circulation of the distilled ^{131}I vapor through circular coil glass tubing would render it free from TeO_2 . In the present study, the same TeO_2 trap has been repeatedly used for retaining TeO_2 generated during the distillation, up to 20 batches without disconnecting it from the main distillation assembly.

2A.3.2.5 Trapping of ^{131}I

With a view to utilize the ^{131}I solution for formulation of ^{131}I -labeled radiopharmaceuticals using proteins and other macromolecules, it was required to be concentrated in a very small volume. Although a variety of bases have been found to be suitable for trapping $^{131}\text{I}_2$, sodium hydroxide is preferred. The exact chemical form of the radioiodine released from the TeO_2 target is not known. One postulate is that oxides of iodine are formed, while other stipulates the occurrence of free radicals [53]. Within all the unknowns and uncertainties related to the chemical form of the radioiodine released from the TeO_2 target, the scope of using sodium hydroxide was found to be productive in trapping ^{131}I . Iodine-131 get trapped in sodium hydroxide according to the reaction



In order to facilitate the reduction of iodate ion, IO_3^- to I^- , it is essential to add either thiosulphate ($\text{S}_2\text{O}_3^{2-}$) or sulfite (SO_3^{2-}), according to the following equations:



In view of perceived need to obtain ^{131}I as NaI , addition of either $\text{Na}_2\text{S}_2\text{O}_3$ or Na_2SO_3 to NaOH solution constitutes a necessity. When it is employed, the resulting iodine is obtained in the form of sodium iodide and hence suitable for medical use. In the present investigation, Na_2SO_3 was used.

Iodine-131 carried by the flow of carrier gas was allowed to pass through two traps containing a solution of 20 mL 0.1 M NaOH containing 0.2 mg mL^{-1} Na_2SO_3 connected in series. The distilled volatile iodine ($^{131}\text{I}_2$) reacts with sodium sulphite and sodium hydroxide solution in the trap solution. To enhance the ^{131}I trapping, the NaOH trap was maintained at low temperature.

We preferred to use two traps connected serially containing small amount ($< 20 \text{ mL}$) of 0.01 M NaOH solution to collect the ^{131}I species in order to achieve a better control on the radioactive concentration of ^{131}I for subsequent radiolabeling.

Although NaOH and Na_2SO_3 was used in this investigation for trapping $^{131}\text{I}_2$ vapor, other bases such as sodium carbonate, potassium hydroxide, ammonium hydroxide, calcium hydroxide can also be employed if the radioactive iodine is intended for other than medical uses.

2A.4 Optimized protocol for radiochemical separation of ^{131}I from neutron irradiated TeO_2 target

Based on the experimental results described in the previous sections, the optimized protocol for radiochemical separation of ^{131}I from neutron irradiated TeO_2 target, in the flow chart illustrated in Fig. 2A.23.

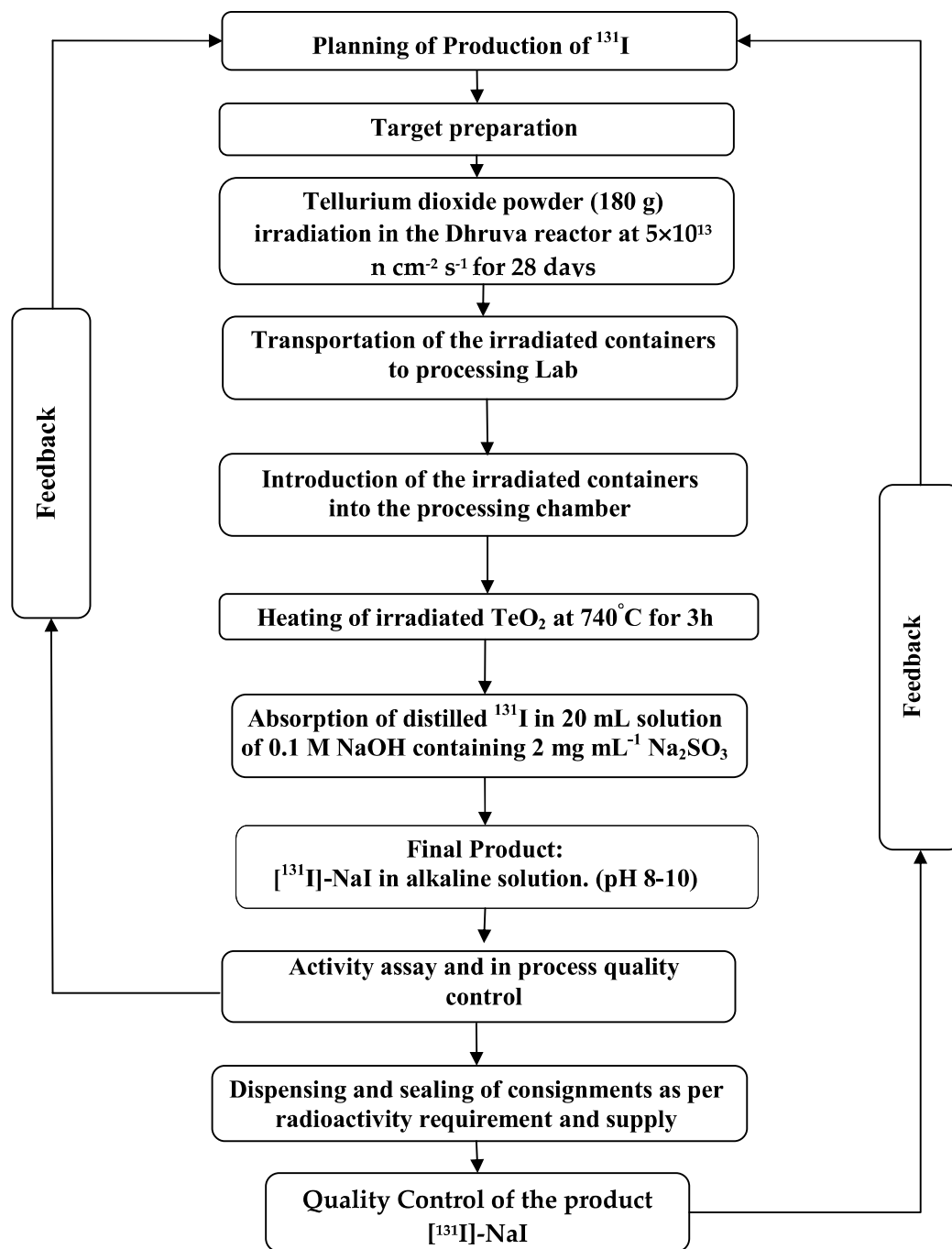


Fig. 2A.23: Flow sheet of protocol for radiochemical processing of ^{131}I

CHAPTER-2B

Large Scale Production, Separation and Purification of Iodine-131 Using Dry Distillation Technique

“One worthwhile task carried to a successful conclusion is worth half-a-hundred half-finished tasks”

Malcolm S. Forbes

This chapter describes the development of facility and detailed procedure for large scale radiochemical processing of ^{131}I inside the lead shielded glove box adhering to radiological safety requirements. Radiochemical separation of ^{131}I upto a level of 1.85 TBq (50 Ci) per batch suitable for use in nuclear medicine procedures has been achieved using the developed procedure. Experience of operating the facility over a period of four years is also illustrated.

2B.1 Materials and equipments

An induction furnace specially designed, was used for heating the irradiated target material during processing. In order to reduce the radiation exposure and perform the operation in a remotely operated shielded facility, special operation specific process apparatus were designed and fabricated in house. All other chemicals and equipments used in the studies were same as specified in the section 2A.3.1.

2B.2 Neutron irradiation

Tellurium dioxide 20 g in a 1S aluminum container was encapsulated and in total 9 containers ($9 \times 20 \text{ g TeO}_2$) were irradiated in the Dhruva reactor at a neutron flux of $\sim 5 \times 10^{13} \text{ n cm}^{-2} \text{ s}^{-1}$ for 21 days. After irradiation of TeO_2 , the container were kept in a 7 inch thick lead shielded flask and transported into radiochemical processing laboratory.

2B.3 Facility for large-scale radiochemical separation of ^{131}I

The facility of large-scale radiochemical separation of ^{131}I consists of three numbers of 150 mm lead shielded stainless steel (SS) plants (Plant-I, Plant-II and Plant-III). The plants are divided into two portions. In the upper portion of the plants, all the radiochemical processing is done and in the lower portion where all liquid and solid waste generated during

radiochemical processing are stored temporarily. Photograph of the shielded facility is shown in Fig. 2B.1.

Dimensions of each plant is 1800 mm (L) x 1200 mm (H) x 1000 mm (W) of upper chamber and 1800 mm (L) x 600 mm (H) x 1000 mm (W) of lower chamber having 3 mm wall thickness allover placed on a mild steel (MS) table with adjustable legs. The boxes have perspex panels in front and back with provision for fixing glove port rings to accommodate remote handling tongs and neoprene gloves. The plants are interconnected serially through SS tunnels of dimension 75 cm (L) x 60 cm (W) using suitable gaskets (EPDM, Ethylene Propylene Diene Monomer, 6 mm thick) and fastened with M-6 hexagonal SS nuts and bolts by putting gasket in between the tunnel. The tunnels used for inter cell transfers on both sides have pneumatically operated sliding doors for isolation of plants which can be operated from the switches on the electric panel/ HMI (Human Machine Interface) on the front side of the plants.

Plant II (loading chamber) has transfer port at the backside opening outside. It is provided with pneumatic doors from inside the plants and hand operated door opening to the outside. This port facilitates the transfer of materials, chemicals and reagents from outside to inside of the plant when required during operation. This plant also has circular opening on the floor of the box and is provided with pneumatic door to facilitate loading and unloading of lead casks containing the irradiated target directly into the plant. All the plants are provided with electrical tube light fixture placed on the top perspex panel and with service lines for circulation of water, compressed air, vacuum which can be controlled through the valves and switches mounted on the front panel. The containment boxes are connected to the main laboratory exhaust system through 2 numbers of charcoal filters assemblies mounted outside the plant on top of the boxes. The control panels fixed at overhead are equipped with controls for ion chamber, electric switches etc. Each cell is provided with radiation shielding windows,

remote handling tongs to facilitate remote operation and maintenance of different equipment and systems. Equipment and systems inside the cell were manipulated with remote handling tongs that passed through the front working face. The facility is capable of handling up to 3.7 TBq (100 Ci) of ^{131}I per batch.



Fig. 2B.1: Photographic image of 150 mm lead shielded radiochemical processing plant

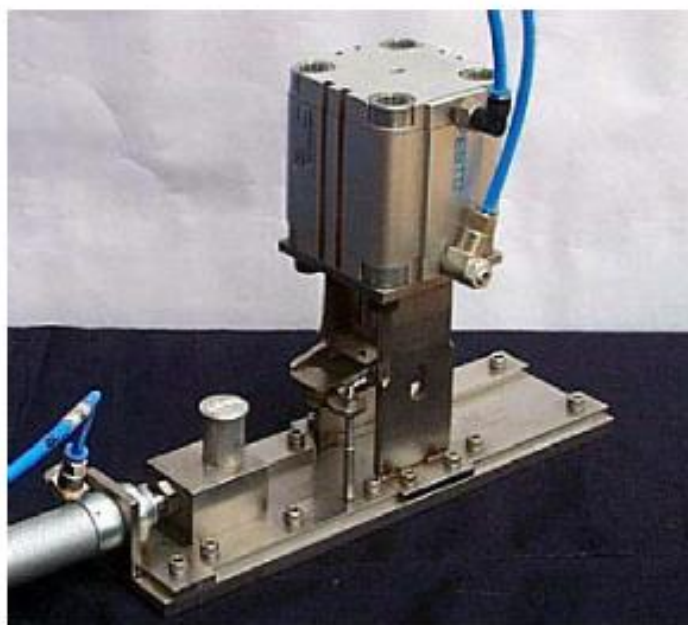
2B.4 Remotely operated custom made gadgets

In order to simplify operation in the remotely operated shielded facility, few non standard equipments, gadgetry and furnace necessary for the processing of irradiated TeO_2 target and separation of ^{131}I were designed, fabricated in-house and used. Details of these custom made devices are given below.

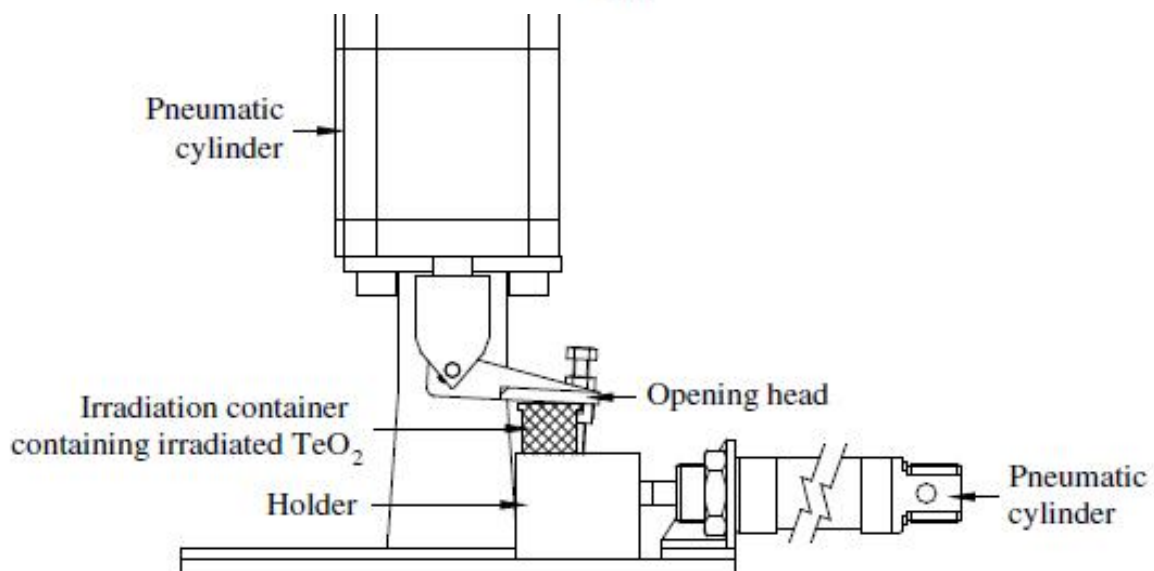
2B.4.1 Irradiation container opening unit

After neutron irradiation, the seal of the irradiation container containing neutron irradiated TeO_2 target was opened with the help of a semi-automatic irradiation container opening unit (Fig. 2B.2) to retrieve the irradiated target for distillation. The irradiation container is inserted in the holder remotely by the tong and pushed towards the tool by a pneumatic cylinder. After

the irradiation container engages with the tool, the valve is brought to the mid position to allow the irradiation container holder to move freely closer to the tool to open. The neutron irradiated TeO_2 target was transferred into a quartz crucible (180 g of TeO_2 /crucible) and the crucible was then kept inside the distillation flask.



(a)



(b)

Fig. 2B.2: Semi-automatic irradiation container opening unit (a) photographic image of actual unit (b) schematic diagram

2B.4.2 Semi-automated crucible holder

The quartz crucible containing irradiated TeO_2 is kept at the loading station with the help of semi-automated crucible gripper and then it is transferred into the distillation flask for further processing. The crucible handling gripper is having 4-fingers to hold the quartz crucible and operates by a pneumatic cylinder (as shown in fig. 2B.3). The fingers are padded with neoprene for soft handling of crucible. The plunger is a long rod, which is normally spring – loaded in the downward direction keeps 4-fingers in open condition. When the solenoid is energized, it pulls the plunger rod up to close the fingers which then to be put inside the quartz crucible and operate the solenoid valve to grip hold the quartz crucible at the opening. A stopper is attached above the gripper, which sits over the flange of the distillation flask during loading and limits the travel of the crucible into the flask and also locates the fingers at the required level for gripping during unloading. The holder positioned manually on quartz crucible containing irradiated TeO_2 and operates the holder from outside. It grips the crucible automatically and moves the holder to the distillation flask manually and de-grips it into the distillation flask inside the furnace.



Fig. 2B.3: Semi-automatic crucible holder (photographic image of actual unit)

2B.4.3 Semi-automated flange lid holder

The distillation flask is closed with flange lid (as shown in Fig. 2B.4). After loading irradiated TeO_2 into quartz crucible, it is transferred to the distillation flask. Then the flange lid with gasket closes the distillation flask with the help of semi-automated flange lid holder leak tight as shown in Fig. 2B.4 before starting the distillation. A semi-automatic device is designed which holds the flange lid and can be operated from outside to close the distillation flask.

The flange lid is held in a SS316 metal casing, which carries 4-jaw gripper for clamping at the bottom and the actuating pneumatic cylinder at the top. This assembly is hanged from the top ceiling of the SS Glove box at specified location using spring balancer. The pneumatic cylinder pushes the 4-jaws down and the jaws expand during their downward movement. The clamps are normally kept in open condition away from the flask. To close and clamp the flask, this flange lid holder is gripped by the remotely operated tong and brought onto the top of the flask. The clamp in the open condition is lowered on the flask. After resting the lid on the flask flange, pneumatic cylinder is actuated. At the end of the stroke, fingers contact the flange of flask and pull it up against the lid on top, causing the gasket to compress and seal. The lid is kept in sealed leak tight position till the completion of distillation of ^{131}I .



Fig. 2B.4: Semi-automated flange lid holder (photographic image of actual unit)

2B.4.4 Inconel Cylinder

During distillation, a metallic cylinder made up inconel-601 (Composition in weight % is Fe: 14 %, Ni: 61 %, Cr: 23 %, Al: 1.4 %, Ti: 0.5 %, C: 0.1 %) in the form of bucket acting as receptor was heated inductively, and the heat energy was transmitted by radiation to the irradiated target. Schematic diagram of the inconel cylinder [63 mm (Φ) \times 80 mm (L) \times 2 mm (t)] is shown in Fig. 2B.5. It is kept inside the distillation flask to hold the quartz crucible inside it.

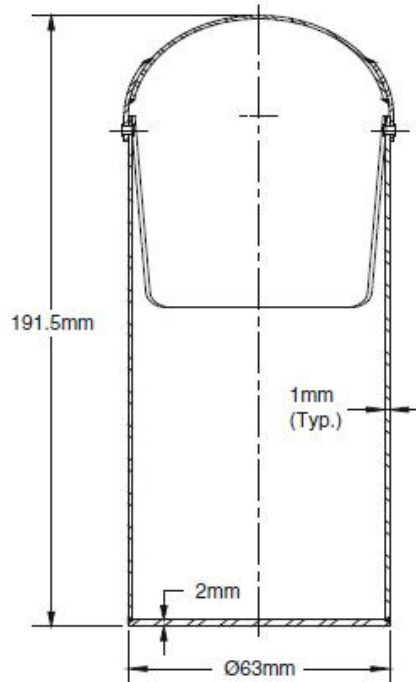


Fig: 2B.5: Schematic diagram of inconel cylinder for induction furnace

2B.4.5 Induction Furnace

A light weight induction furnace suitable for manipulation by remote-handling tongs inside a shielded facility and capable of working up to 1,000 °C was designed and fabricated. A schematic block diagram of the induction heating system is shown in Fig. 2B.6. An inconel cylinder is placed inside the copper coil [88 mm (H) × 109 mm (ID)] known as inductor. The inductor serves as the transformer primary and gets heated. Copper tubes [88 mm (H) × 109 mm (ID)] with uniform internal diameter duly insulated and internally coated with refractory castables forms the inductor coil. The coil is kept inside the lead shielded glove box and the controller unit outside the box. The required temperature of 740 ± 5 °C was achieved within 10 min time. The electromagnetic force (e.m.f.) of a thermoelement placed within the inconel cylinder serves both as a temperature sensor and controller of the generator performance.

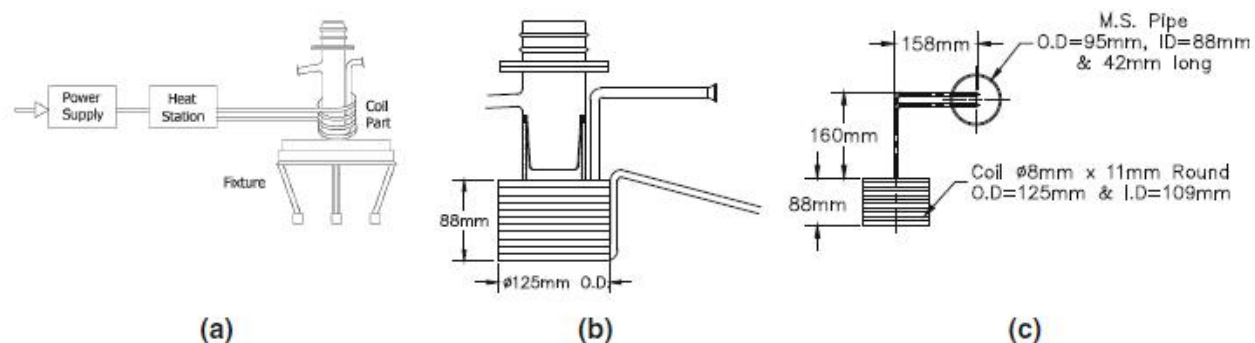


Fig. 2B.6: Induction heating system (a) block diagram; (b) induction coil around the quartz cylinder containing inconel cylinder; (c) side view of induction coil

2B.5 Complete processing set-up

A schematic diagram of the quartzwares, glasswares and gadgets for processing of ^{131}I inside the glove box cell is give in Fig. 2B.7.

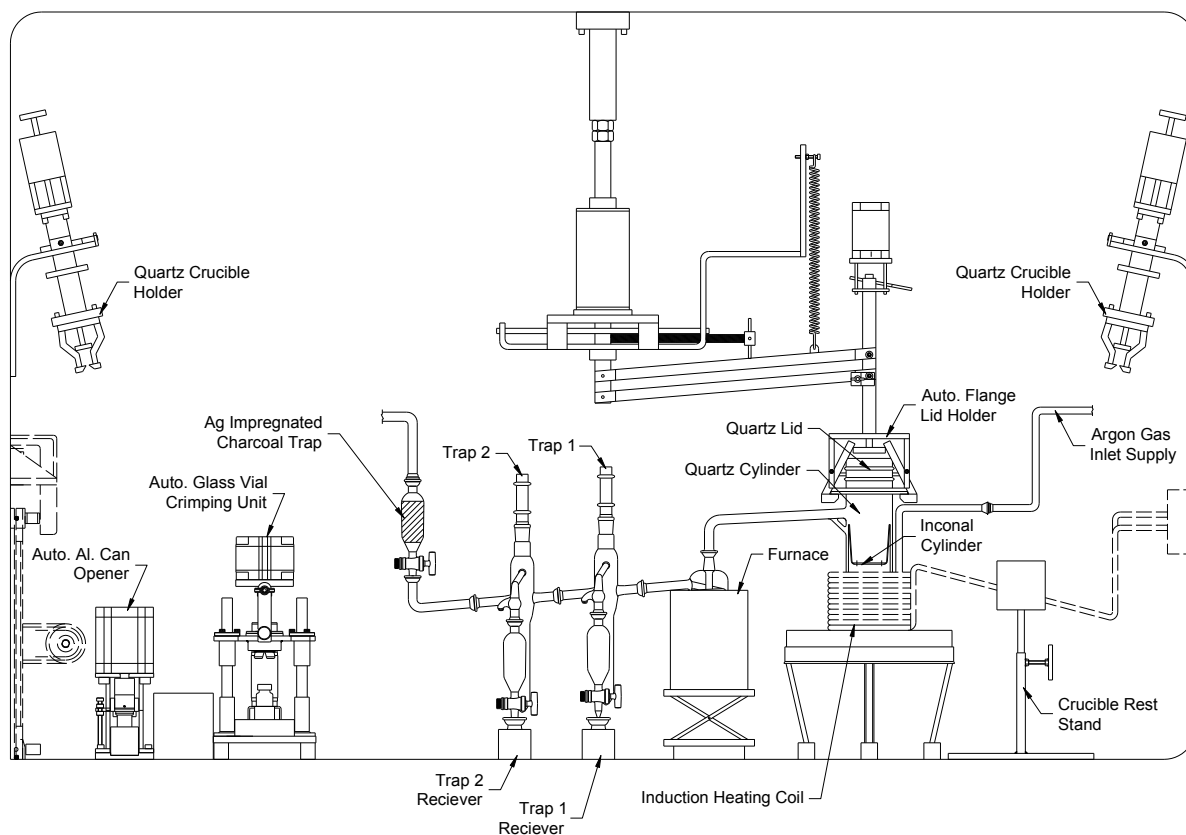


Fig. 2B.7: Schematic of complete dry distillation set-up for regular large-scale production

of ^{131}I

2B.6 Radiochemical separation of ^{131}I by dry distillation method

The quartz crucible containing irradiated tellurium dioxide target was transferred into the distillation flask and the lid was placed back. This provided a firm and tight fitting which ensured a leak-tight seal to the container. One end of the distillation flask was connected to a tellurium trap which contains circular coil glass tubing maintained at 100 °C, the other end being connected to an argon cylinder which supplies Ar gas to the distillation flask. The lid was then pressed from the top in order to reconfirm that the sealing was normal. The argon flow was put on to flow through the distillation flask containing TeO_2 . Flowrate of 20–30 mL min^{-1} was adjusted. The induction furnace was operated in conjunction with an inconel cylinder which acts as a receptor to get heated inductively, and transmit the heat energy to the irradiated target by radiation. The furnace was heated up to a temperature of 740 °C, which was above the melting point of TeO_2 . At this temperature, the neutron irradiated TeO_2 melts and simultaneously releases ^{131}I entrapped in the crystal lattice. The experimental set up used for the separation of ^{131}I from neutron irradiated TeO_2 is schematically presented in Fig. 2B.7. The ^{131}I release from the target was monitored by measuring the ion current measured by an ion chamber kept close to trap 1 (of ^{131}I). In order to obtain optimum ^{131}I separation yields (~90 %), it was necessary to keep the TeO_2 target molten for 90 min. The distillation assembly was fitted to a spiral glass coil tubes directly behind the end of the furnace. The distilled radioiodine was then circulated through a spiral glass coil tubes to trap trace amount of volatile TeO_2 present in distilled ^{131}I vapor. After leaving the TeO_2 trap, ^{131}I vapor carried by the flow of Ar gas was allowed to pass through two traps known as primary (trap-1) and secondary (trap-2) connected in series. Before mounting, each trap was prewashed with a small volume of 0.1 M aqueous NaOH solution. Each trap contains 20.0 mL solution of 0.1 M NaOH containing 0.2 mg mL^{-1} Na_2SO_3 . In order to collect the un-trapped volatile ^{131}I , a secondary NaOH trap was placed downstream of the primary ^{131}I trap. After distillation, the

trap was opened, and the radioiodine was collected using a remote arm from the trap. In this process, the resulting ^{131}I was obtained in the form of sodium iodide and hence suitable for medical use. In an attempt to preclude the inadvertent release of ^{131}I into the general ventilation system, a glass trap packed with silver coated charcoal was placed downstream of the secondary NaOH trap. After about 20 production runs, the silver coated charcoal column was changed.

Trapping of ^{131}I : To get ^{131}I -[NaI], presence of 0.01 M NaOH containing 0.2 mg mL⁻¹ Na₂SO₃ is essential. We preferred to use two traps connected serially containing small amount (~20 mL) of 0.01 M NaOH solution to collect the ^{131}I species in order to achieve a better control on the radioactive concentration (RAC) of ^{131}I for subsequent radiolabeling. Table 2B.1 provides the data on the ^{131}I activities collected in the primary and secondary trap for 5 different batches.

It was seen from the result that separated ^{131}I radionuclide was successfully collected in the two successive traps containing Na₂SO₃ in sodium hydroxide solution. The activity was distributed in the order of ~70 % in the primary trap and ~30 % in the secondary trap. As required, ^{131}I activity adsorbed in the charcoal trap was very small compared to that retained in the two traps. ^{131}I trapped in the primary trap has significantly higher RAC than that in secondary trap. ^{131}I obtained from the primary trap possessing higher RAC was used for the preparation of ^{131}I -NaI therapeutic capsules, ^{131}I -MIBG, ^{131}I -Lipiodol and ^{131}I -labeled tositumomab and supplied to the nuclear medicine centers for clinical applications. On the other hand, ^{131}I collected from the secondary trap was used for diagnosis and treatment of thyroid disorders.

With the system and procedures described and based on the aforementioned results, a number of batches of ^{131}I (about 45–50 Ci of ^{131}I per batch) were processed from neutron irradiated TeO₂ targets. The total time required for irradiated target handling and radiochemical

separation amounted to ~3 h. Results of ^{131}I production carried out from 5 typical batches are presented in Table 2B.2.

Variations in the yield of ^{131}I from batch to batch are mostly due to the differences in the reactor irradiation conditions, such as the exact duration, intervening shut-down, and the variation of neutron flux level due to the power level of the reactor operation. It was not practicable to normalize the reactor irradiation conditions in the multi-purpose research reactor. It was imperative to point out that appropriate radiologic safety measures were in place during the production of ^{131}I .

Table: 2B.1: ^{131}I activities collected in different batches

Batch No.	Total distilled activity GBq (Ci)	Activity in primary trap GBq (Ci)	Activity in secondary trap GBq (Ci)	Activity in Charcoal trap GBq (Ci)
1	1,905 (51.49)	1,267.2 (34.25)	634.5 (17.15)	2.9 (0.078)
2	1,692 (45.73)	1,138.4 (30.77)	550.5 (14.88)	3.1 (0.084)
3	1,766 (47.73)	1,181.3 (31.93)	580.4 (15.69)	4.3 (0.116)
4	1,697 (45.86)	1,133.5 (30.64)	561.4 (15.17)	2.1 (0.057)
5	1,943 (52.51)	1,296.3 (35.04)	643.5 (17.39)	3.2 (0.086)
Weight of TeO_2 : ~180 g in each batch				

Table: 2B.2: Production of ^{131}I using natural TeO_2 target at Dhruva reactor

Batch No.	^{131}I activity [GBq (Ci)]		% Recovery	RNP %	RCP %
	Expected	Recovered			
1	2,119 (57.27)	1,905 (51.49)	89.90	89.90	99.2
2	1,991 (53.81)	1,692 (45.73)	84.98	84.98	99.4
3	2,029 (54.84)	1,766 (47.73)	87.04	87.04	98.3
4	1,974 (53.35)	1,697 (45.86)	85.97	85.97	97.9
5	2,393 (64.68)	1,943 (52.51)	81.20	81.20	99.1
Weight of TeO_2 : ~180 g in each batch					

2B.7 Quality control of separated ^{131}I

Quality control of the separated ^{131}I solution is an important pre-requisite for its clinical use.

^{131}I separated from irradiated TeO_2 target would be an active pharmaceutical ingredient (API) as [^{131}I]-NaI for the preparation of radiopharmaceuticals.

2B.7.1 Activity measurement

The radioactivity content was measured by both a pre-calibrated ion-chamber and later on, after appropriate dilution and sampling, by gamma ray spectrometry as well. While undertaking the measurement of activity in an ion chamber, the sealed vial containing ^{131}I solution was inserted into the ionization chamber with a dedicated holder in order to allow the vial to be accurately centered in the maximum response position of the measuring volume.

The ion current 'I' was measured and the activity 'A' was calculated by the relation

$$A = \frac{I}{\epsilon} \text{ MBq}$$

where ' ϵ ' is the ionization factor of the ionization chamber in pA/MBq.

^{131}I activity was monitored for 300 s at a suitable geometry and counts acquired under the 364.5 keV photopeak was used for assay of activity. The detection efficiency at this energy was derived by counting a standard ^{152}Eu source. The ^{131}I activity was calculated from the measured count rate and dividing it by the average efficiency.

The use of ion chamber for the determination of activity of the separated ^{131}I solution seems to be an ideal proposition as it was capable of producing ionization in gas filled detectors. While measuring ^{131}I solution activity in an ion chamber, care was taken to place the sealed vial containing solution inside the ionization chamber with a dedicated holder in the maximum response position of the measuring volume.

Experimentally it was ascertained that the percentage deviation between activity measurement values obtained by gamma spectrometric and ionization current techniques lies within ± 3.1 %. Radioactivity assessment of batch control samples of ^{131}I was therefore done

using well type ionization chamber for routine measurements due to rapidity and operational simplicity.

Radioactive concentration: Radioactive concentration (RAC) was determined by measuring the activity of known volume of the ^{131}I solution in an ion chamber after determining the efficiency of the ionization factor.

Therapeutic applications require routine availability of ^{131}I with a specific volume sufficient for the radiolabeling of biomolecules with ^{131}I for clinical use. The reported method provides ^{131}I in a RAC of 130–148 GBq (3.5–4.0 Ci)/mL, which will suffice for the formulation of clinical agents such as ^{131}I -MIBG, ^{131}I -Lipidol and ^{131}I -tositumomab.

2B.7.2 Radionuclidic purity

Radionuclidic purity was determined by recording γ -ray spectrum of the appropriately diluted sample solutions using an HPGe detector for 1 h. Table of Isotopes [50] and Gamma Ray Catalogue [51] were used for confirmation of the measured gamma energies. Gamma ray spectra of the processed products were recorded for each batch at regular time intervals. Samples measured initially for the assay of ^{131}I were preserved for complete decay of ^{131}I and re-assayed to determine presence of long lived radionuclide impurities.

The radionuclidic purity of the separated ^{131}I depends on the chemical purity of the target material and the decontamination from non-isotopic impurities achieved during distillation. Radionuclidic purity of the separated ^{131}I solution was assessed using gamma-ray spectrometric technique in which the samples were monitored for appropriate time at a suitable geometry after the end of distillation and after a decay period of upto 120 days. The corresponding radionuclidic purity was found to be $> 99.99\%$ ^{131}I (Fig. 2B.8 (a)). The radionuclidic purity of ^{131}I was further verified, from the corresponding decay curve (Fig. 2B.8 (b)), with the characteristic half-life of 8.02 days.

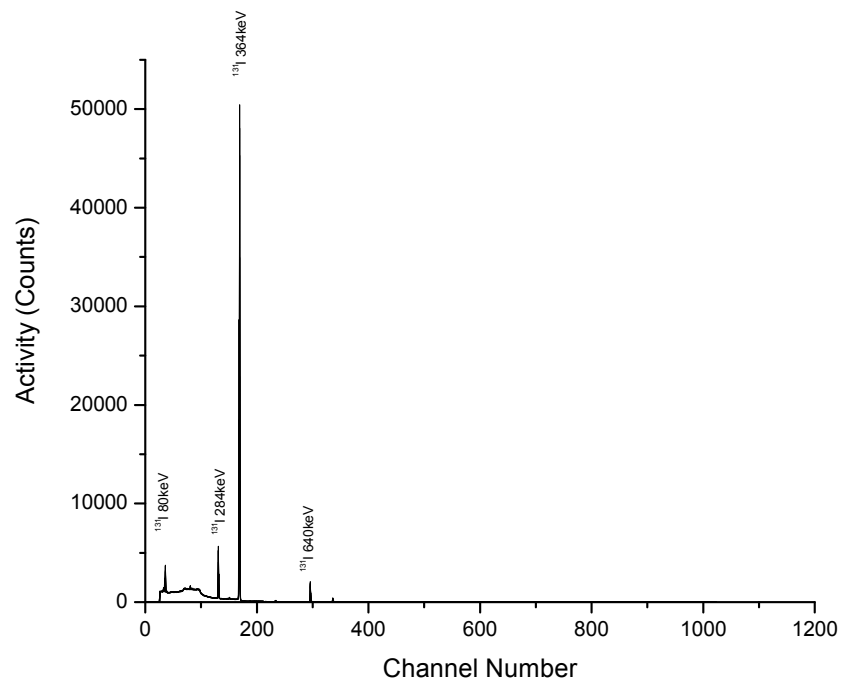


Fig. 2B.8 (a): Gamma ray spectrum of ^{131}I

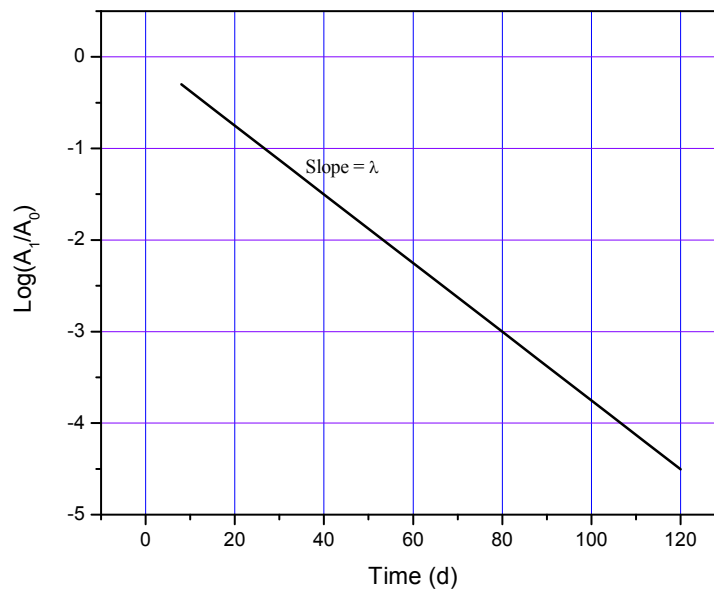


Fig. 2B.8 (b): Decay curve for ^{131}I

2B.7.3 pH of ^{131}I solution

A universal indicator non-bleeding paper of pH range 0-14 was used for pH measurement. A small drop of ^{131}I -[NaI] was spotted on the pH paper strip and the test color was matched with standard pH color paper. It was found that the pH of the solution was 8-10.

2B.7.4 Radiochemical purity

Radiochemical purity of ^{131}I was determined by paper electrophoresis technique. Whatman 3 MM paper (2.5 cm \times 25 cm) was presoaked in 0.025 M sodium phosphate buffer and placed in the electrophoresis bath containing 0.025 M phosphate buffer and 200 V constant voltage was applied for about 15 min. Following equilibration, 2–5 μL of the sample was spotted at middle of the strip and voltage was applied for another 1 h. After electrophoresis, the strips were dried and counted in NaI(Tl) detector by cutting it into 1 cm pieces.

Radiochemical purity is an essential parameter which determines the oxidation state in which ^{131}I is present in the solution. The presence of ^{131}I in the I^- ion form is desirable. As radioiodine is known to exist in several oxidation states in varying proportions, it is obligatory to determine the radiochemical purity to ascertain its suitability for clinical use. A typical paper electrophoresis pattern of separated ^{131}I is shown in Fig. 2B.9. The paper electrophoresis pattern of ^{131}I was examined for several batches and it was observed that >98 % of ^{131}I in the alkaline solution was present in the form of $^{131}\text{I}^-$.

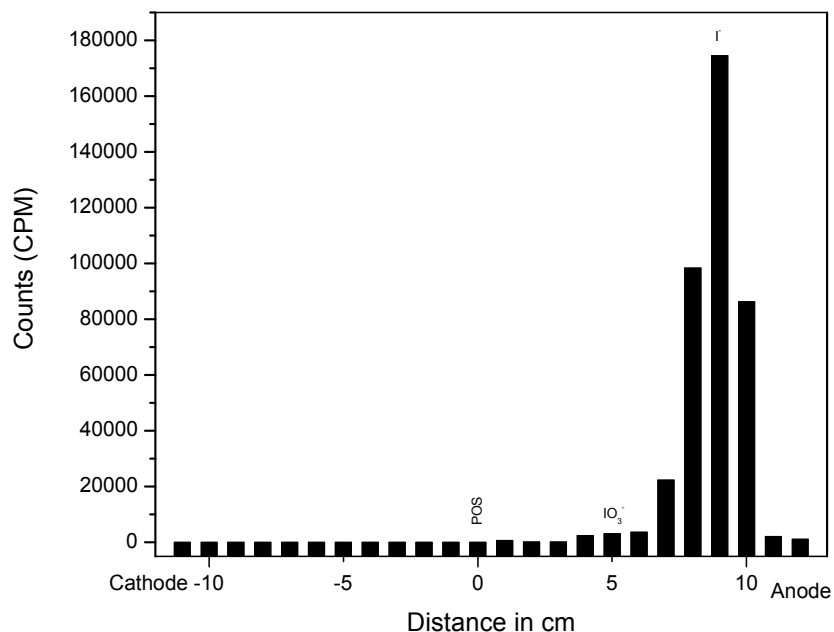


Fig. 2B.9: Paper electrophoresis pattern of ^{131}I

2B.7.5 Chemical purity

The major inactive impurity expected in the separated radioiodine was Te. The amount of nonradioactive Te in each batch of radioiodine was determined as per the method described in 2A.1.1.1 (f).

Tellurium contamination in the separated ^{131}I solution, as a stable chemical impurity, was checked and was found to be $< 1 \mu\text{g mL}^{-1}$ limit [13].

2B.8 ^{131}I product specifications: Results

The pH of the separated ^{131}I -[NaI] was found to be in the alkaline range (pH 8–10) as desired. The RAC was 130–148 GBq (3.5–4.0 Ci) mL^{-1} , and this is sufficient for the iodination reactions. Radionuclidic purity of $> 99.9\%$ was obtained. Radiochemical purity of the ^{131}I obtained was $> 98\%$ in all the lots analyzed (Table 2B.3). Typical batch quality control

report from the end user involved in formulation of ^{131}I radiopharmaceuticals is given below in Fig. 2B.10.

Table 2B.3: Report on analysis of Sodium Iodide (I-131) solution

Code: I-2 (I-131 as sodium iodide in alkaline solution)			
Sr. No	Test/ parameter	Desired value	Result obtained
1	Description	A clear colourless solution upon standing both the solution and glass container may darken	As expected
2	Radionuclide Identification	By the photopeak corresponding to its principal gamma emission of 364 keV	Identified as ^{131}I by γ -ray spectrometry
3	Radionuclidic purity	> 99.9 %	> 99.99 % was observed
4	pH	8-10	~ 9
5	Radiochemical purity	> 95% of $^{131}\text{I}[\text{I}^-]$	> 98 % of $^{131}\text{I}[\text{I}^-]$
6	Sodium sulphite content	< 1 mg/ 100 mCi of ^{131}I	< 0.1 mg / 100 mCi ^{131}I
7	“Te” content	< 5 $\mu\text{g/mL}$ by spot test	< 5 $\mu\text{g/ mL}$ obtained

COA NO:- 99 ; Dt:- 12/8/16

BOARD OF RADIATION AND ISOTOPE TECHNOLOGY
Radiopharmaceuticals Operation
Quality Control 1895

Report on Analysis of Sodium Iodide (I-131) Solution (Raw Material)

Code : I-2 Batch No. 124/229/001/9.8.16 Date of preparation 10.8.16

Batch Control 1x 2.0

Sr. No.	Test	Expected (as per BARC monograph)	Observed	Remarks
1	Description	A clear colourless solution upon standing both the solution and glass container may darken.	A clear colourless solution	Passes/ Does not pass
2	Radionuclide identification	By the photopeak corresponding to its principal gamma emission of 0.36 Mev.	Complies	Passes/ Does not pass
3	Radionuclidic purity	No other extraneous gamma emitting radionuclide is detectable in the gamma ray spectrum	Complies	Passes/ Does not pass
4	pH	7.0 — 10.0	~9	Passes/ Does not pass
5	Radiochemical purity	The activity in the sodium iodide (I-131) zone shall not be less than 95 percent of the total activity.	99.26% 11/8/2016	Passes/ Does not pass
6	Sodium sulphite content	< 1 mg/100 Ci	0.058 mg per 100 mCi of I-131 at 12 hrs on 11/8/16	Passes
7	Assay for radioactivity	Reps Result	217 mCi per ml at 10.5 hrs. on 10.8.2016	—
8	"Te" content	< 5 ug/ml by spot test	< 5 ug/ml	Passes/ Does not pass
9	Storage	To be stored at room temperature in a safe place with adequate shielding	Complies	—

Remarks :

The batch No. 124/229/001/9.8.16 of Sodium Iodide I-131 Solution Code I-2 complies with the prescribed specifications of the BARC Monograph. ~~does not comply~~

Analysed by: 11/8/16

Manager
Quality Control 12.8.16

To
Manager
Production

Dr. Sudipta
Asso. CRP

cc : Manager, RCRSO, BRIT, RLG, BARC

Fig. 2B.10: Typical report on analysis of ^{131}I -[NaI]

2B.9 Results of employment of the dry distillation technology for regular production and supply of ^{131}I -[NaI]

The dry distillation technology is being employed for radiochemical separation of ^{131}I for its clinical use and the results are summed up for last four years (2015-2018) in Table 2B.3. The ^{131}I produced was also subjected to quality control which is reported in the table.

Table 2B.4: Results of Production of ^{131}I by dry distillation technology

Sr. No.	Year	Number of batches	Weight of TeO_2 per batch (g)	Activity Recovered in each batch GBq (Ci)	RAC GBq mL^{-1} (Ci mL^{-1})	Te content (mg mL^{-1})	RNP %	RCP (%)
1	2015	44	130 ± 27	1,972 ± 559 (53.31 ± 15.1)	97.68 ± 27.38 (2.64 ± 0.74)	< 5	>99.9	97.56 ± 1.02
2	2016	44	115 ± 17	1,461 ± 418 (39.49 ± 11.3)	71.78 ± 21.83 (1.94 ± 0.59)	< 5	>99.9	97.90 ± 1.1
3	2017	47	106 ± 25	1,111 ± 459 (30.04 ± 12.4)	54.76 ± 20.72 (1.48 ± 0.56)	< 5	>99.9	97.82 ± 1.07
4	2018	39	106 ± 22	1,144 ± 355 (30.92 ± 6.9)	56.24 ± 15.54 (1.52 ± 0.42)	< 5	>99.9	97.94 ± 0.99

2B.10 Radiological safety

Appropriate procedure of radioactivity handling was followed during the entire radiochemical processing steps involved. In light of the need to achieve ALARA (as low as reasonably

achievable), all the radiochemical processing steps were carried out after proper planning and executed cautiously. Radiation exposure levels were monitored for by TLD (Thermoluminescent dosimetry). Continuous radioactivity monitoring of air in the working area was performed to provide an immediate warning when air concentrations exceeded safe radioactive levels for maintaining radiological safety. Air activity during processing of ^{131}I was found to be 0.1- 0.2 Derived Air Concentration (DAC) inside the processing laboratory (For ^{131}I , 1 DAC = 400 Bq M^{-3}). Average absorbed radiation dose to the operator was < 10 μSv per batch of 50 Ci. Background radiation dose to the operating area was found to be 0.1- 0.5 mR/h during processing of ^{131}I .

2B.11 Radioactive waste handling

Although the radioactive waste generated during the production of ^{131}I through dry distillation process was relatively in small volumes with low levels of radio-activity, its management was an integral and important part of ^{131}I production. The concept of waste minimization during the radiochemical processing of irradiated TeO_2 target was followed scrupulously. All process consumables such as Al irradiation container, quartz crucible, charcoal trap etc. are used for only one production run. After each run, they were collected, segregated, and stored in a specially designed lead cell to allow for decay of the contaminated radionuclides. The overall philosophy for the management of radioactive waste generated during ^{131}I production relies on the concepts of delay and decay as the longest lived radionuclide in tellurium radioactive waste was $^{121\text{m}}\text{Te}$ ($T_{1/2} = 154$ days). Their activity decayed to 0.1 % after 10 half life (4.22 years) and after 8 years its activity reached ~0.0005 % of original activity. The radioactive waste was decayed for 8–10 years in centralized radioactive waste management facility of the institution.

2B.12 Discussion

The role of ^{131}I , either as ionic or bound to a carrier moiety, in clinical diagnosis and treatment of malignant disease needs hardly to be reiterated. The striking diffusion and the exciting perspective of ^{131}I in nuclear medicine are mainly attributable to its attractive nuclear properties, favorable chemistry and cost effective availability. ^{131}I would continue to play a significant role in nuclear medicine for today as well as in the foreseeable future, notwithstanding the introduction of new exotic radionuclides. The Isotope program of the Bhabha Atomic Research Centre has been following a wet distillation technology for the large scale production of ^{131}I for the last 50 years. As the demand for ^{131}I from the nuclear medicine community were increasing over the years, the production levels could not be augmented beyond 740 GBq (20 Ci) per batch in the wet distillation process and hence the need for setting up the dry distillation technology was an essential requirement of the program. The options were either procuring a ready to use technology from one of the providers at a high cost; or develop the technology indigenously. The latter route was adapted; and the technology developed is documented in this thesis, for the benefit of potential other isotope producers.

Conscientious harnessing of the dry distillation technique to separate ^{131}I from neutron irradiated Te target will not only reinvigorate the ^{131}I production technology but can foster sustainability. While the outlook of dry distillation technique in term of physical and chemical principles seems to be quite promising, devising an effective technology requires a blend of science and engineering. Even though there is no technical impediment to adapt dry distillation technique, there are concerns about the handling of radioactive irradiated target at GBq level in hostile radiation environment, containment of gaseous ^{131}I during distillation as well as transformation of gaseous ^{131}I into an acceptable chemical form and adherence to RAC as well as purity of the final ^{131}I solution. In light of the explicit need to produce ^{131}I

week after week all through the year, it is not only essential to have a very high degree of robustness of the operational systems but also crucial to enforce adequate radiological safety systems. In view of such demanding conditions, large scale production capabilities of ^{131}I are thus restricted to a small number of suppliers in the world despite huge demands; and the technology hardly diverged. This is the main reason for most countries prefer to follow the soft option of purchasing commercially available ^{131}I radiochemical in bulk to meet their requirements for the formulation of radiopharmaceuticals. The primary endeavor of this investigation is an attempt to unlock the potential of dry distillation technique that can be unambiguously implemented for the routine production of clinical grade ^{131}I adaptable to the existing and foreseeable demands.

Our pursuit of ^{131}I production technology development was driven mainly by four considerations, namely, (i) availability of operating research reactors capable of providing moderate neutron flux (up to $1 \times 10^{14} \text{ n cm}^{-2} \text{ s}^{-1}$), (ii) need to replace the wet chemical distillation ^{131}I production technique in use in India since 1960s, (iii) ease on dependency on import of ^{131}I , and (iv) establish the necessary capacity to produce ^{131}I to meet increased local demands.

Since an oxygen containing atmosphere at 750°C and molten tellurium dioxide are rather corrosive, selection of quartz distillation assembly seemed attractive at first sight owing to the attributes such as ready availability, inexpensive, chemical resistance against oxygen and tellurium dioxide at 750°C and satisfactory thermal conductivity. While release of ^{131}I from the neutron irradiated TeO_2 target during distillation depends on a number of factors, its dependence on temperature is arguably the strongest and is of key importance. Although distillation of ^{131}I using conventional resistance coil heating system has tangible benefits, use of induction heating system is a desirable proposition owing to rapid attainment of melting temperature of TeO_2 and successful curtailing the volatilization of TeO_2 to $\sim 0.5\%$ [53]. With

a view to remove trace amount of TeO_2 in distilled ^{131}I , the scope of circulating the distilled ^{131}I vapor through glass coil tube is enticing because it is generally succinct, rugged and unsusceptible to subtle variation in the operational conditions. The major advantage of this purification technique lies in the compactness and simplicity in the design that paved the way for unambiguous adoption in a remotely operated shielded facility.

With a sensible strategy, adequate resources, and sustained determination, extensive investigations on dry distillation technique led to a steady progress, achieved both in terms of process technology development and final performance. Concurrent to process technology development, a 150 mm thick lead-shielded facility comprising 3 interconnected cells was erected. Spurred by the perceived need to realize process robustness, operation-specific gadgets were designed, developed, fabricated, installed and commissioned. Before undertaking hot run, every remotely operating step has been examined scrupulously not only to ensure operational requirements but also to guarantee the safety of the processes. The developed process was validated by conducting a series of successive scale-up studies beginning with laboratory-scale process confirmation experiments, initially with simulated irradiated TeO_2 target and proceeding to limited scale under radioactive conditions with representative materials. These exploratory studies were essential primarily to acquire basic knowledge of the process chemistry, integrated testing of the technique and equipment, feasibility assessment of the key processing steps and identification of the problem areas. The obtained results were also conscientiously used for the technical as well as economic feasibility studies and overall safety assessment of the process.

While the indigenous ^{131}I production technology development had passed many milestones, achieved spectacular success and has been prolific in providing ^{131}I , the process as well as obtained ^{131}I must comply with local legislative, regulatory and institutional regulations. Review of the radiological safety features of the processing facility was carried out by the

regulatory body of the institution and granted approval for processing 3.7 TBq (100 Ci) of ^{131}I activity per batch. This indigenous method of producing ^{131}I represents a new paradigm and ^{131}I obtained from this process, therefore, needs to be complying with qualification and validation protocols established by national pharmacopoeia regulations to ensure its safety and efficacy for human use as ^{131}I is considered as an active pharmaceutical ingredient (API) either used as such or in the preparation of radiopharmaceuticals. The quality of the ^{131}I obtained from the aforementioned procedure was reviewed by the Radiopharmaceutical Committee (RPC), the regulatory body responsible for clearing radiopharmaceuticals in India and based on the documentation relating to establishment of chemical, radiochemical and radionuclidic purity of ^{131}I , granted approval for widespread use in daily nuclear medicine routine. It is important to point out that before undertaking clinical use, every single batch of ^{131}I obtained from the process were subjected to on-site quality assurance at the institutional level to ensure that it is within the stipulated limit of the pharmacopoeias.

Each ^{131}I production technology developed has its own distinct advantages and disadvantages but since every institution has different scientific and technical resources, each option would be expected to have a place. The reported ^{131}I production strategy does indeed represent a leap forward in pursuit of self-sufficiency in the radioisotope production technology. Self-reliance through indigenous production and utilization of ^{131}I represents a bold initiative to circumvent possibility of delay or unacceptable disruptions in radioisotope supplies through import. Local production capability of ^{131}I of required quantity and quality offered numerous benefits like reducing dependence on import, and therefore security of supply risk, as well as cost savings. Reliable availability of ^{131}I on demand would not only promote the beneficial use of ^{131}I in well entrenched area of nuclear medicine procedures, but also invigorate basic research as well as development of clinically-oriented radiopharmaceuticals that will hopefully pave the way for the sustained growth and future expansion of ^{131}I radiopharmacy.

2B.13 Conclusion

The objective of development of a ^{131}I production and chemical processing strategy making use of dry distillation technique, capable of providing ^{131}I of acceptable quality, commensurate with clinical requirements, has been successfully achieved. The developed process was found to be facile, robust, efficient, cost-effective, easily up scalable, uses simple apparatus and generates minimum amount of radioactive waste. The reported method has been successfully used for the routine production of ^{131}I at a TBq level [1.85–3.7 TBq (50–100 Ci)]. ^{131}I produced from this method would suffice for the preparation of ^{131}I -MIBG, ^{131}I -[NaI] therapeutic capsules, ^{131}I -tositumomab, ^{131}I -Lipiodol and other ^{131}I labeled biomolecules. With ready availability of ^{131}I , further research development of ^{131}I labeled molecules for various applications is expected to increase. While technical realization of the dry distillation technique for routine ^{131}I production has been a long and winding journey fraught with peril and stumbling blocks around every corner, payoff of success was substantial. The distillation procedure described in the thesis is generic in nature and expected to be useful for the production of other isotopes of iodine such as ^{124}I , ^{123}I from reactor or cyclotron irradiated tellurium matrices.

CHAPTER-3

Post-processing Concentration of I-131 for Therapeutic Applications

“paṭisaṅkhānabalā bahussutā.”

“Experience comes from careful judgement.”

23/227, aṅguttaranikāyā aṭṭhaka

3.1 Introduction

The last few years have witnessed an exceptional growth in the development of advanced sorbent materials which play a crucial role in radiochemical procedures for obtaining the medically important radioisotopes in desired formulations for clinical use [54-56]. Also there is huge advancement in the development and application of ordered mesoporous metal oxides in different technologies [57, 58]. Inorganic sorbent materials such as mesoporous metal oxides with attractive properties like high surface areas, tailorable pore shapes and sizes, possibility of having a wide variety of structures and a multitude of compositions and amenability for functionalization meets the requirements as ‘new generation’ of advanced sorbent materials for radiochemical applications [59]. The desired radioisotope can be selectively absorbed in the mesopores with high sorption capacity due to the large surface area and enhanced pore volume of mesoporous metal oxides.

Despite excellent attributes of such materials as sorbents, their large scale synthesis with well-defined mesoporous structures is still a challenge that limits their practical utility [60, 61]. The optimization of simple, cost-effective protocol for large scale synthesis of the sorbent maintaining constructive structural characteristics is challenging in the development of advanced sorbent material. For the synthesis of mesoporous metal oxides, synthesis routes based on soft-templating (surfactants or block copolymers as templates), colloidal crystal templating (3D ordered colloidal particles as templates), hard-templating (mesoporous silica or carbon as sacrificial templates), etc. have been reported [57, 58, 62]. Employing these routes has its inherent technical hitches in removal of template material which complicate the synthesis process. Also the conventional strategies require precise control on the synthesis parameters to achieve well-defined mesoporous structure. The overall yield of the final product is low in majority of cases which makes it inadequate for practical use as a sorbent in radiochemical separations for clinical use.

Solid state mechanochemical synthesis of mesoporous sorbents is an emerging concept in materials chemistry that is expected to play an imperative role in making clinically translatable advances in nuclear medicine industry [59]. Solid state synthesis route is promising for synthesis of mesoporous metal oxides, which are useful for applications in radiochemical separations [63-66]. Mechanochemical synthesis process is simple, efficient, rapid, cost-effective, environment friendly and offers feasibility of industrially significant scale-up while maintaining the optimal structural characteristics of the material. This approach comes in arena of 'green Chemistry' because of solvent-free chemical reactions. In solid state synthesis, reactions are performed at very high reactant concentrations because no solvents are used.

Iodine-131 remains the premier, one of the oldest and the most widely used therapeutic radioisotope in nuclear medicine [67]. The immense utility of this radioisotope for treatment of benign and malignant thyroid diseases is clinically well-established [68]. Iodine-131 production route followed is described in Chapter 2 of the thesis. Generally, for treatment of thyroid disorders, ^{131}I encapsulated in hard gelatin capsule is orally administered to the patients [69, 70]. Since, the volume of the capsule is fixed and it is pre-filled with an inert matrix, a very small volume (not exceeding 100 μL) of ^{131}I solution can actually be accommodated in the capsule [63]. Therefore, in order to prepare therapeutic capsules of large radioactive dosage ($\geq 7.4 \text{ GBq}$, $\geq 200 \text{ mCi}$) while maintaining the safety requirements, the concentration of ^{131}I solution should be as high as possible. Maximum radioactive concentration of ^{131}I achievable was $97.68 \text{ GBq mL}^{-1}$ (2.64 Ci mL^{-1}) as described in chapter 2B. For thyroid carcinoma recommended dose for 70 Kg adult patient is 3.7 – 7.4 GBq (100-200 mCi) ^{131}I for ablation of normal thyroid tissues and subsequent treatment [71]. To make a 7.4 GBq (200 mCi) capsule, the required radioactive concentration of ^{131}I should be $> 259 \text{ GBq mL}^{-1}$ ($>7.0 \text{ Ci mL}^{-1}$) on preparation day [71]. This essentially mandates post-processing

concentration of ^{131}I prior to preparation of therapeutic capsules. The conventional evaporation based procedure is not amenable for concentration of ^{131}I due to volatility of iodine which may lead to release of the radioactivity [72-74]. It is anticipated that solid state synthesis of mesoporous alumina may serve as a robust and cost-effective approach for large scale preparation of high capacity sorbent to be used during post processing concentration of ^{131}I from routine clinical perspective. In this context, assessing the potential of column chromatography using mesoporous metal oxide sorbent seemed promising as a practically viable method for concentration of ^{131}I in a hot cell facility for preparation of large-dose therapeutic capsules.

In this chapter the synthesis of mesoporous alumina by a novel solid state mechanochemical route is described. The high mesoporosity and pH dependent surface properties of the synthesized material could be used in development of a solid phase extraction procedure for radiochemical concentration of ^{131}I . The high porosity of mesoporous alumina is expected to enable significant permeability of the liquid containing iodide ions through the pores of the sorbent. Therefore, sorption can take place not only at the surface of the individual grains, but also, at the grain boundaries and at the interface between grains resulting in high I^- (iodide ion) sorption capacity. The structural characteristics and sorption behavior of the material were investigated and the utility of this material towards post processing concentration of ^{131}I was demonstrated. The quality of concentrated ^{131}I for preparation of therapeutic capsule was assessed.

3.2 Experimental

3.2.1 Materials

Aluminum chloride (99.9 % purity) was obtained from BDH chemicals, Mumbai, India; Ammonium carbonate was procured from Thomas Baker, Mumbai, India and D-(+)-glucose

(> 99.5 % purity) was purchased from Sigma-Aldrich, India. Hydrochloric acid, sodium hydroxide, potassium iodide and sodium sulfite were of Guaranteed Reagent (GR) grade and were procured from Merck, India. HPLC grade water was purchased from E. Merck, Germany. Paper chromatography (PC) strips (3 MM Chr, 20 mm width) were purchased from Whatman International Limited, England. The chemicals and reagents were used as such without further modification. Zeta-potential of the suspensions was measured at different pH using a zeta potential analyzer, Zetasizer Nano ZS/ZEN3600, Malvern Instruments Ltd., UK. The trace levels of the metal ion contamination in the decayed samples were determined by inductively coupled plasma-atomic emission spectroscopy using ICP-AES JY-238 spectrometer, Emission Horiba Group, France.

Iodine-131 was produced by irradiation of natural TeO₂ target in the Dhruva reactor via ¹³⁰Te (n,γ) ¹³¹Te $\xrightarrow{\beta^-}$ ¹³¹I nuclear reaction and was radiochemically separated from the irradiated target by dry distillation process to obtain ¹³¹I-[NaI] solution as reported in earlier chapter. Radioactivity measurements were carried out using a pre-calibrated well-type ion-chamber.

3.2.2 Methods

Mesoporous alumina was synthesized by solid state mechanochemical reaction of aluminum chloride, ammonium carbonate and glucose mixed in 1:1.5:1.5 molar ratios. The reaction mixture was ground manually in an agate mortar for 1 h at room temperature and subsequently calcinated at 600 °C for 2 h in a furnace. After calcination, the material was obtained in the form of lumps which were mechanically crushed to obtain free flowing particles. The particle size distributions of the reaction mixture (after grinding and before calcination) and the final product were determined by laser diffraction particle size analyzer. Particle size distributions of the powdered samples were obtained using the CILAS 1090 dual

LASER particle-size-analyzer (Cilas Particle Size, USA). For particle size distribution measurement, a well dispersed suspension of the powder was prepared in de-ionized water by thorough ultrasonication for ~ 30 min. The synthesized material was also characterized by various analytical techniques such as X-ray diffraction (XRD), field emission scanning electron microscopy (FESEM), energy dispersive x-ray spectroscopy (EDS), transmission electron microscopy (TEM), small angle neutron/X-ray scattering (SANS/SAXS), Brunauer–Emmett–Teller (BET) surface area and pore size analyses. The pH dependent variation in surface charge (zeta potential) of mesoporous alumina was determined using a zeta potential analyzer.

3.2.2.1 Structural characterization of mesoporous alumina

XRD data were collected on the powder sample for the phase identification and crystallite size estimation, using monochromatized Cu-K α radiation on a PANalytical X-ray diffractometer (X'pert PRO). The instrument was operated at 40 kV and 30 mA. Silicon was used as an external standard for the correction due to instrumental line broadening. The mesoporous alumina powder was grinded and loaded in the groove of the perspex sample holder. XRD pattern was recorded in the 2θ range of 10-80° for 1 h with a scan step size of 0.02°. Scanning electron microscope (JEOL JSM-7600F FEG-SEM) was used for scanning electron microscopy (SEM) analysis. The chemical composition was obtained by energy dispersive X-ray spectroscopy (EDS) analysis (Oxford, model INCA E350). TEM data were recorded using a JEOL FX microscope (Jeol Ltd., Tokyo, Japan), on the powder sample. The preparation of samples for TEM analysis involved sonication in ethanol for 5 min and deposition on a carbon-coated copper grid. The accelerating voltage of the electron beam was 200 kV.

The small-angle X-ray scattering (SAXS) experiment on powder sample was performed using a lab-based SAXS facility with Cu-K α X-ray radiation. The scattering intensity of X-

rays from the sample was recorded as a function of scattering angle θ . The magnitude of the wave vector transfer q is defined as $q=4\pi\sin\theta/\lambda$, where λ is the wavelength of the X-rays ($\lambda=1.54$ Å). The wave vector transfer in present experiment was $0.1\text{--}2.5\text{ nm}^{-1}$. In order to access further lower q , a double crystal based medium resolution small-angle scattering (MSANS) facility [75] at Dhruva reactor of Bhabha Atomic Research Centre was utilized. The accessible q -range in the MSANS measurements was $\sim 0.003\text{--}0.11\text{ nm}^{-1}$. The combined SAXS and MSANS data provide a wide- q range and thus offer unique opportunity to probe both the mesopores and agglomeration nature of the synthesized alumina.

Nitrogen adsorption-desorption isotherms of the samples were determined at 77 K using a Quantachrome, Autosorb-1 analyzer (Quantachrome Instruments, FL 33426 USA). The surface area analysis was carried out by multipoint BET (Brunauer, Emmett and Teller) method at a relative pressure (P/P_0) range of 0.05–0.30 and BJH (Barrett, Joyner, and Halenda) method was used to measure the total pore volume.

3.2.2.2 Determination of zeta-potential of mesoporous alumina

The zeta potential of mesoporous alumina was studied at different pH environments. The samples were prepared by adding 5 mg of material to 50 mL of de-ionized water and the pH of the suspension was adjusted using HCl and NH_4OH solution. Zeta-potential of the suspensions was measured at different pH using a zeta potential analyzer (Zetasizer Nano ZS/ZEN3600, Malvern Instruments Ltd., UK). Folded capillary zeta cell (product number: DTS1070) was used for determination of the zeta potential of the samples.

3.2.2.3 Determination of distribution coefficients (K_d) of I^- ions

The K_d values of I^- ions in mesoporous alumina sorbent were determined by batch equilibration method. 50 mL solution at different pH (1–14) spiked with 3.7 MBq (0.1 mCi)

of I^- radiotracer in a stoppered conical flask having 200 mg of mesoporous alumina were used. It was shaken for 1 h at room temperature (25°C). The solution allowed to settle and supernatant solution was filtered through a Whatman filter paper (No. 542). Before and after equilibrium, radioactivities of the solution were measured in a well calibrated HPGe detector coupled with MCA (Canberra Eurisys, France) using 364 keV photopeak of ^{131}I . The K_d values were calculated by using the following expression:

$$K_d = \frac{(R_i - R_{eq})V}{R_{eq} m} \text{ L g}^{-1} \dots\dots\dots (1)$$

where, R_i is the initial total radioactivity of 1 mL the solution,

R_{eq} is the unadsorbed activity in 1 mL of the solution at equilibrium,

V is the solution volume (mL) and

m is the mass (g) of the sorbent.

All equilibration experiments were carried out in triplicate. The distribution coefficient (K_d) of I^- ions in mesoporous alumina sorbent were determined at different pH.

3.2.2.4 Determination of time required to attain sorption equilibrium

Time dependence of sorption of ^{131}I onto mesoporous alumina was studied by determining K_d of $^{131}\text{I}^-$ ions for pH 6 at different time intervals. The equilibrium condition was indicated by constant K_d value after a certain period of time.

3.2.2.5 Determination of $^{131}\text{I}^-$ sorption capacity of mesoporous alumina

The sorption capacity of mesoporous alumina was evaluated under both static and dynamic conditions [59].

(a) Static sorption capacity

The static sorption capacity of mesoporous alumina for I^- was determined by batch equilibration method. An accurately weighed amount of mesoporous alumina (~ 200 mg) was taken in a stoppered glass conical flask and equilibrated with 50 mL solution of NaI (0.2 mg I^- per mL, pH 6) spiked with 37 MBq of ^{131}I for 20 min. The solution was filtered through Whatman filter paper (No. 542). The activities of ^{131}I in the solution before and after adsorption were measured in 1 mL aliquot by using HPGe-MCA detector system by measuring the counts at 364 keV peak corresponding to ^{131}I . All measurements were carried out at 25° C in triplicate.

The capacity was given by:

$$\text{Capacity} = \frac{(R_0 - R_e)VC_0}{R_0 m}, \dots\dots\dots(2)$$

Where, R_0 and R_e represented the radioactivity of ^{131}I in 1 mL of supernatant solution before and after sorption, respectively,

C_0 was the total I content (0.2 mg) in 1 mL of solution before sorption,

V was the volume of solution and

m was the mass (g) of the sorbent.

(b) Breakthrough pattern under dynamic conditions

To evaluate the I^- ion sorption capacity under dynamic conditions, a borosilicate glass column of dimension 6 cm (H) \times 0.5 cm (ID) with a sintered disc (G_0) at the bottom was packed with 200 mg of the sorbent. The column was conditioned with pH 6 solution. Total 50 mL NaI solution (0.2 mg I^- mL⁻¹, pH 6) spiked with 37 MBq ^{131}I radiotracer was passed through the column at a flow rate of 0.5 mL min⁻¹. From the feed ^{131}I solution, 1 mL was kept as reference (A_0) and eluted solution was collected in 1 mL aliquots. The radioactivity associated with the reference solution (A_0), as well as each fraction (A_i) was measured in a HPGe detector coupled with MCA by counting the 364 keV peak of ^{131}I .

(c) Practical sorption capacity

To evaluate the I^- sorption capacity under column flow conditions, a borosilicate glass column of dimension 6 cm (H) \times 0.5 cm (ID) with a sintered disc (G_0) at the bottom was packed with 200 mg of the sorbent. The column was conditioned with pH 6 solution. 50 mL NaI solution ($0.2 \text{ mg I}^- \text{ mL}^{-1}$, pH 6) spiked with 37 MBq ^{131}I radiotracer was passed through the column at a flow rate of 0.5 mL min^{-1} . Subsequently, the column was washed with 200 mL of pH 6 solution and the activities of the effluent and the washing were measured.

3.2.2.6 $^{131}\text{I}^-$ ion Desorption characteristics of mesoporous alumina**(a) Optimization of desorption concentration**

In order to study the conditions for retrieval of ^{131}I , a borosilicate glass column of dimension 6 cm (H) \times 0.5 cm (ID) with a sintered disc (G_0) at the bottom containing 200 mg of mesoporous alumina was used. After conditioning the column with pH 6 solution, each column was loaded with ^{131}I by passing NaI solution. It contained 1 mg I^- ions in 20 mL volume spiked with 185 MBq of ^{131}I through the column at a flow rate of 0.5 mL min^{-1} . The adsorbed ^{131}I was recovered by passing 5 mL of NaOH solutions of concentrations ranging from 0.01 to 0.03 M (with an increment of 0.05M) through the columns. The activities in the eluates were measured. Thus optimization of the concentration of NaOH solutions for elution of ^{131}I absorbed in the column was carried out. The kinetics of sorption was evaluated by determining the K_d values at different time intervals.

(b) Optimization of flow rate of elution

Similarly from the optimal concentration of NaOH solution another column was prepared and loaded with ^{131}I activity as explained in (a) above. 5 mL of NaOH solution of the optimal

concentration was passed through the columns at different flow rates. After each flow rate the eluates were collected and the activities were measured.

(c) Elution profile of the desorption of ^{131}I from the sorbent

Similarly from the optimal concentration of NaOH solution another column was prepared and loaded with ^{131}I activity as explained in (a) above. After optimizing the optimal concentration of NaOH for elution, the optimized concentration was used for elution profile study. The eluates were collected in a series of 0.25 mL aliquots and the activity of each sample was measured to plot the elution profile of I^- through the sorbent.

3.2.2.7 Practical utility of the sorbent

The practical utility of the mesoporous alumina in chromatographic process was demonstrated by concentration of ^{131}I solutions, simulated to represent different activity levels (37 – 3700 GBq). The simulated solutions were prepared by adding appropriate amount of inactive NaI carrier to ^{131}I solutions containing tracer level of activity (~ 185 MBq). The volumes of the radioactive solutions were varied in the range of 10-100 mL. The radioactivity was loaded in chromatographic columns containing 200 mg of mesoporous alumina under the optimized conditions as described above. Subsequently, ^{131}I was eluted in 2 mL of 0.1 M NaOH solution, maintaining a flow rate of 0.5 mL min^{-1} . The overall yield of ^{131}I obtained was determined by measuring the activity in a pre-calibrated ion chamber and the radioactive concentration of the product was determined.

3.2.2.8 Quality control of processed ^{131}I

(i) Radiochemical purity of ^{131}I

The radiochemical purity of ^{131}I (in the form of I^- ions) was determined by paper electrophoresis method as reported earlier in chapter 2B [76].

(ii) Chemical purity of ^{131}I

To determine the presence of chemical impurities in the form of metal ions in the ^{131}I -eluate, the samples were allowed to decay for 80 days. The trace levels of the metal ion contamination in the decayed samples were determined by inductively coupled plasma-atomic emission spectroscopy (ICP-AES) using ICP-AES JY-238 spectrometer, Emission Horiba Group, France. The calibration curves for these ions were obtained by using standard solutions having known concentration of these ions.

3.3. Results and Discussion

Mechanochemical synthesis of mesoporous alumina and its utilization in post-processing concentration of ^{131}I by column chromatographic method is schematically illustrated in Fig.3.1.

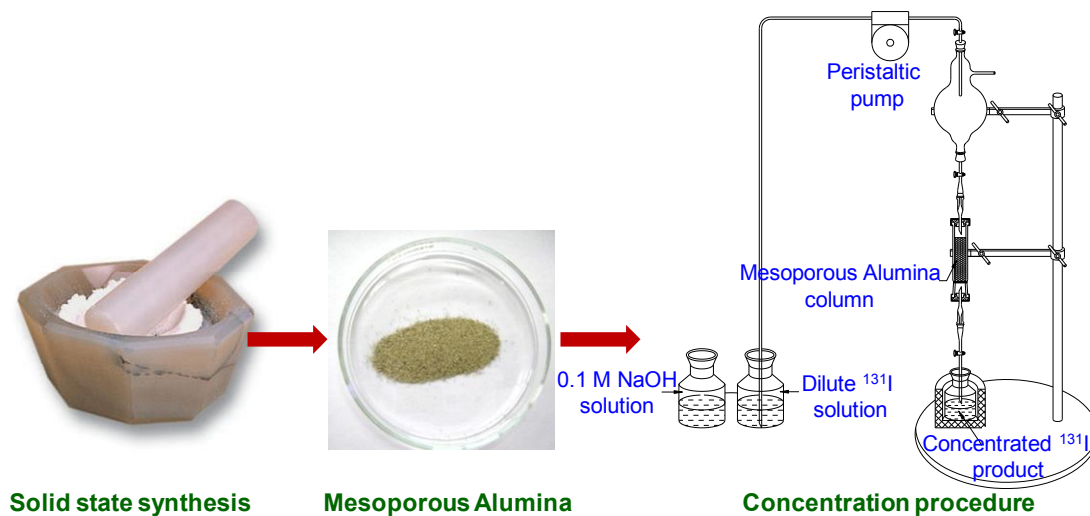
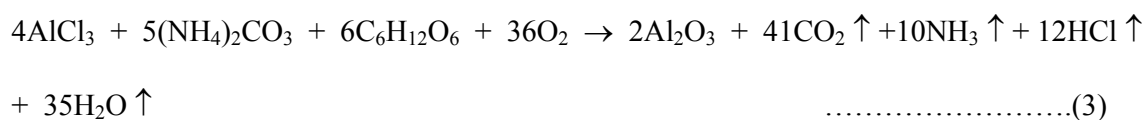


Fig.3.1: Schematic diagram showing synthesis of mesoporous alumina by solid state mechanochemical approach and its utilization as a sorbent in concentration of ^{131}I .

3.3.1 Synthesis and characterization of mesoporous alumina

Mesoporous alumina was synthesized by solid state mechanochemical reaction of aluminum chloride with ammonium carbonate and glucose, followed by calcination at 600 °C. On mechanical grinding of aluminum chloride with ammonium carbonate in presence of glucose, a mixture was formed. The mean diameter of agglomerated particles was 40.1 µm as particle size distribution shown in Fig. 3.2. On heating at 600 °C, the reaction mixture decomposed with evolution of gaseous products, such as, CO₂, NH₃, HCl and H₂O. Evolution of these gases was responsible for increasing the porosity of the material. Especially, the presence of glucose template was responsible for formation of the mesoporous structure as thermal decomposition of the carbonaceous material led to evolution of CO₂ gas, which prevented collapsing of the pores during the calcination step [59]. The balanced chemical reaction for this process can be written as:



The final material obtained after sieving was granular and demonstrated free flowing characteristics. The mean diameter of agglomerated particles was 58.3 µm as per the particle size distribution study (shown in Fig. 3.3) with good mechanical integrity for use as a sorbent in column chromatography applications.

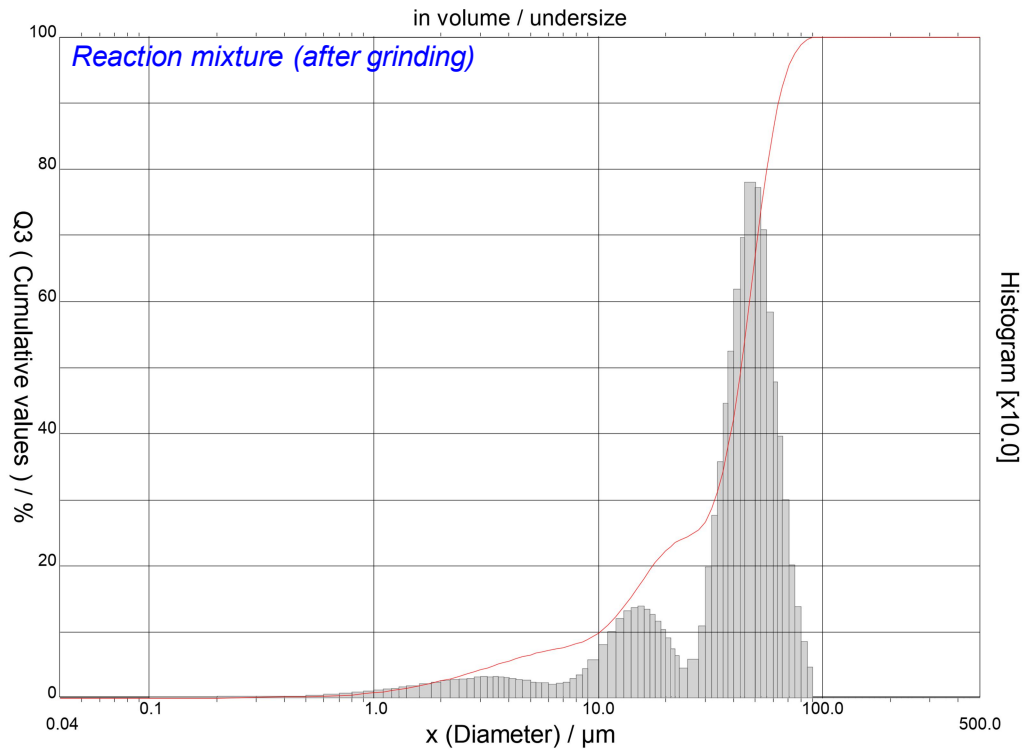


Fig. 3.2: Particle size distribution of the reaction mixture after grinding

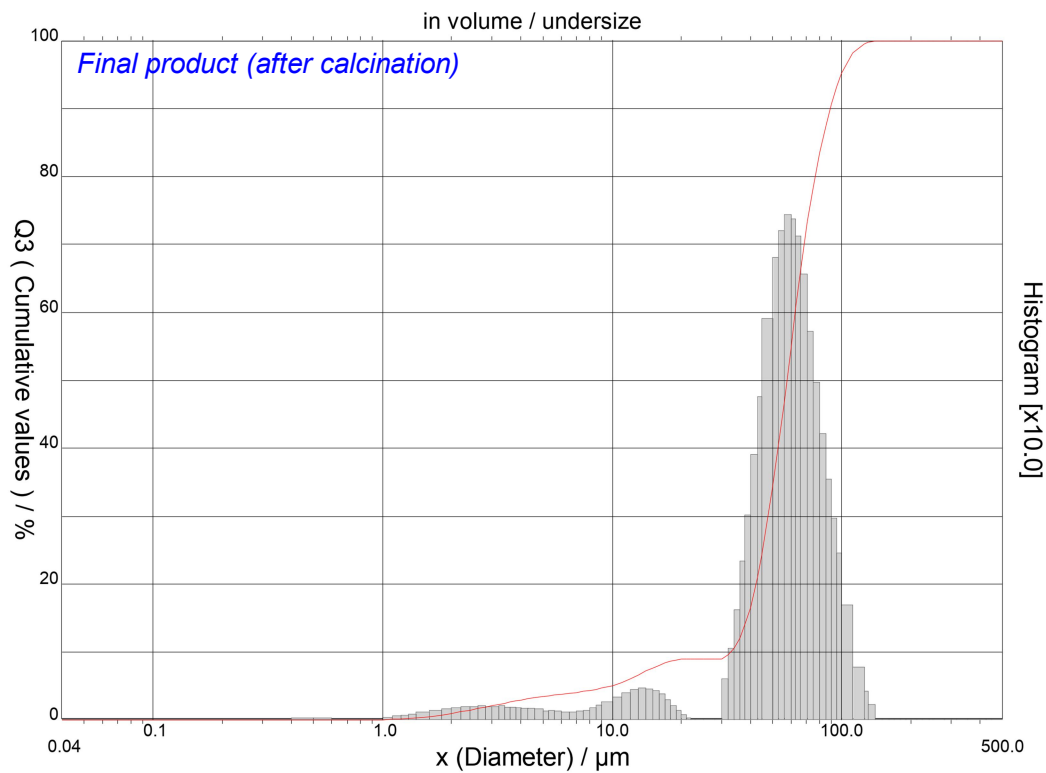


Fig. 3.3: Particle size distribution of the product after calcination

The XRD pattern of mesoporous alumina showed that the material was nanocrystalline and comprised of cubic γ -phase (Fig. 3.4). The peaks in the XRD pattern could be assigned to (3 1 1), (4 0 0), (5 1 1) and (4 4 0) planes of cubic alumina (space group. Fd3m, $a = 7.905 \text{ \AA}$). The average crystallite size of the nanoparticles as determined from the XRD studies using standard Scherrer's formula was $12 \pm 2 \text{ nm}$ [59] which was calculated from the full length and half-maximum (FWHM) of the (4 0 0) peak as given below.

$$D = \frac{0.9\lambda}{B_{2\theta} \cos \theta_{\max}} \dots\dots\dots (4)$$

where, D is the average crystallite size in \AA , λ is the characteristic wavelength of X-ray used (1.5406 \AA), 2θ is the diffraction angle, $B_{2\theta}$ is the angular width in radian at an intensity equal to half of the maximum peak intensity after correcting it for instrumental line broadening.

The SEM micrograph indicated that the synthesized material was porous (Fig. 3.5). The chemical characterization of mesoporous alumina was carried out by EDS, which showed peaks corresponding to Al, O, Cl and C (Fig. 3.6). The light brownish coloration in the sample is due to the presence of carbonaceous material, which could not be completely removed during the calcination procedure. The TEM micrograph of the material showed that was nanocrystalline but highly agglomerated (Fig. 3.7). Agglomeration of nanoparticles is essential in order to utilize them as sorbents for column chromatography applications [55, 59]. As determined from the TEM, the crystallite size of the nanoparticles varied in the range of 10-15 nm and it thus substantiated the results obtained from XRD studies.

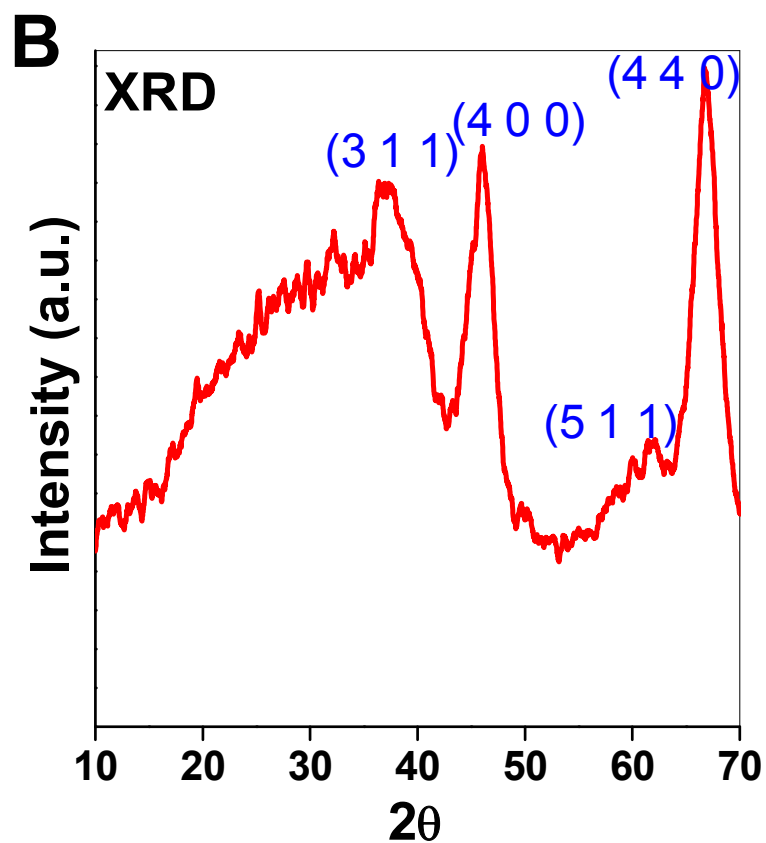


Fig. 3.4: XRD pattern of mesoporous alumina.

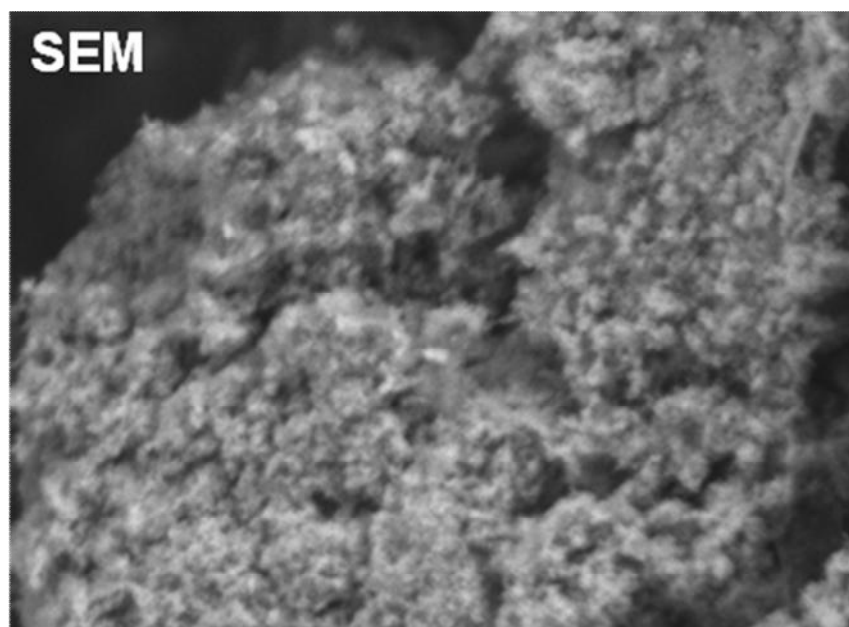


Fig. 3.5: SEM image of mesoporous alumina.

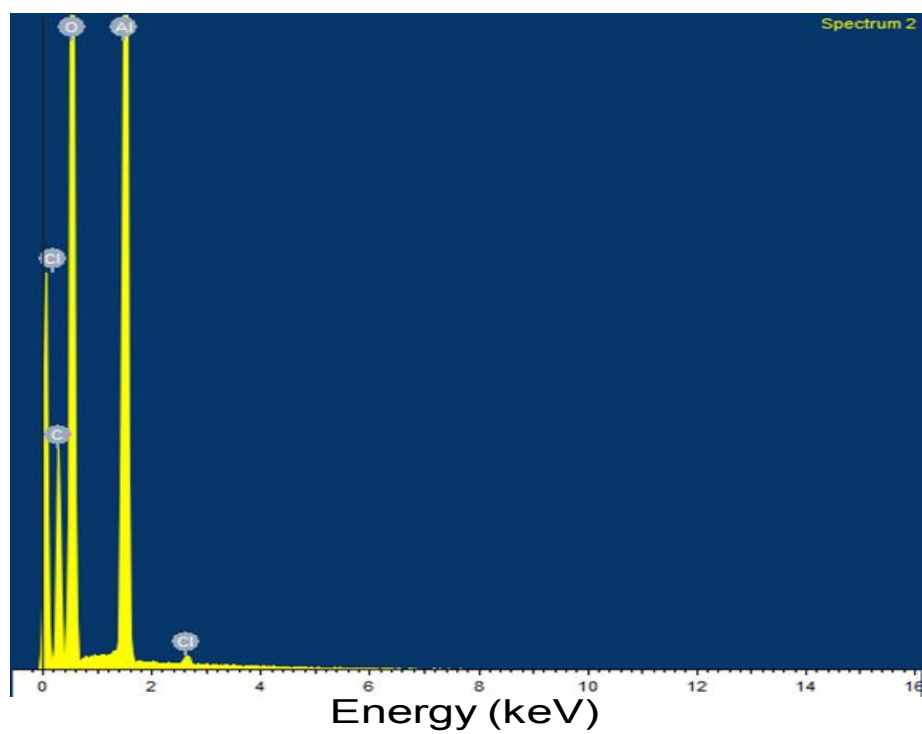


Fig. 3.6: EDS spectrum of mesoporous alumina

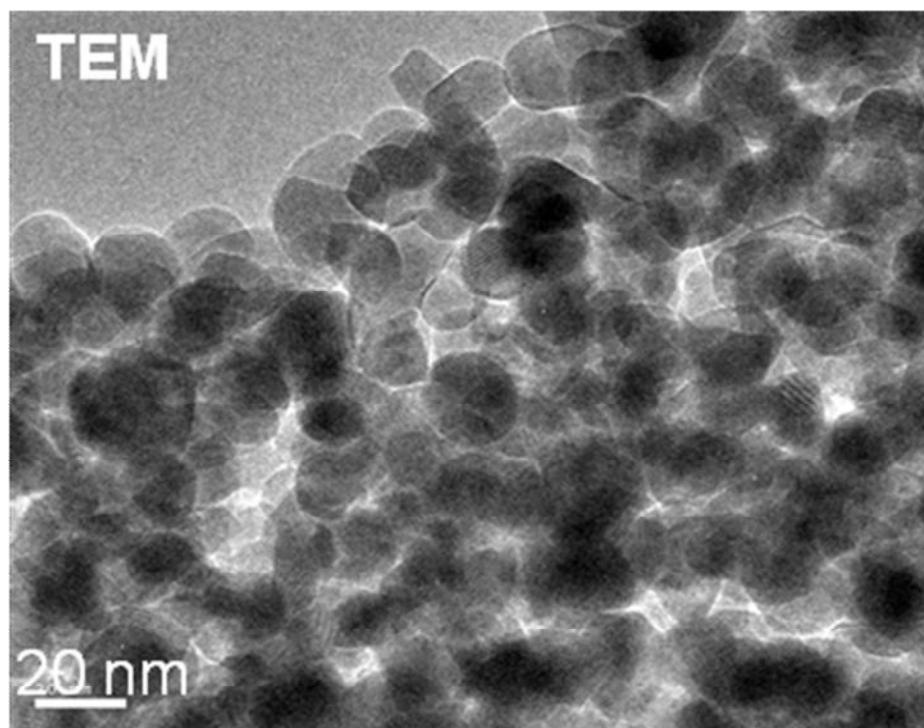


Fig. 3.7: TEM image of mesoporous alumina.

The porosity of synthesized material was evaluated by SANS/SAXS study (Fig. 3.8) [59, 77]. The SANS and SAXS measurements on the sample were carried out to access low and high wave vector transfer regime, ($q = 4\pi\sin\theta/\lambda$, 2θ is the scattering angle and λ is the wavelength of probe radiation), respectively. A double crystal based medium resolution small angle neutron scattering (MSANS) instrument [78] located at Dhruva reactor, Mumbai, India has been used to access low q scattering whereas SAXS measurements have been carried out using a laboratory based set up for accessing high q . Due to reciprocity relation between q and real space dimension, it is evident that MSANS instrument probes larger length scales in the material whereas SAXS instrument probes smaller length scale. The combined SANS/SAXS profile depicted in Fig. 3.8 (i) does not show any diffraction peak indicating the absence of ordered pores. The polydisperse sphere model is appropriate for fitting high- q data whereas the low- q data can be well represented by fractal model in such mesoporous materials [78]. The pore size distribution obtained from the scattering profile is shown in Fig. 3.8 (ii). The average pore diameter of mesoporous alumina was estimated to be 6.8 ± 0.7 nm from this study and therefore the synthesized material could be considered as mesoporous. The porosity of the material was also analyzed by conventional nitrogen adsorption-desorption process. The nitrogen adsorption-desorption isotherm of the material is of type V and the pore size was estimated to be 6.2 ± 0.4 nm, in accordance with the findings from the SAXS study (Fig. 3.9). The surface area of the material as estimated by BET method was 292 ± 28 m²/g, which was appreciably high for the material to demonstrate high ¹³¹I sorption capacity.

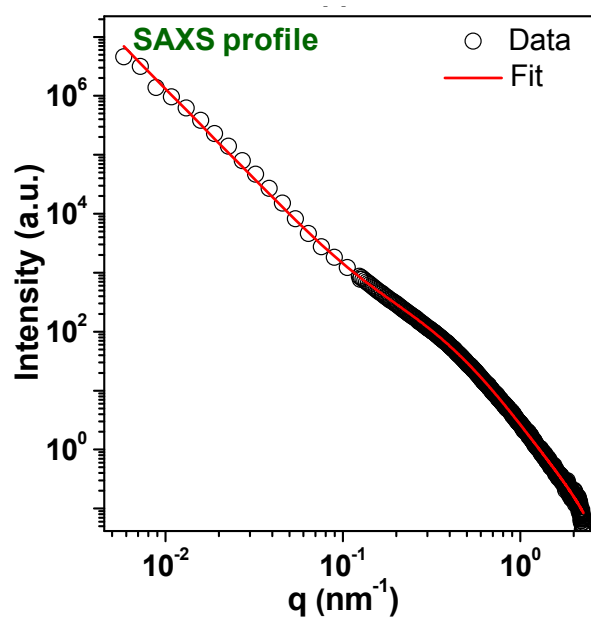


Fig. 3.8 (i) Combined SANS and SAXS profile of mesoporous alumina plotted on a double logarithmic scale.

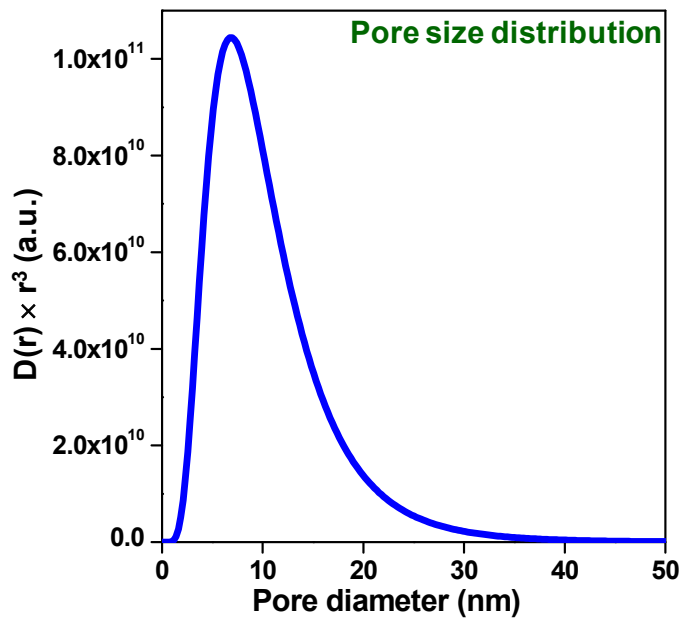


Fig. 3.8 (ii) Pore size distribution as obtained from the scattering profile.

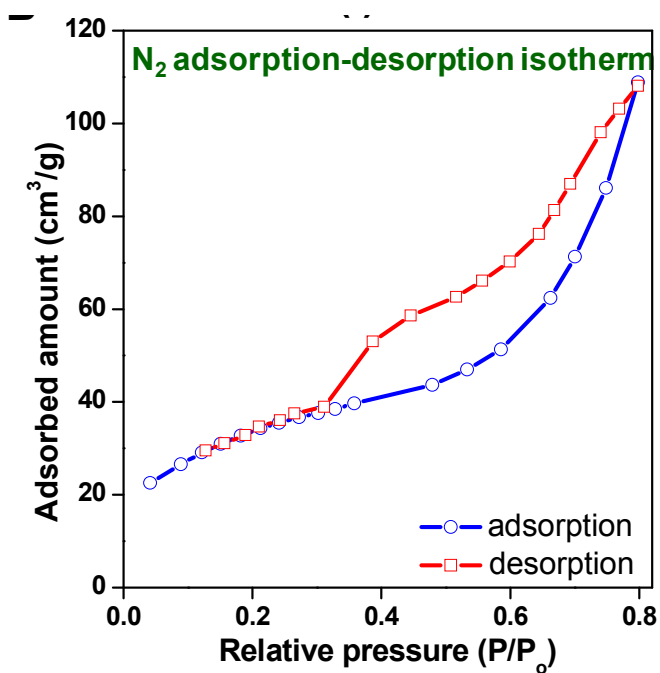


Fig. 3.9 (i): Nitrogen adsorption/desorption isotherms for mesoporous alumina.

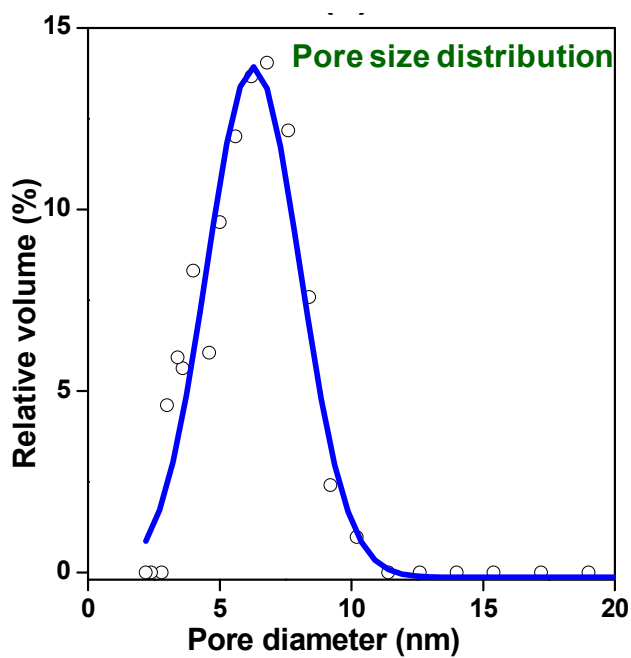


Fig. 3.9 (ii): Pore size distribution as obtained from nitrogen absorption-desorption study.

3.3.2 Zeta potential of mesoporous alumina

The effective electric charge on the surface of mesoporous alumina was determined at different pH environments by measuring the corresponding zeta potential. In order to understand the pH dependent sorption characteristics of mesoporous alumina, its zeta potential was determined by dispersing the sorbent in solutions of different pH (Fig. 3.10). When dispersed in aqueous medium, mesoporous alumina particles are hydrated, and Al-OH groups cover their surface completely. These amphoteric -OH groups can undergo reaction with either H^+ or OH^- and develop positive or negative charges on the surface depending on the pH. The zeta potential of the sorbent was positive in the acidic pH range of 1-6. On further increase in pH, the zeta potential became zero (attained isoelectric point) between pH 6 and 7. The zeta potential became increasingly negative with further rise in pH of the medium (Fig. 3.10). The magnitude of the zeta potential provides information about particle stability, with particles with higher magnitude zeta potentials exhibiting increased stability due to a larger electrostatic repulsion between particles. From the results of this study, it was expected that the positively charged sorbent would adsorb negatively charged $^{131}I^-$ ions under acidic conditions, which could subsequently be retrieved in alkaline medium when surface charge on the sorbent was negative.

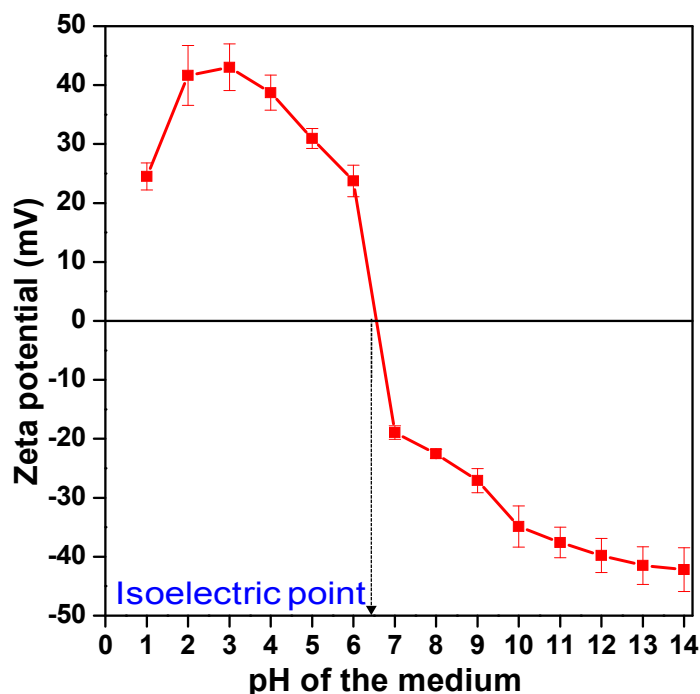


Fig. 3.10: Zeta potential of mesoporous alumina at different pH.

3.3.3 Sorption characteristics of mesoporous alumina

The distribution coefficient (K_d) is a measure of affinity of the sorbent towards iodide ion.

This phenomenon was practically demonstrated by determining the K_d values for I^- ions in mesoporous alumina sorbent (Fig. 3.11). As expected, the K_d values for I^- ions were high under acidic conditions and attained the maximum value at $pH \sim 3$, when the positive surface charge on the sorbent was maximum. Therefore, this medium was most suitable for attaining highest ^{131}I (in the form of I^- ions) sorption. However, it is well known that highly acidic conditions enhance the chances of oxidation of NaI to elemental (free) iodine, thereby, increasing the volatility of ^{131}I solution [74, 79]. Therefore, $pH \sim 6$ was considered to be the most suitable medium for sorption of ^{131}I in mesoporous alumina. At $pH \sim 13$, the K_d value of I^- was negligibly low and hence was suitable for elution of ^{131}I . The sorption equilibrium was attained within 20 min, which indicated reasonably fast kinetics (Fig. 3.12).

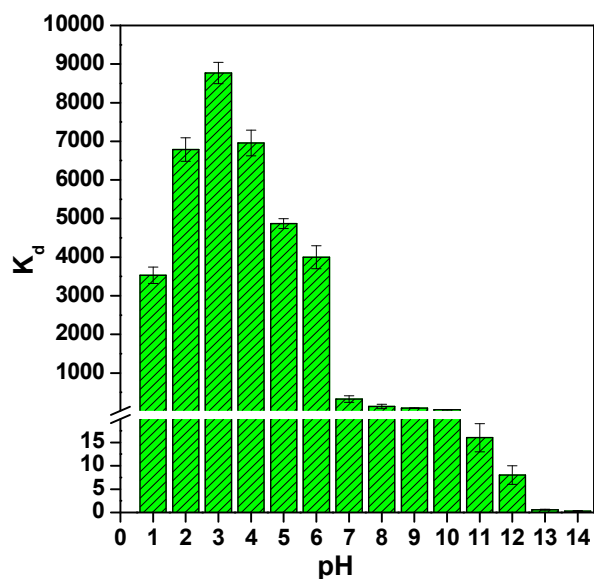


Fig. 3.11: K_d values for I^- ions in mesoporous alumina sorbent at different pH.

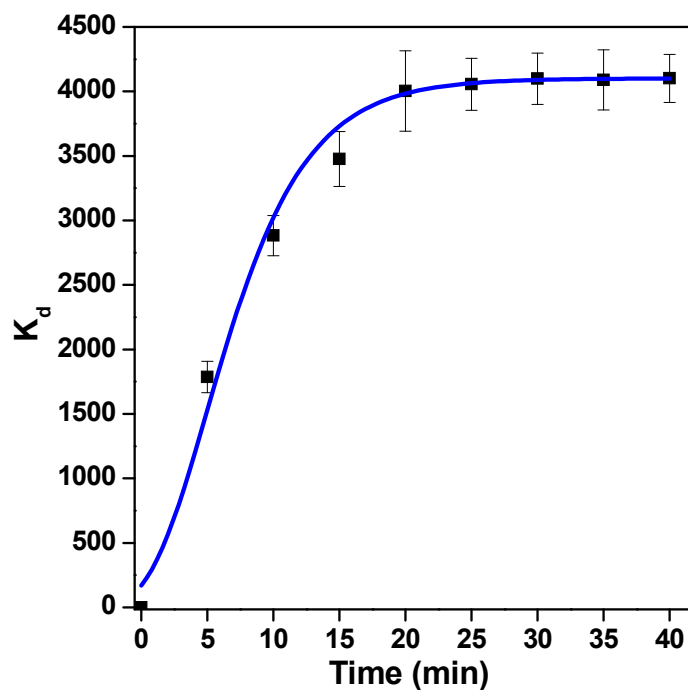


Fig. 3.12: Kinetics of I^- sorption in mesoporous alumina.

Under batch equilibration conditions, the sorption capacity of mesoporous alumina was determined to be 30.2 ± 1.8 mg I^- ions per g of sorbent. The practical sorption capacity was

determined from the breakthrough profile developed by passing I^- ions through a chromatographic column containing mesoporous alumina, at a flow rate of 0.5 mL/min (Fig. 3.13). The breakthrough capacity was determined to be 10.3 ± 0.7 mg I^- ions per g of sorbent. This essentially means that > 200 GBq (> 5.4 Ci) of no-carrier added (NCA) ^{131}I could be quantitatively adsorbed by passing the radioactive solution through a small chromatographic column packed with just 200 mg of mesoporous alumina sorbent.

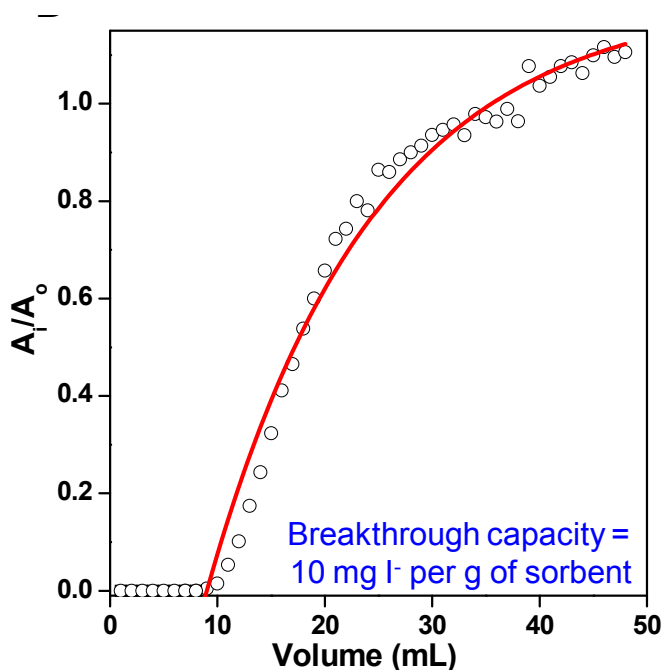


Fig. 3.13: Breakthrough profile of ^{131}I in a column packed with 200 mg of mesoporous alumina sorbent. The radioactive solution was passed through the column at a flow rate of 0.5 mL min^{-1} .

3.3.4 Desorption characteristics of mesoporous alumina

For elution of ^{131}I sorbed in mesoporous alumina column, a minimum concentration of 0.1 M of NaOH solution was required to achieve $> 90\%$ elution yield (Fig. 3.14). The elution

behavior of ^{131}I from the chromatographic column was highly dependent on the flow rate of elution (Fig. 3.15). An optimal flow rate of 0.5 mL min^{-1} was found adequate for achieving > 90 % elution yield. The elution profile of ^{131}I at a flow rate of 0.5 mL min^{-1} was reasonably sharp and near quantitative elution of ^{131}I could be achieved in just 2 mL volume of eluent (Fig. 3.16).

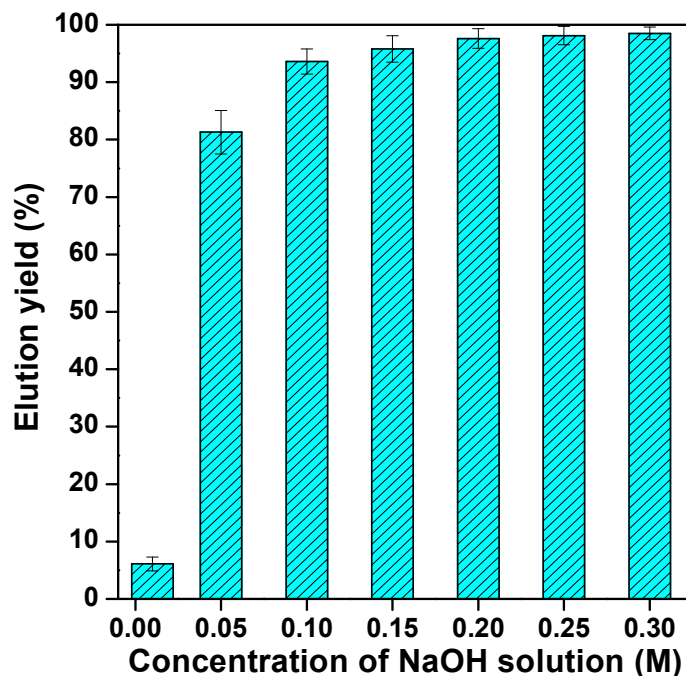


Fig. 3.14: Optimization of the concentration of NaOH solution for elution of ^{131}I adsorbed in the column.

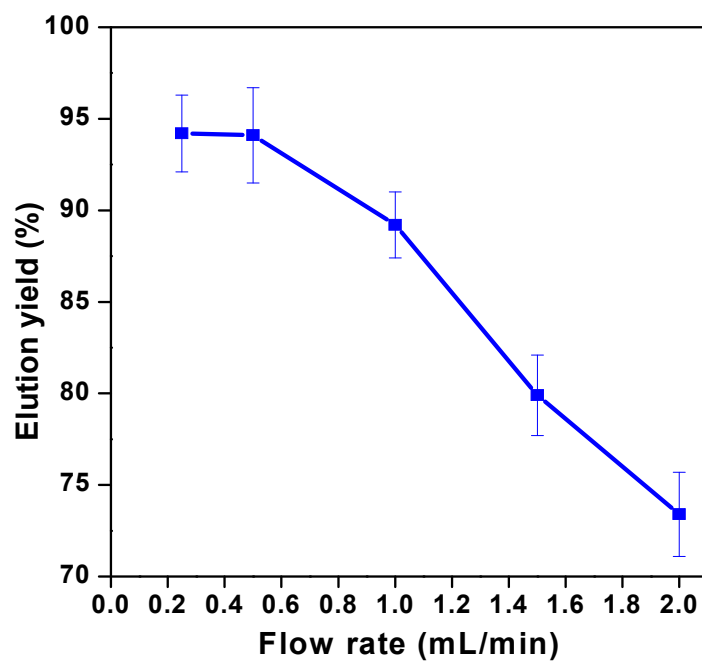


Fig. 3.15: Optimization of flow rate of elution.

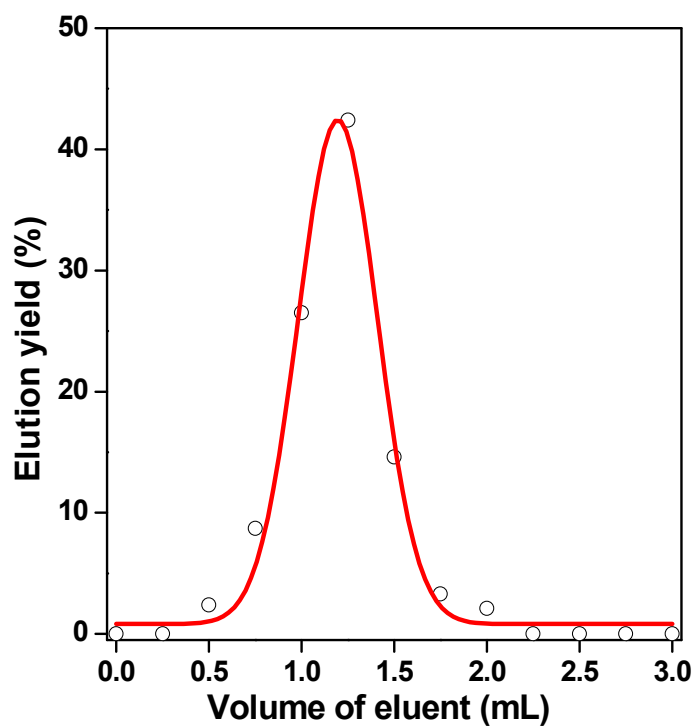


Fig. 3.16: Elution profile of ^{131}I .

3.3.5 Process demonstration for increasing radioactive concentration of ^{131}I

The column chromatographic concentration process was demonstrated by using solutions simulated to represent different activity levels of ^{131}I , prepared by adding requisite quantity of NaI carrier in tracer level of ^{131}I solutions maintained at pH ~ 6 and the results are summarized in Table 3.1. It can be seen from the table that irrespective of the initial activity and volume of ^{131}I feed solution; the final product could be obtained in just 2 mL of 0.1 M NaOH solution with $> 90\%$ yield. The radiochemical purity of the concentrated ^{131}I in the form of I^- ions is an important quality control parameter to determine its suitability for use in nuclear medicine [76]. By paper electrophoresis method, it was found that the radiochemical purity of ^{131}I was $> 98\%$ (Fig. 3.17). The presence of Al ions as chemical impurity in the concentrated ^{131}I -NaI solution could not be detected by ICP-AES analysis (detection limit $0.01\text{ }\mu\text{g/mL}$). The maximum radioactive concentration of ^{131}I that could be attained by this chromatographic process was 1.7 TBq mL^{-1} ($\sim 45\text{ Ci}$), which was more than adequate for preparation of large dose ($> 7.4\text{ GBq}$ per capsule) therapeutic capsules for use in nuclear medicine.

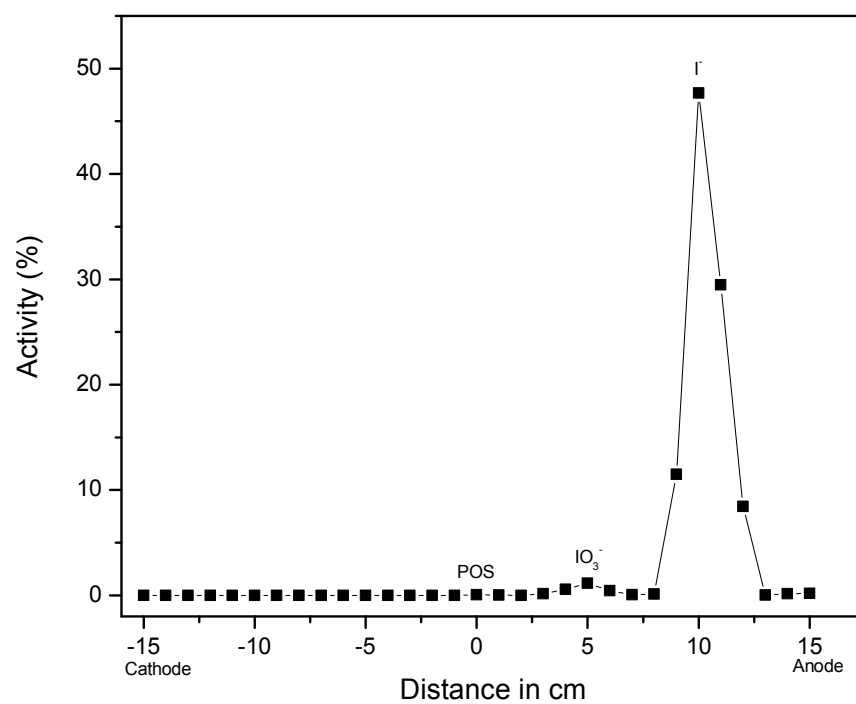


Fig. 3.17: Paper electrophoresis pattern of ^{131}I solution obtained after the concentration procedure.

Table 3.1: Concentration of ^{131}I by solid phase extraction procedure

Batch No.	Simulated activity of ^{131}I in the feed solution GBq (Ci)	Before concentration procedure		After concentration procedure		Percentage of initial ^{131}I activity recovered in the final concentrated solution (%)
		Initial volume of solution mL	Initial radioactive concentration GBq/mL (Ci/mL)	Final volume of solution mL	Final radioactive concentration GBq/mL (Ci/mL)	
1	37 (1)	10	3.7 (0.1)	2	17.3 (0.46)	93.6
2	37 (1)	20	1.9 (0.05)	2	17.4 (0.47)	94.1
3	37 (1)	50	0.7 (0.019)	2	17.1 (0.46)	92.7
4	74 (2)	10	7.4 (0.2)	2	34.4 (0.93)	92.9
5	74 (2)	20	3.7 (0.1)	2	34.4 (0.93)	93.1
6	74 (2)	50	1.5 (0.04)	2	34.3 (0.93)	92.8
7	740 (20)	10	74.0 (2)	2	341.5 (9.23)	92.3
8	740 (20)	20	37.0 (1)	2	345.2 (9.33)	93.3
9	740 (20)	50	14.8 (0.4)	2	348.5 (9.42)	94.2
10	1480 (40)	20	74.0 (2)	2	688.9 (18.62)	93.1
11	1480 (40)	50	29.6 (0.8)	2	692.6 (18.72)	93.6
12	3700 (100)	100	37.0 (1)	2	1713.1 (46.3)	92.6

3.4. Conclusions

The objective of developing a column chromatographic process for post-processing concentration of ^{131}I has been successfully accomplished. Adequately high radioactive concentration of ^{131}I could be achieved and it met the requirements for clinical use. The proposed chromatographic method is simple, rapid, efficient and amenable for automation. This study also demonstrates the practicality of solid state mechanochemical approach for synthesis of 'new generation' sorbent materials for use in solid phase extraction procedures. Widespread adoption of this procedure is expected to enhance the cost-effective availability of large-dose therapeutic ^{131}I capsules for the benefit of millions of thyroid cancer patients all over the world.

CHAPTER-4

Formulation of Patient Dose of ^{131}I -Lipiodol and Its Clinical Utilization for the Treatment of Hepatocellular Carcinoma

“mahāpurisabhāvassa lakkhaṇaṃ karuṇāsaho”

“To be moved by compassion is a character of a great person”

HRH Prince Vajirañāṇavarorasa

4.1 Introduction

Hepatocellular carcinoma (HCC) is the most common type of liver cancer, with an annual global incidence of more than 1 million and is the third highest cause of cancer related deaths worldwide [80-82]. Especially in the Asian and African regions, it is the most frequent cause of cancer-induced deaths [83, 84]. The high incidence of HCC in developing countries is mostly due to the high rates of chronic hepatitis B virus (HBV) infection and higher dietary exposure to the fungal aflatoxin B1 [85]. Because of the late appearance of symptoms of HCC, the disease commonly presents in an inoperable scenario with poor patient prognosis and > 95 % of patients do not survive five years past the initial diagnosis [86, 87]. Resective surgery is an efficacious treatment modality but practically possible only for 10-37 % of HCC patients due to complications arising from concomitant cirrhosis and loss of hepatic function [88, 89]. Systemic chemotherapy with various known anti-cancer agents also has proven singularly ineffective for treatment of the disease in terms of survival benefit [80, 90, 91], while external beam radiotherapy, in view of the radiosensitivity of normal hepatic tissue, carries the risk of radiation induced liver disease (RILD) [92].

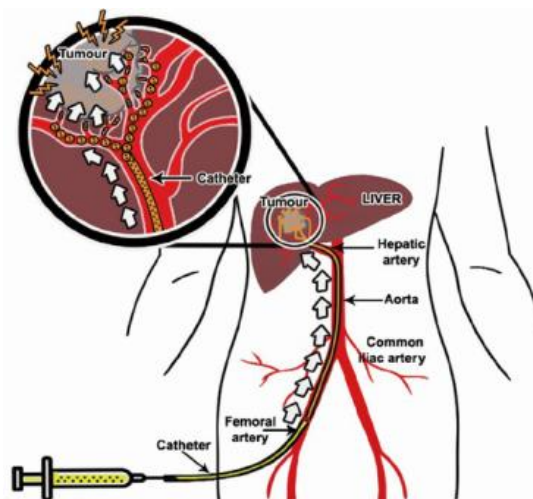


Fig. 4.1: Schematic of injection of therapeutic agent via hepatic artery to liver cancer

80-85 % of normal liver tissue is primarily supplied with nutrients and oxygen via the portal vein. And neoangiogenic vessels provide blood supply to growing tumors, is primarily fed by the hepatic artery as shown in Fig. 4.1. Hence, intra-arterial injection of therapeutic agent is expected to preferentially localize in the region of growing tumors with minimal accumulation in adjacent normal liver tissue, thus offering an effective treatment modality for primary HCC and for liver metastases of tumors of other origin. This is the principle of Trans-Arterial Chemo-Embolization (TACE). For locoregional therapy, TACE using drugs like cisplatin, doxorubicin, methotrexate, paclitaxel has been employed in conjunction with Lipiodol [93-95] where Lipiodol serves as both drug carrier and embolizing agent. Intra-vascular retention of Lipiodol leads to starvation of tumor cells of nutrients and oxygen supply and deliver high doses of the drug(s) loco-regionally, which provides greater chemotherapeutic effect than the systemic route. Embolization in conjunction with a radiotherapy agent is known as radio-embolization. There are two main categories of radio-embolic agents approved for clinical use [96]. First category is based on micron-range particulates that encapsulate or adsorb therapeutic radionuclides, like ^{90}Y -bearing glass spheres (Therasphere[®]) and polymeric selective internal radiation spheres (SIR-spheres[®]). Another is Lipiodol or related embolic substances tagged with therapeutic radionuclide. Lipiodol or Ethiodised oil is a mixture of naturally iodinated fatty acid ethyl esters of poppy seed oil (37%w/w of iodine), including Ethyl 9, 10 di-iodostearate, iodinated ethyl ester (Fig. 4.2) [97, 98]. However, the exact structure of Lipiodol is not known. It is employed as a magnetic resonance imaging (MRI) contrast agent for the liver and has also been labeled with therapeutic radionuclides such as ^{131}I and ^{188}Re for HCC treatment. ^{131}I -Lipiodol was the first radiolabeled agent to be used for the treatment of HCC [99]. Rhenium-188-N-(DEDC)₂ /Lipiodol (abbreviated as $^{188}\text{ReN-DEDC}$, where DEDC = monoanionic diethyldithiocarbamate) is also used for the therapy of unresectable HCC through Trans Arterial Radio-Embolization (TARE) [100].

Isotopic exchange is used to label iodine rich Lipiodol with ^{131}I to prepare radioiodinated Lipiodol, while ^{188}Re -labeled 4-hexadecyl-1-2,9,9-tetramethyl-4,7-diaza-1,10-decanethiol (HDD) is dispersed in Lipiodol for ^{188}Re -labeled radioembolizing agent [101]. A comparison of major radioembolic agents is given in Table 4.1. ^{188}Re -HDD/Lipiodol has the advantage of shorter radionuclidic half-life (16.9 h), but it calls for the use of $^{188}\text{W}/^{188}\text{Re}$ generator and requires specialized facilities for labeling and quality control of therapeutic radiopharmaceutical at the hospital radiopharmacy. Requirement of double neutron capture reaction for ^{188}W production limits the availability of $^{188}\text{W}/^{188}\text{Re}$ generators. However, compared to generator produced ^{188}Re , ^{131}I radioisotope is available at a lower cost due to its reactor production route and dry distillation processing method [76]. ^{131}I is easily produced by irradiation of Tellurium target in nuclear reactors and the dry distillation process for ^{131}I production leads to availability of large quantities of ^{131}I on regular basis as described in Chapter 2. Low cost of ^{131}I -Lipiodol compared to other agents makes it a promising therapeutic agent especially for cancer patients in developing countries [102]. ^{131}I -Lipiodol can be prepared and supplied from a centralized radiopharmacy owing to suitable half-life of ^{131}I , allowing convenient logistics of production and quality control checks prior to patient administration.

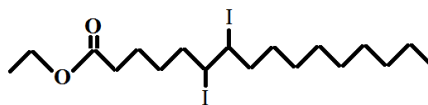


Fig. 4.2: Ethyl 9, 10 di-iodostearate, iodinated ethyl ester

Table 4.1: Therapeutic agents used in treatment of hepatocellular carcinoma (HCC)

	Glass spheres (Therasphere®)	Polymeric SIR- spheres®.	¹⁸⁸ Re-HDD- Lipiodol	¹³¹ I-labeled Lipiodol
Radioisotope	⁹⁰ Y	⁹⁰ Y	¹⁸⁸ Re	¹³¹ I
Nuclear Emissions	E _{βmax} : 2.28 MeV No γ	E _{βmax} : 2.28 MeV No γ	E _{βmax} : 2.12 MeV, 1.97 MeV E _γ : 155 keV	E _{βmax} : 610 keV E _γ : 364 keV; 637 keV
Half-Life	64.1 h	64.1 h	17 h	8 d
Production route of radionuclide	⁹⁰ Sr/ ⁹⁰ Y Generator	⁹⁰ Sr/ ⁹⁰ Y Generator	¹⁸⁸ W/ ¹⁸⁸ Re Generator	Nuclear Reactor
Material	Glass	Resin	Oil	Oil

Biodistribution, *in-vivo* kinetics and dosimetry of ¹³¹I-Lipiodol was first reported in the year 1988 [103-105]. Since then, a number of studies by various groups have reported improved recurrence-free and overall survival benefit with ¹³¹I-Lipiodol compared with surgery alone in an adjuvant setting and in a palliative setting in patients with HCC and portal vein thrombosis (PVT). Efficacy of the agent was also compared with chemoembolization and in the patients with advanced clinical staging or PVT and it was found that there was a significant survival advantage for patients treated with ¹³¹I-Lipiodol [101]. This agent was also reported to be useful for small nodules not accessible for surgery or percutaneous treatment [106]. European Association of Nuclear Medicine (EANM) guidelines for ¹³¹I-Lipiodol therapy were reported in the year 2011 mentioning standard activity of 2.22 GBq (60 mCi) ¹³¹I-Lipiodol for administration in patients by slow intra arterial injection under

fluoroscopic guidance [107]. Overall ^{131}I -Lipiodol is reported as a safe and effective treatment for patients with HCC and PVT in an adjuvant setting after surgical resection [108-110]. Lipiocis[®] (^{131}I -Lipiodol) is licensed in France for the treatment of patients with HCC and PVT. However, till now in India, there was no indigenous source of radioiodinated Lipiodol and the imported radiopharmaceutical formulation is less favorable in terms of convenient logistics to the clinic and economic affordability to the patient. Additionally, the high-energy gamma radiations (364 keV, 81 % abundance) of ^{131}I pose considerable safety related limitations for preparation of patient doses of ^{131}I -Lipiodol with high amounts of initial activity ($> 3.7 \text{ GBq}$) of ^{131}I . Few reports are available on the preparation of therapeutic radiopharmaceuticals using automated or semi-automated modules [111, 112]. Hence, a semi-automated modular system was designed and fabricated to ensure operator safety, as well as pharmaceutical purity and safety of the product. Quality control tests were carried out to estimate radiochemical yield (RCY), radiochemical purity (RCP) and to determine sterility and apyrogenicity of the preparation. Preclinical evaluation was done in Wistar rats to ascertain liver retention of ^{131}I -Lipiodol. Preparation of patient dose of ^{131}I -lipiodol using the semi-automated module, quality control analysis of the product and evaluation of the agent in patients with histologically confirmed HCC for its clinical utilization has been described in this chapter.

4.2 Characteristics of ^{131}I -Lipiodol

Basic characteristics of ^{131}I -Lipiodol:

- ^{131}I is a beta emitting radionuclide with a physical half life of 8.02 days.
 - The maximum and mean beta particle energies are 0.61 MeV and 0.192 MeV respectively.
 - Additionally, ^{131}I emits a principal gamma photon of 364 keV (81% abundance).
-

- The beta radiation of ^{131}I is responsible for its therapeutic effects while gamma radiation makes the distribution of the radiopharmaceutical visible through imaging.
- As iodine is an integral part of lipiodol, its radiolabeling with ^{131}I is by simple exchange method.

4.3 Radiolabeling process optimization for ^{131}I -Lipiodol formulation

4.3.1 Materials and methods

a) Materials

Lipiodol[®] Ultra Fluid, 4.8 g Iodine per 10 mL (38 % w/w) was procured from Guerbet (Asia Pacific). No carrier added (NCA) ^{131}I -sodium iodide solution of > 99.99 % radionuclidic purity, $\sim 18.5 \text{ GBq mL}^{-1}$ radioactive concentration and > 98 % radiochemical purity was produced in-house as described in chapter 2 [76]. Analytical grade ethanol used for cleaning of module was obtained from Brampton, Canada. Whatman 3 MM paper (12 cm \times 2 cm) was used for paper chromatography. During patient dose production, gamma sterilized disposable sterile syringes, needles, gloves, clothing and Polytetrafluoroethylene (PTFE) filters (0.22 μm) were used. All glassware and accessories used for production were cleaned and processed to render them sterile and apyrogenic. Semi-automated module and control panel were fabricated and assembled indigenously at Texol Engineering Ltd, Pune, India. Radioactivity assay of ^{131}I activity was carried out by high-resolution gamma ray spectrometry using an HPGe detector (Eurysis Measures, France) coupled to a 4K multichannel analyzer system. And higher radioactivity measurements were done using pre-calibrated ion chamber. Sterility test kits containing Fluid thioglycollate media and Soybean casein media were obtained from Himedia Laboratories, India. Endotoxin standards and LAL reagents, pyrogen free water for endotoxin detection were procured from Charles River Laboratories India Pvt. Ltd.

4.3.1.1 Design and fabrication of semi-automated module

An independent stand alone modular system suitable for mini hot cell was designed and fabricated for the present work. Schematic of semi-automated module for production of patient dose of ^{131}I -Lipiodol is depicted in Fig 4.3. The module holds two lead pots of 30 mm thickness. The lead pot containing Na^{131}I can easily slide on the base plate of the module and the radioactivity vial gets firmly held with the help of a precisely designed bottle guard plate for safe operations. The reaction vessel assembly is enclosed in a silicon glycerin bath, fitted at rear end of the base plate of the module.

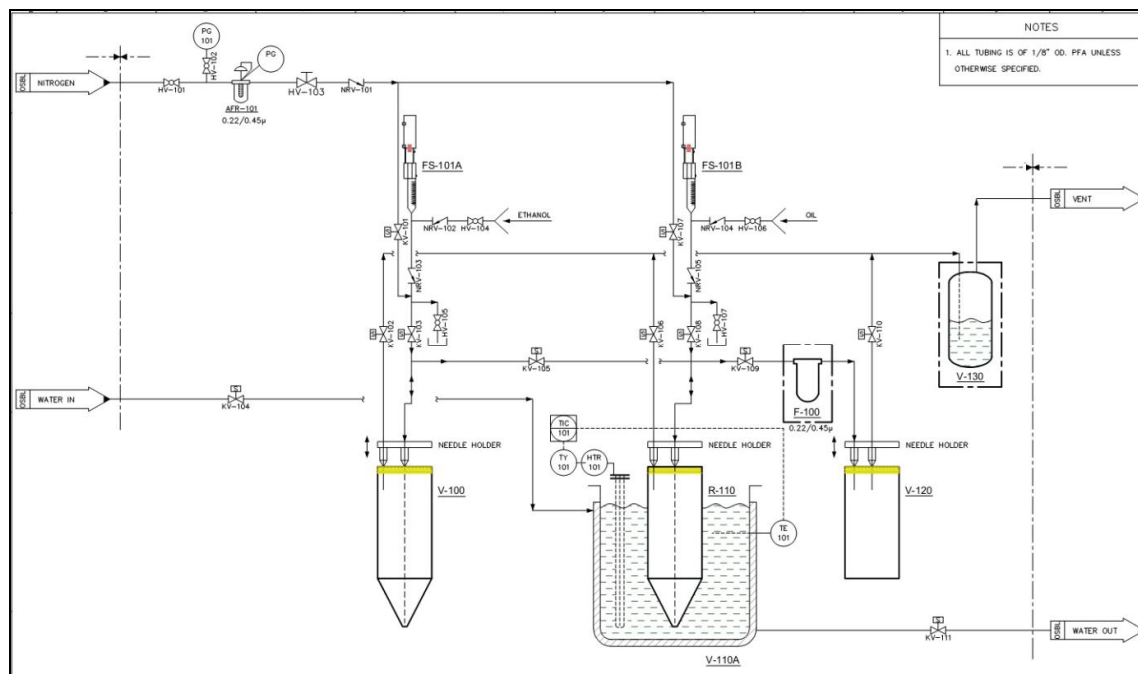


Fig. 4.3: Schematic of semi-automated module for ^{131}I -Lipiodol processing

Facility is made for remote addition of reagents to vial containing Na^{131}I activity as well as to reaction vessel. The heating of reaction vessel is precisely carried out in a heating oil bath using K-type thermocouple as sensor. Pressurized high purity nitrogen gas is used for transfer of all solutions through tubings connected to solenoid valves which are mounted on SS plate and connected to junction box. The valves, tubing and connectors used for fabrication are

compatible with organic solvents.

The module is placed inside indigenously designed and fabricated shielded facility similar to commercially available mini hot cell with adequate lead shielding having negative pressure and charcoal filters fitted at release duct. For external surface sterilization of this set-up ultraviolet light is installed and kept on for minimum three hours prior to formulation of the agent. Electrical valve operations and heating controls are placed separately on control panel, which are operated manually by simple on/off switch away from module. The system could be upgraded to PLC (Programmable Logic Controller) based operations, if desired. Valve operation sequence was standardized based on optimized reaction parameters. Step-wise scaling-up of reaction was carried out towards preparation of patient dose. Radiation field, air activity and activity released through charcoal trap were monitored during all operations.

4.3.2 Preparation of ^{131}I -Lipiodol using module

Isotope exchange reaction between organic iodine of Lipiodol with ionic ^{131}I was carried out with slight modifications in the reported procedure [96]. The initial standardization of optimum time and temperature for formulation of ^{131}I -Lipiodol was carried out. During this standardization trace amounts of radioiodine was used and volume of aqueous ethanol and Lipiodol was kept equal for patient dose formulation. Typically 2 mL of absolute ethanol was injected to the ^{131}I activity (> 740 MBq in 0.1 mL) vial at R_1 as shown in Fig. 4.4 followed by transfer of complete activity (by pressurizing with nitrogen at R_1) into the reaction vessel reactor at R_2 . It was heated to 55 °C by heater (H) for 15 minutes under nitrogen gas flow. 2 mL Lipiodol was injected directly into the reaction vessel R_2 , and the isotopic exchange reaction was carried out by heating Lipiodol with ^{131}I -[NaI] in ethanol at 80 °C for 20 minutes and subsequently, at 100 °C for 30 minutes. The reaction mixture was allowed to cool and the product was transferred to product vial P through 0.22 μm sterile filter F.

Additional 500 μL Lipiodol was added to the reaction vial, mixed and the product was transferred to two other similar (500 μL) vials for quality control analyses. The reaction was monitored for ^{131}I activity measurement at all the stages of production. Radioactive assay of the product was carried out using pre-calibrated ion chamber and yield of the product was calculated. The percentage reaction yield was calculated by measuring activity in the product vials compared to starting activity by applying decay correction. Quality control analysis by physicochemical tests was done immediately after preparation for all the batches of ^{131}I -Lipiodol, while biological tests as per Indian Pharmacopoeia were done after decay of ^{131}I activity. Initial optimization of process parameters for formulation of ^{131}I -Lipiodol was carried out and radiochemical yield was optimized. The product was biologically evaluated by injecting into normal adult Wistar rats.

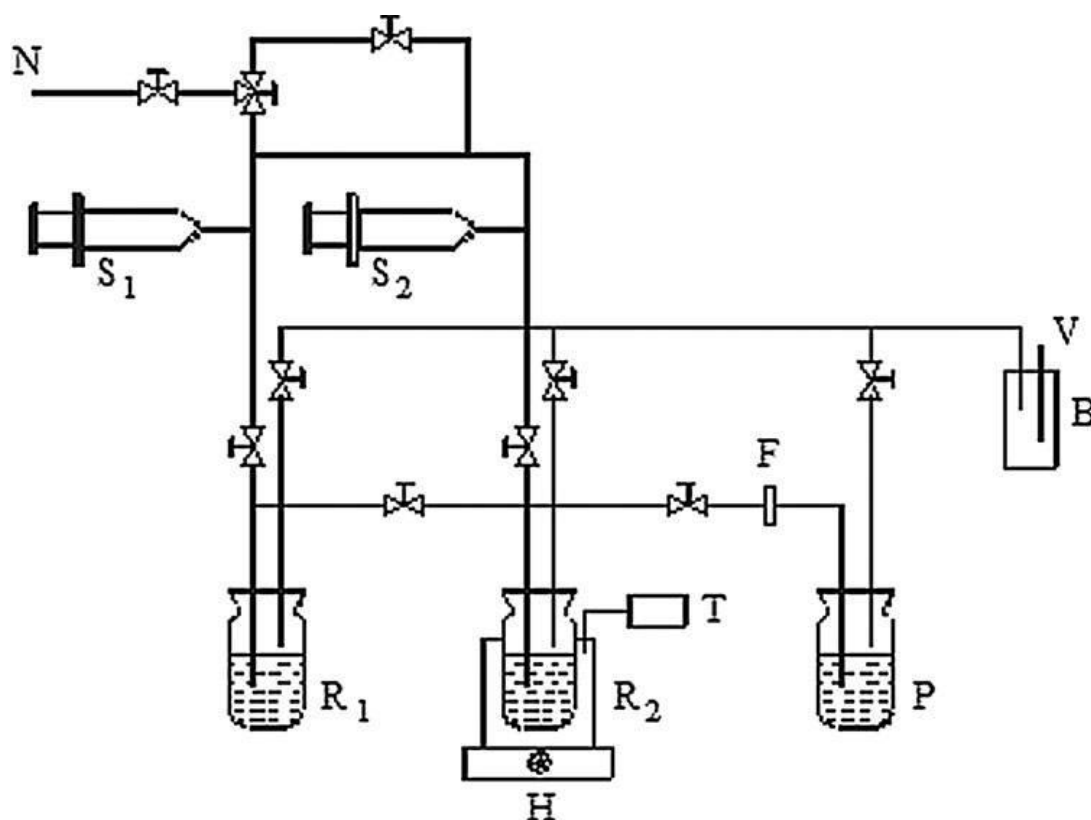


Fig. 4.4: Schematics of the process system for production of ^{131}I -Lipiodol

(B, bubbler; F, sterile membrane filter; H, heater; N, Nitrogen gas inlet; P, sterile apyrogenic product vial; R₁, vial containing Na¹³¹I placed inside a lead pot; R₂, reaction vessel; S₁ and S₂, syringe ports; T, thermocouple; V, vent)

4.3.3 Quality control tests of ¹³¹I-Lipiodol

In-process checks and physicochemical and biological quality control studies were carried out for the finished product.

4.3.3.1 Tests of radionuclide identification and radionuclidic purity

The gamma-ray spectrum of the preparation was taken as per standard procedure of gamma ray spectrometry using a high-purity germanium (HPGe) detector assembly coupled Multi-Channel Analyzer (MCA). The most prominent gamma photon of 364 keV energy was examined to estimate radionuclide purity of ¹³¹I. Not less than 99.9 % of the total activity should be due to ¹³¹I.

4.3.3.2 Assay of radioactivity

The radioactivity in MBq (mCi) per ml of ¹³¹I-Lipiodol shall be measured directly using pre-calibrated ion chamber.

4.3.3.3 Test of radiochemical purity (RCP)

The RCP of ¹³¹I-Lipiodol was determined by paper chromatography. Two microliter aliquots of carrier solution (1.5 % Potassium Iodide solution) and radiolabeled product were spotted on two Whatman 3 MM paper chromatography strips (12 cm × 2 cm), which were then developed in two different solvent systems, namely 85% methanol and ether/petroleum ether

(1:2, v/v), respectively, by ascending chromatography. The movement of ionic $^{131}\text{I}^-$ and the radiolabeled product was measured using NaI (TI) detector. In 85% methanol solvent system, R_f of ^{131}I -Lipiodol is 0 - 0.3 and R_f of iodide ion is 0.8-0.9. In solvent, ethyl ether: petroleum ether (1:2, v/v) R_f of ^{131}I -Lipiodol is 0.9 -1.0 and R_f of Iodide ion is 0 - 0.1. The strips were counted using the radiochromatogram scanner or cut into 1 cm sections and counted in a well-type scintillation counter. The activity at the Lipiodol zone shall not be less than 95 % of the total radioactivity.

4.3.3.4 Stability

The product was stored at 4 °C protected from light and tested repeatedly for RCP using paper chromatography technique as described in the previous section for up to 3 weeks, post-preparation.

4.3.3.5 Sterility and bacterial endotoxin test (BET)

To ensure pharmaceutical purity of the product, sterility and bacterial endotoxin testing (BET) was carried out as per Indian Pharmacopoeia procedures listed in General Chapter on Radiopharmaceuticals [98]. 0.1 mL of ^{131}I -Lipiodol was diluted with 1.9 mL of Lipiodol and used for sterility and BET.

Test for Sterility: 0.6 ml of ^{131}I -Lipiodol is divided equally in fluid thioglycolate and soyabean casein digest media and incubated at 37 °C and 25 °C, respectively with positive and negative controls. Incubation was done for up to 14 days, with repeated optical examination for evidence of microbial contamination.

Bacterial Endotoxin Testing: Product is tested for bacterial endotoxins using *Limulus Amebocyte Lysate* (LAL) reagent test [98]. Bacterial endotoxin content (in Endotoxin Units, EU) not more than 175 EU per V mL, V being maximum recommended dose in mL (or 25

EU/mL). Alternatively the preparation should pass pyrogen test as per Indian Pharmacopoeia. Sterility and BET test may be carried out on decayed sample for each batch. In the event of any batch not complying with sterility or BET tests, the production process needs to be revalidated.

4.3.3.6 Biological evaluation

In-vivo distribution studies of ^{131}I -Lipiodol were carried out in normal adult Wistar rats (male, ~200–225 g). The animals were fasted for 6 hours before the procedure. Approximately 100 μL of ^{131}I -Lipiodol was administered through portal vein following a previously reported protocol of viable surgery under Ketamine: Xylazine (10:1) induced anesthesia [99]. Animals were sacrificed at different time points, and the relevant organs and tissues were dissected. The percentage of injected activity associated with different organs/tissue was determined. Blood, bone and muscle were presumed to account for 7, 10 and 40 % of the total body weight of the animals respectively, and associated radioactivity was extrapolated accordingly [113].

4.4 Formulation of actual patient dose of ^{131}I -Lipiodol for clinical utilization

The process of formulation of patient dose of ^{131}I -Lipiodol was optimized. Initial ^{131}I -[NaI] activity was measured and taken for the required patient dose. The flow sheet of the operation was illustrated in Fig. 4.5

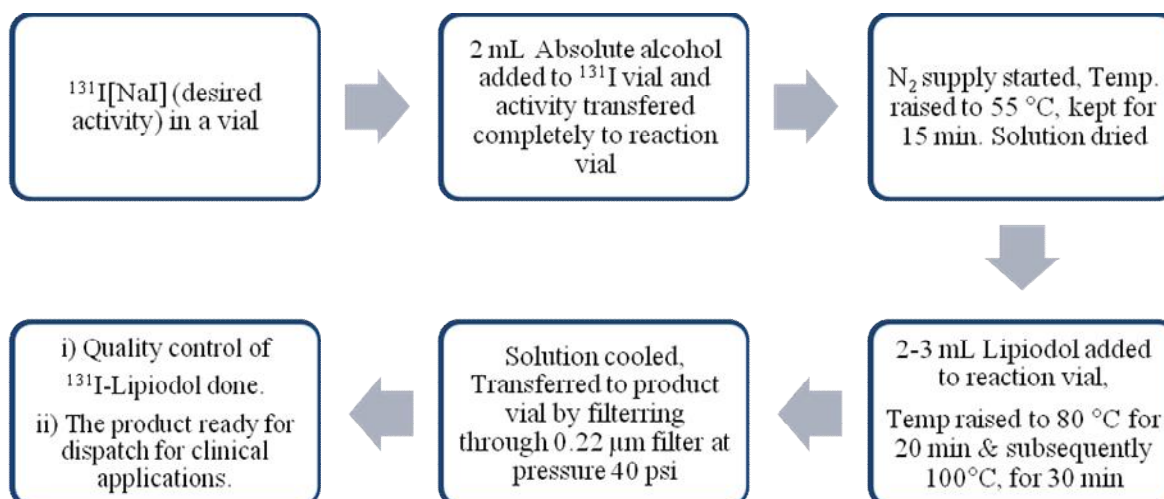


Fig. 4.5: Flow sheet of ¹³¹I-Lipiodol formulation

4.5 Results and discussion

4.5.1 Design and fabrication of Semi-automated module

The fabricated module remotely enables precise liquid transfers and controlled heating leading to consistent yields of radiolabeling when isotope exchange reaction was carried out. The simple remote operating procedures standardized for production of ¹³¹I-Lipiodol considerably reduce dose exposure to the radiation worker and also assured pharmaceutical purity and safety of the product. Fig. 4.3 depicts the schematics of the semi-automated synthesis module. Photograph of module with two lead pots, valve mounting plate, junction box, etc. and control panel illustrated in Fig 4.6 (a) & (b). All the operations during formulation of ¹³¹I-Lipiodol were carried out remotely with the help of control panel kept outside the shielded cell. In this module, ¹³¹I radioactivity is confined safely inside the vials and transferred through tubing and thus reduces free activity inside the cell. The safety features that were included while designing the module resulted in significantly reducing the radiation exposure to the operator. The cleaning and drying procedures of module carried out before the formulation and collection of final product in sterile pyrogen-free vial through sterile membrane filter ensured compliance with good manufacturing practices. The

optimized cleaning protocol after batch preparations removes most of the residual activity, which aids in maintenance of module parts.

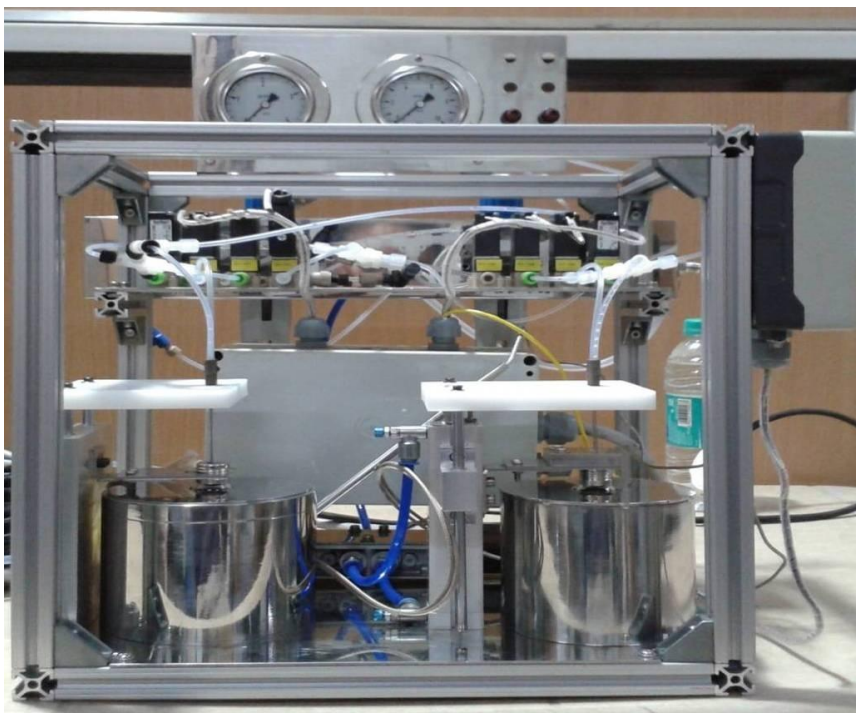


Fig. 4.6 (a) Photograph of internal set up for ^{131}I -Lipiodol processing

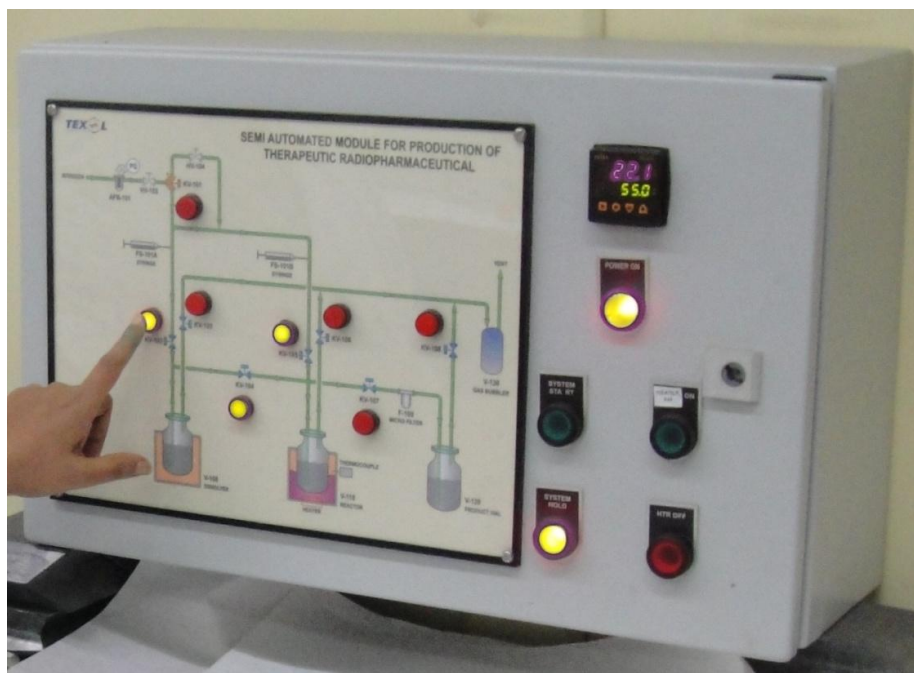


Fig. 4.6 (b) Photograph of control panel for remote operations in ^{131}I -Lipiodol processing

4.5.2 Preparation of ^{131}I -Lipiodol using module

The dose escalation studies were safely carried out inside the plant without measurable radioactive iodine release. The operation protocol allows safe and user friendly remote operation. The cleaning protocols and feasibility of filter sterilization of final product ensures pharmaceutical purity and safety of the product. It was observed that under controlled nitrogen flow, complete drying of aqueous alkaline solution of Na^{131}I in ethanol occurs within 10 minutes of heating at 55 °C. The radiolabeling yields varied between 50 % and 70 % when 2 mL of Lipiodol was used. The yield was found to be consistent when temperature was increased from 80 °C to 100 °C. However, heating for a longer period at 100 °C did not result in substantial increase of radiolabeling yields. Diluting reaction mixture with additional 1 mL Lipiodol resulted in > 80 % recovery of the product from the reaction vessel without compromising quality. The activity distribution determined as in-process quality control (QC) parameter showed low retention (< 3 % to 5 %) of ^{131}I -[NaI] activity in vial, indicating almost complete transfer to the reaction vessel. The activity recovered in ethanol during distillation was ~5 % to 7 %, and the activity trapped in charcoal was ~10 % to 15 %. The sterile syringe filter used for terminal filtration showed < 2 % retention of the product.

4.5.3 Quality control tests of ^{131}I -Lipiodol

4.5.3.1 Test for radionuclide purity

The principal gamma photon energy peaks of 364 and 640 keV (± 5 keV) were observed for all the samples of ^{131}I -Lipiodol in gamma ray spectrum fulfilling the test of radionuclide identification (Fig. 4.7).

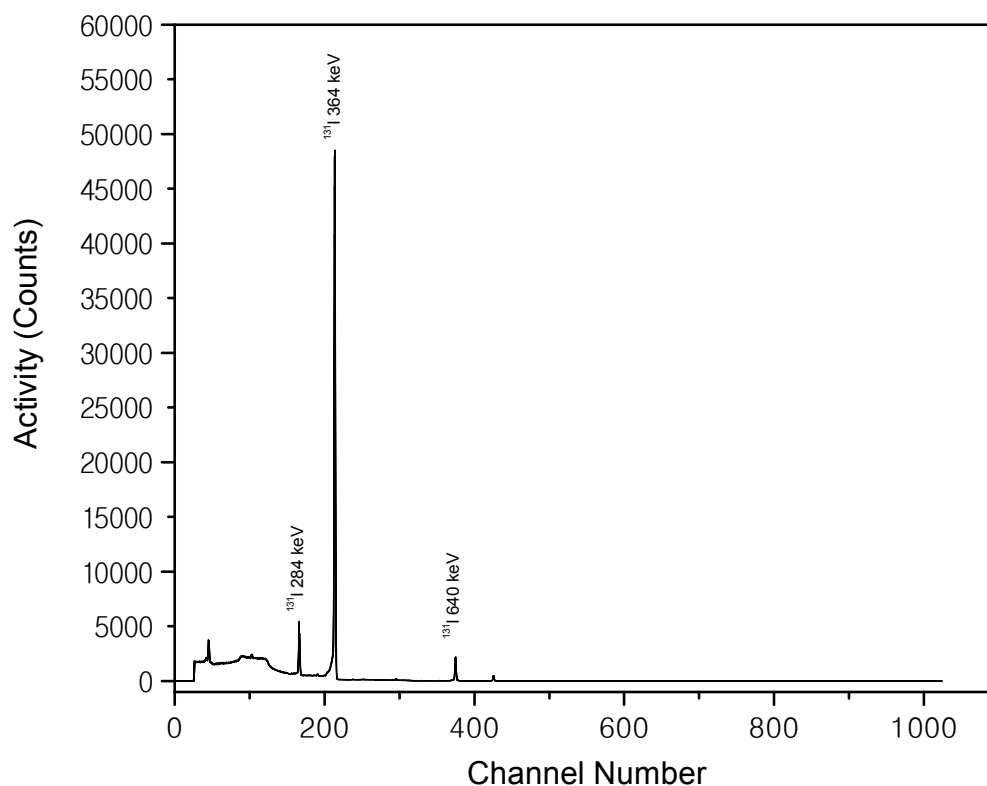


Fig. 4.7: Radionuclidic identification and purity of ^{131}I -Lipiodol

4.5.3.2 Test for radiochemical purity (RCP)

RCP of the product ^{131}I -Lipiodol was > 95 % when estimated by paper chromatography in two different solvent systems. In 85 % methanol as solvent, ^{131}I -Lipiodol shows R_f of 0–0.2, while R_f of free iodide ion is 0.8–0.9 (Fig. 4.8 (a)). Another solvent system, ethyl ether/petroleum ether, wherein ^{131}I -Lipiodol shows R_f of 0.8-0.9 and R_f of free iodide ion as 0–0.1 (Fig. 4.8 (b)), was used for comparison. RCP values of different batches of ^{131}I -Lipiodol estimated on next day and 2 weeks after preparation are tabulated in Table 4.2.

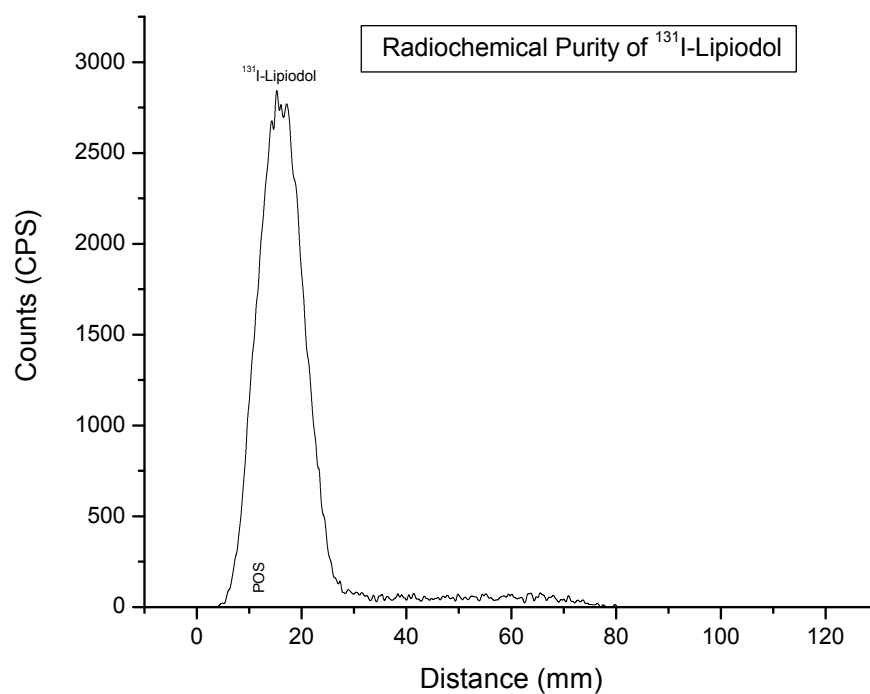


Fig.4.8 (a): Radiochemical purity of ^{131}I -Lipiodol (Methanol Solvent)

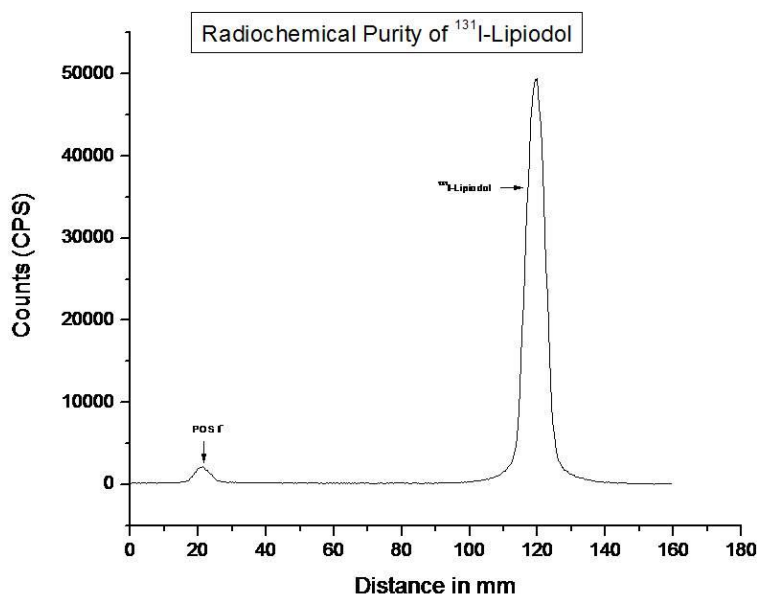


Fig. 4.8 (b): Radiochemical purity of ^{131}I -Lipiodol (ethyl ether/petroleum ether solvent)

Table 4.2: Radiochemical Purity of ^{131}I -Lipiodol

Batch. no.	% RCP ^{131}I -Lipiodol	
	Next day of preparation	After 2 weeks
1	95.1 \pm 1.2	94.6 \pm 1.1
2	97.2 \pm 1.6	96.3 \pm 2.6
3	97.3 \pm 0.9	98.2 \pm 1.7
4	97.1 \pm 1.2	96.6 \pm 2.1
5	97.0 \pm 1.6	97.9 \pm 1.3
6	95.6 \pm 3.8	96.3 \pm 2.9
7	96.2 \pm 2.9	97.7 \pm 1.5
8	95.6 \pm 3.2	96.2 \pm 2.7
RCP: Radiochemical Purity		
*The figures are rounded off to the nearest integers to one decimal point.		

4.5.3.3 Stability

The stability of the product evaluated over a period of 3 weeks after preparation ascertains the logistics of supply to other nuclear medicine centers. The product was stable for two weeks post-preparation when stored in dark at ambient temperature.

4.5.3.4 Sterility and bacterial endotoxin testing (BET)

Product also qualified the tests for sterility and apyrogenicity as per the established methods as prescribed by Pharmacopoeia. Endotoxin levels were found to be below 10 EU/mL,

significantly less than the permitted limits for radiopharmaceuticals (25 EU/mL or 175 EU/V mL).

4.5.3.5 Biological evaluation

There are not many reports on preclinical animal biodistribution studies of ^{131}I -Lipiodol. Hence our pharmacokinetic studies extended till 5 day post-injection gives more insight to the *in-vivo* fate of the product. The results of *in-vivo* distribution studies are given in Table 4.3. At 24 hours post administration, more than 90 % of injected ^{131}I activity was associated with the liver with negligible activity in the non-target tissues and organs (Table 4.3). Good localization and retention of the labeled preparation in the hepatic tissue were observed. At 3 days post-surgery, around 80 % of ^{131}I -Lipiodol was retained in the liver, while after 5 days liver activity was decreased to 70 % compared to > 90 % at 24 hours. Normal liver tissue contains specific macrophages (Kupffer cells), which are known to metabolize Lipiodol and cause its release from the liver over a period of days [101]. It is expected that in HCC tissue, which lacks macrophages, such loss of radiolabeled Lipiodol will not be observed ensuring retention and *in-vivo* stability of the product after locoregional intravascular application. Other organs did not show any appreciable accumulation of the activity, and most of the activity was excreted through urine. It is notable that the thyroid, known to absorb iodine from the bloodstream, did not harbor any mentionable radioactivity from the preparation, indicating that ^{131}I -iodine remains stably associated with Lipiodol. Bio-distribution studies revealed retention of injected product in liver without significant leakage of activity to other organs including thyroid.

Table 4.3: In-vivo distribution data (% ID/Organ) of ^{131}I -Lipiodol in normal Wistar rats

Organ/tissue	Avg \pm SD ($n = 4$)		
	1 Day	3 Days	5 Days
Liver	93.87 \pm 1.66	77.81 \pm 7.61	69.99 \pm 6.56
Intestine	0.62 \pm 0.04	2.81 \pm 1.02	1.31 \pm 0.51
Stomach	0.41 \pm 0.04	1.41 \pm 0.19	1.27 \pm 0.99
Kidney	0.10 \pm 0.02	0.40 \pm 0.22	0.17 \pm 0.19
Heart	0.02 \pm 0.00	0.15 \pm 0.05	0.00 \pm 0.00
Lungs	0.04 \pm 0.02	0.80 \pm 0.49	0.73 \pm 1.01
Spleen	0.03 \pm 0.01	0.06 \pm 0.05	0.17 \pm 0.29
Muscle	1.73 \pm 0.76	1.09 \pm 0.39	1.69 \pm 0.40
Blood	0.35 \pm 0.16	1.15 \pm 0.94	0.22 \pm 0.29
Bone	0.60 \pm 0.13	0.59 \pm 1.03	0.00 \pm 0.00
Thyroid	0.13 \pm 0.01	0.45 \pm 0.04	0.19 \pm 0.05
Urine	2.13 \pm 0.62	13.72 \pm 7.21	28.04 \pm 5.89

4.5.3.6 Radiochemical yield of ^{131}I -Lipiodol and its specification

Table 4.4 depicts RCYs (60 % – 70 %) obtained when production of ^{131}I -Lipiodol was carried out by varying ^{131}I activity from 222 to 5180 MBq. The final specifications and QC acceptance criteria are given in Table 4.5.

**Table 4.4: Scaling-up of radiosynthesis of ^{131}I -Lipiodol under optimized conditions
with semi-automated module**

Batch no.	^{131}I -[NaI] activity before batch preparation (MBq)	^{131}I -Lipiodol produced (MBq)	% RCY (Radiochemical yield)
1	222	141	63.3
2	600	410	68.5
3	1685	1147	68.0
4	2812	1776	63.0
5	3053	2138	70.0
6	3774	2571	68.0
7	4810	3248	67.4
8	5180	3675	71.0

Table 4.5: Specifications/Acceptance criteria of ^{131}I -Lipiodol injection

Product Code	^{131}I -Lipiodol injection
Description	^{131}I -Lipiodol is ready to use sterile, pyrogen free injectable formulation. The formulation contains ^{131}I Iodinated ethyl esters of fatty acids of poppy seed oil (^{131}I -Lipiodol)
Appearance	Clear yellow to light brown liquid
Radionuclide identification	Principal Energy peaks 364 & 640 keV (\pm 5 keV)
Radionuclide Purity	> 99.9 %
Radiochemical purity	> 95 %
Radioactive concentration	740-925 MBq /mL
Sterility test	Complies with IP (no microbial growth till 14 days in FTG and SCD growth mediums)
BET	Complies with IP (< 175 EU per total volume or 25 EU per mL)
Biodistribution/ imaging	> 90 % retention of activity in the liver up to 24 h
Storage	Stored between 10 to 25 °C in dark with adequate shielding
Expiry	Seven days from the date of preparation
BET, bacterial endotoxin testing; FTG, fluid thioglycollate medium; RNP, radionuclide purity; SCD, soybean casein digest medium; IP, Indian Pharmacopoeia	

4.6 Formulation of actual patient dose of ^{131}I -Lipiodol for clinical utilization

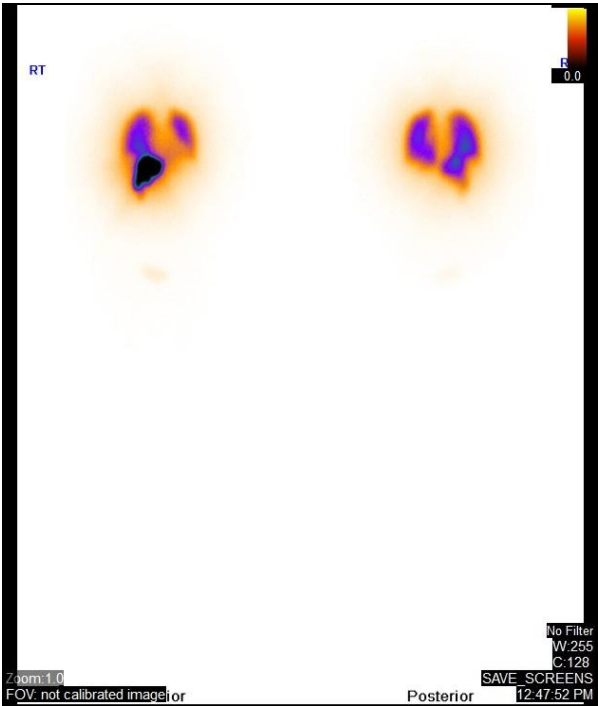
Thirteen patient doses of ^{131}I -Lipiodol were successfully prepared using semi-automated module. In all the thirteen batches the radionuclidic purity was $> 99.9\%$. Radiochemical yield of ^{131}I -Lipiodol was found to be in the range of 48-78 % and radiochemical purity of the product was $97.9 \pm 1.2\%$ (n=13) (Table 4.6). On the day of formulation of ^{131}I -Lipiodol, radioactivity concentration was 550-3080 MBq/mL (15-83 mCi /mL). Endotoxin levels were found to be below 10 EU/mL (BET < 175 EU/V mL), significantly less than the permitted limits for radiopharmaceuticals (25 EU/mL or 175 EU/V mL). Sterility of the product was as per the Indian pharmacopoeia standards. The product ^{131}I -Lipiodol complied all specifications and QC acceptance criteria of ^{131}I -lipiodol injection as mentioned in Table 4.5. Decay corrected quantities of therapeutic doses of ^{131}I -Lipiodol injection were supplied to nuclear medicine centre for clinical studies in liver cancer patients.

Table 4.6: Data of actual patient dose preparation of ^{131}I -Lipiodol

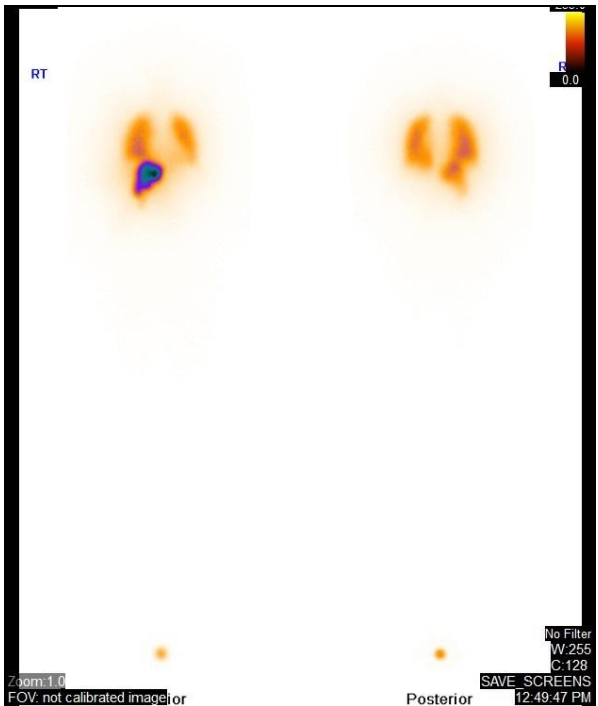
Batch No.	^{131}I -[NaI] initial activity (MBq)	^{131}I -Lipiodol final activity (MBq)	Radiochemical Yield (%)	Radiochemical Purity (%)
1	17333	9250	53.36	99.4
2	15074	7093	47.05	96.0
3	12469	7929	63.59	97.2
4	9384	7289	77.68	96.2
5	11581	8954	78.06	97.3
6	9839	5735	58.28	99.1
7	6590	3552	53.89	98.2
8	4558	2528	55.46	97.8
9	5469	2627	48.06	98.4
10	3409	1647	48.31	98.9
11	17597	8018	45.56	99.3
12	6163	3330	54.03	97.7
13	6882	5365	77.95	96.6

4.7 Clinical evaluation:

Patients suffering from unresectable hepatocellular carcinoma (HCC) were treated with ^{131}I -Lipiodol administered through hepatic artery. SPECT images of the patients at 24 h, 48 h and 72 h post injection revealed desired retention of ^{131}I activity in the liver [Fig. 4.9 (a), 4.9 (b), 4.9 (c)]. It can be seen from the images that there is no accumulation in the thyroid gland which shows that ^{131}I remained bound to Lipiodol even after 72 h of administration (Fig. 4.9).



(a)



(b)



Fig. 4.9: Whole body scan of patient treated with ^{131}I -Lipiodol

(a) 24 h post-administration (anterior and posterior view),

(b) 48 h post-administration (anterior and posterior view),

(c) 72 h post-administration (anterior and posterior view)

4.8 Safety features during formulation of patient dose ^{131}I -Lipiodol

- 100 mm lead shielded containment for semi-automated modular system with additional 30 mm sliding door ensured adequate radiation shielding
- 150 mm lead glass viewing window in it.
- 50 g charcoal filter at the outlet of vent of the system changed after every batch.
- Extra charcoal filter (~ 300 g charcoal) at the outlet of exhaust of the containment which was used in regular production of ^{131}I .

- Continuous air monitor (CAM) at the proximity to the process chamber to monitor air borne ^{131}I activity during processing.

4.9 Discussion

Hepatocellular carcinoma (HCC) is the fifth most common human cancer, with approximately 7,50,000 new cases occurring worldwide each year. Eighty percent of global HCCs occur in developing countries in Asia and Sub-Saharan Africa. HCC ranks third in annual global cancer mortality rates and has the shortest survival time among all cancers in both males and females [90]. Among agents for Trans Arterial Radio Embolization (TARE), ^{131}I -Lipiodol could be prepared in multiple patient doses at relatively low cost compared to other agents. Suitable half-life of ^{131}I allows convenient logistics of production and quality control checks prior to patient administration. The indigenously developed semi-automated module allowed for convenient and operator-safe production of ^{131}I -Lipiodol through exchange labeling. The results of the quality control studies to assess the physico-chemical characteristics of the radiolabeled formulation indicate expected yield and *in-vitro* stability suitable for its clinical application. The studies of sterility and BET estimation indicated a sufficiently aseptic and non-pyrogenic product that can be employed for patient therapy. *In-vivo* studies in established animal model showed adequate localization of the formulation in the liver with minimal escape to non-target organ/tissue and negligible loss of product stability inside the body. Using the above described automated synthesis protocol, ^{131}I -Lipiodol could be made available to the patients in developing countries at low cost for treatment of HCC and PVT. Thirteen batches of ^{131}I -Lipiodol were safely processed and it was utilized successfully for treating thirteen patients with liver cancer.

4.10 Conclusions

The indigenously designed and fabricated module for remote handling of radioactivity is successfully applied for patient dose preparation of ^{131}I -Lipiodol. ^{131}I -Lipiodol can be easily and safely synthesized by installing such modules inside mini hot cells in centralized or hospital radiopharmacy. Preparation of other therapeutic radiopharmaceuticals can also be envisaged using similar modules for radiosynthesis. Initial clinical results are promising with major retention of activity in liver up to 72 h post injection for therapeutic response. ^{131}I -Lipiodol is a very promising therapeutic agent available as a cost effective alternative for treatment of HCC.

==== ===== ===XXXX=====

REFERENCES

- [1]. Pierre Radvanyi, Jacques Villain *C. R. Physique*, **2017**, 18, 544–550
 - [2]. Ramamoorthy N. *IANCAS Bulletin*, **2007**, 5, 59-67.
 - [3]. Richards P, Tucker WD, Srivastava SC. *Int J Appl Radiat Isot*, **1982**, 33, 793-799 .
 - [4]. Silberstein E. B., *Seminars in Nucl Med*, **May 2012**, 42,3,164-170
 - [5]. Fermi E. *Nature*, **1934**,122,201
 - [6]. Livingood J.J, Seaborg G.T., *Phys.* 1938, 53,1015 (article available at, http://prola.aps.org/abstract/PR/v53/i12/p1015_2).
 - [7]. Bauduer F., Tankersley K. B., *Medical Hypotheses*, **Sept. 2018**, 118, 6-8.
 - [8]. Galton V. A., *Molecular and Cellular Endocrinology*, **2017**, 458, 105-111.
 - [9]. *The Journal of Nuclear Medicine* , **May 2015**, Vol. 56, No. 5 (Suppl 2)
 - [10]. https://www.nucleonica.com/Application/ReducedDecaySchemes/I131_TXT.htm seen on 14/11/2019
 - [11]. Friedlander G, Kennedy JW, Macias ES, Miller JM. *Nuclear and Radiochemistry. 3rd edition, John Wiley and Sons, New York; 1981*, p 110-190.
 - [12]. Manual for reactor produced radioisotopes *IAEA TECDOC-1340*
 - [13]. Technical Reports Series No. 128, *Radioisotope Production And Quality Control IAEA*, 1971
 - [14]. *IANCAS Bulletin*, January **2002**, Vol. I, No.1, 20
 - [15]. Sawka AM, Brierley JD, Tsang RW, Thabane L, Rotstein L, Gafni A, Straus S, Goldstein DP *Endocrinol Metab Clin N Am* **2008**, 37,457–480
 - [16]. Middendorp M, Grünwald F *Semin Nucl Med* **2010**, 40,145–152
-

- [17]. Luster M, Clarke SE, Dietlein M, Lassmann M, Lind P, Oyen WJ, Tennvall J, Bombardieri E European association of nuclear medicine (EANM). *Eur J Nucl Med Mol Imaging* **2008**, 35,1941–1959
 - [18]. Lee SL *Curr Opin Endocrinol Diabetes Obes* **2012**, 19,420–428
 - [19]. Reiners C, Hänscheid H, Luster M, Lassmann M, Verburg FA *Nat Rev Endocrinol* 2011, 7,589–595
 - [20]. Haymart MR, Banerjee M, Yang D, Stewart AK, Koenig RJ, Griggs JJ *Cancer* **2013**, 119,259–265
 - [21]. Ronald J, Weigel I, McDougall R *Surg Oncol Clin N Am* **2006**,15,625–638 J Radioanal Nucl Chem
 - [22]. Van Nostrand D, Wartofsky L. *Endocrinol Metab Clin N Am* **2007**,36,807–822
 - [23]. Vöö S, Bucerius J, Mottaghy FM. *Methods* **2011**, 55,238–245
 - [24]. Rufini V, Treglia G, Castaldi P, Perotti G, Giordano A. *Q J Nucl Med Mol Imaging* **2013**, 57,122–133
 - [25]. Rufini V, Treglia G, Perotti G, Giordano A. *Hormones (Athens)* **2013**, 12,58–68
 - [26]. Vallabhajosula S, Nikolopoulou A, *Semin Nucl Med* **2011**, 41,324–333
 - [27]. Grünwald F, Ezziddin S. *Semin Nucl Med* 2010, 40,153–163
 - [28]. Zelenetz AD. *Semin Oncol* **2003**, 30(Suppl4),22–30
 - [29]. Knox SK, Meredith RF, Coleman M, Kaminski MS, Zelenetz AD, Vose JM. *Int J Radiat Oncol Biol Phys* **2004**, 60,S220
 - [30]. Wahl RL. *J Nucl Med* **2005**, 46(Suppl 1),128S–140S
 - [31]. Davies AJ. *Expert Opin Biol Ther* 2005, 5,577–588
 - [32]. William BM, Bierman PJ. *Expert Opin Biol Ther* **2010**,10,1271–1278
-

- [33]. Friedberg JW, Fisher RI. *Expert Rev Anticancer Ther* **2004**, 4,18–26
 - [34]. Douis M, Rosa U. *US Patent* **1963**, 3,114,608. 12
 - [35]. Kabonza K, Hallaba E. *Isotopenpraxis* **1975**, 11,284–287
 - [36]. Sorantin H, Bildstein H. *J Inorg Nucl Chem* **1965**, 27,521–526
 - [37]. El-Absy MA, El-Garhy MA, El-Amir MA, Fasih TW, El-Shahat MF. *Sep Pur Technol* **2010**, 71,1–12
 - [38]. Tòth G, Repas L, Fàbiàn G. *Int J Appl Radiat Isot* **1975**, 26,781–782
 - [39]. Arino H, Gemmill WJS, Kramer HH. *US Patent* **1973**, 3745067
 - [40]. Shikata E. *J Nucl Sci Technol* **1970**, 7,481–483
 - [41]. Abrashkin S, Radicella R. *Int J Appl Radiat Isot* **1964**, 15:695
 - [42]. El-Absy MA, Aly HF, Mousa MA, Mostafa M. *J. Radioanal Nucl Chem* **2004**, 261:163–172
 - [43]. Mondino AV, Kols HJ, Cristini PR, Furnari JC. *J Radioanal Nucl Chem* **1999**, 240:371–374
 - [44]. Wilkinson MV, Mondino AV, Manzini AC. *J Radioanal Nucl Chem* **2003**, 256:413–415
 - [45]. Nazari K, Ghannadi-Maragheh M, Shamsaii M, Khalafi H. *Appl Radiat Isot* **2001**, 55:605–608
 - [46]. Khalafi H, Nazari K, Ghannadi-Maragheh M. *Ann Nucl Energy* **2005**, 32:729–740
 - [47]. Lavi N. *J Radioanal Nucl Chem* **1975**, 20:41–49
 - [48]. Salacz J. *IAEA-TECDOC-515*, **1989**, 149–154
 - [49]. Case FN, Acree EH. *USAEC Report*, **1966**, ORNL-3840
 - [50]. Firestone R. In, Shirley VS (ed) *Table of isotopes*, 8th edn. John Wiley & Sons Inc, New York **1996**.
-

- [51]. Reus U, Westmeier W, Warnecke I. *Gamma-ray catalog*. GSI Report **1979**, 79-2, Darmstadt, Gesellschaft fur Schwerionenforschung
- [52]. Vo Thi Cam Hoa, Duong Van Dong, Nguyen Thi Thu, Chu Van Khoa, Bui Van Cuong, Mai Phuoc Tho, Pham Ngoc Dien and Nguyen Thanh Binh. The Annual Report for 2006, VAEC, 233-238.
- [53]. Oberdorfer F, Helus F, Mayer-Borst W. *J Radioanal Chem* **1981**, 65, 51–56 J Radioanal Nucl Chem
- [54]. I. Saptiama, Y.V. Kaneti, Y. Suzuki, K. Tsuchiya, N. Fukumitsu, T. Sakae, J. Kim, Y.M. Kang, K. Ariga, Y. Yamauchi, *Small* **2018**, 14 , e1800474.
- [55]. R. Chakravarty, A. Dash, *J. Nanosci. Nanotechnol.* **2013**, 13, 2431-2450.
- [56]. A. Amor-Coarasa, M. Schoendorf, M. Meckel, S. Vallabhajosula, J.W. Babich, *J. Nucl. Med.* **2016**, 57, 1402-1405.
- [57]. Z. Wu, D. Zhao, *Chem. Commun.* **2011**, 47, 3332-3338.
- [58]. Y. Ren, Z. Ma, P.G. Bruce, *Chem. Soc. Rev.* **2012**, 41, 4909-4927.
- [59]. R. Chakravarty, S. Chakraborty, R. Shukla, J. Bahadur, R. Ram, S. Mazumder, H. Dev Sarma, A.K. Tyagi, A. Dash, *Dalton Trans.* **2016**, 45, 13361-13372.
- [60]. Y. Ren, Z. Ma, P.G. Bruce, *Chem. Soc. Rev.* **2012**, 41, 4909-4927.
- [61]. D. Gu, F. Schuth, *Chem. Soc. Rev.* **2014**, 43, 313-344.
- [62]. Z. Jin, M. Xiao, Z. Bao, P. Wang, J. Wang, *Angew. Chem. Int. Ed. Engl.* **2012**, 51, 6406-6410.
- [63]. J.L. Do, T. Friscic, *ACS Cent. Sci.* **2017**, 3, 13-19.
- [64]. D. Tan, F. Garcia, *Chem. Soc. Rev.* **2019**, 48, 2274-2292.
- [65]. M. Leonardi, M. Villacampa, J.C. Menendez, *Chem. Sci.* **2018**, 9, 2042-2064.
- [66]. T. Tsuzuki, P.G. McCormick, *J. Mater. Sci.* **2004**, 39, 5143-5146.
- [67]. T. Das, M.R. Pillai, *Nucl. Med. Biol.* **2013**, 40, 23-32.
-

- [68]. K.L. Parthasarathy, E.S. Crawford, *J. Nucl. Med. Technol.* 2002, 30, 165-171.
- [69]. M. Al Aamri, R. Ravichandran, J.P. Binukumar, N. Al Balushi, *Indian J. Nucl. Med.* **2016**, 31, 176-178.
- [70]. A. Freud, N. Hirshfeld, A. Canfi, Y. Malamud, *IAEC- Annual Report*, **1997**, 51-65. Available online at:
https://inis.iaea.org/collection/NCLCollectionStore/_Public/30/023/30023821.pdf?r=30023821&r=30023821.
- [71]. *Draximage product monograph for I-131 therapeutic capsule* seen on 30/10/2019 at <https://www.draximage.com/wp-content/uploads/2016/12/I-131-cap-therapeutic-mono-CA.pdf>
- [72]. J.M. Bright, T.T. Rees, L.E. Baca, R.L. Green, *J. Nucl. Med. Technol.* **2000**, 28, 52-55.
- [73]. N. Fleck, J. Weichert, L. Trembath, *J. Nucl. Med.* **2008**, 49(S1) 414P.
- [74]. L.W. Luckett, R.E. Stotler, *J. Nucl. Med.* 1980, 21, 477-479.
- [75]. S. Mazumder, D. Sen, T. Saravanan, P.R. Vijayaraghavan, *J. Neutron Res.* **2001**, 9, 39-57.
- [76]. R.N. Ambade, S.N. Shinde, M.S.A. Khan, S.P. Lohar, K.V. Vimalnath, P.V. Joshi, S. Chakraborty, M.R.A. Pillai, A. Dash, *J. Radioanal. Nucl. Chem.* **2015**, 303, 451-467.
- [77]. R. Chakravarty, J. Bahadur, S. Lohar, H.D. Sarma, D. Sen, R. Mishra, S. Chakraborty, A. Dash, *Microporous Mesoporous Mater.* 2019, 287, 271-279.
- [78]. S. Mazumder, V.K. Aswal, D. Sen, J. Bahadur, S. Kumar, A. Das, *Neutron News* **2014**, 25 26-30.
- [79]. G.J. Evans, S.M. Mirbod, R.E. Jervis, *Can. J. Chem. Eng.* 1993, 71, 761-765.
- [80]. Poon RT, Fan ST, Tsang, FH, Wong *J. Ann Surg* **2002**, 235, 466-86.
-

- [81]. Greten TF, Manns MP, Korangy F. *J Hepatol* **2006**, 45, 868-78.
 - [82]. Llovet JM, Burroughs A, Bruix J. *Lancet* **2003**, 362, 1907-17.
 - [83]. Blum HE. *World J Gastroentero* **2005**, 11, 7391-7400.
 - [84]. Sundram FX. *Biomed Imaging Interv J* **2006**, 2, 40.
 - [85]. Dimitrios Dimitroulis, Christos Damaskos, Serena Valsami, Spyridon Davakis, Nikolaos Garmpis, Eleftherios Spartalis, Antonios Athanasiou, Demetrios Moris, Stratigoula Sakellariou, Stylianos Kykalos, Gerasimos Tsouroufflis, Anna Garmpi, Ioanna Delladetsima, Konstantinos Kontzoglou, and Gregory Kouraklis. *World J Gastroenterol*. **2017** Aug 7, 23(29), 5282–5294.
 - [86]. Bruix J, Boix L, Sala M, Llovet JM. *Cancer Cell* **2004**, 5, 215-9.
 - [87]. Barbara L, Benzi G, Gaiani S, Fusconi F, Zironi G, Siringo S, et al. *Hepatology* **1992**, 16, 132-7.
 - [88]. Bruix J, Sherman M, Llovet JM, Beaugrand M, Lencioni R, Burroughs AK, et al. *J Hepatol* **2001**, 35, 421-30.
 - [89]. Sherman M, Klein A. *Hepatology* **2004**, 40, 1465-73.
 - [90]. Yuen MF, Poon RT, Lai CL, Fan ST, Lo CM, Wong KW, et al. *Hepatology* **2002**, 36, 687-91.
 - [91]. Chow PK, Tai BC, Tan CK, Machin D, Win KM, Johnson PJ, et al. *Hepatology* **2002**, 36, 1221-6.
 - [92]. Ibrahim SM, Lewandowski RJ, Sato KT, Gates VL, Kulik L, Mulcahy MF, et al. *World J Gastroentero* **2008**, 14, 1664-9.
 - [93]. Llovet JM, Bruix J. *Hepatology* **2003**, 37, 429-42.
 - [94]. Marelli L, Stigliano R, Triantos C, Senzolo M, Cholongitas E, Davies N, et al. *Cardiovasc Inter Rad* **2007**, 30, 6-25.
-

- [95]. Lewandowski RJ, Geschwind JF, Liapi E, Salem R. *Radiology* **2011**, 259, 641-57.
 - [96]. Riaz A, Salem R. *Eur J Nucl Med Mol Imaging* **2010**, 37, 451-2.
 - [97]. Y.-S. LEE, J.M. JEONG, Y.J. KIM, et al. *Nucl Med Comm.* **2002**, 23, 237-242
 - [98]. Ahmadzadehfar H, Sabet A, Biersack HJ, Risse J. *Hepatocellular Carcinoma - Clinical Research.* **2012**, Dr. Joseph W.Y. Lau (Ed.), InTech.
 - [99]. Raoul JL, Boucher E, Rolland Y, Garin E et al. *Nat. Rev. Gastroenterol. Hepatol.* **2010**, 7,41–49
 - [100]. Madhava B. Mallia, Viju Chirayil, Ashutosh Dash. *Appl Radiat Isot* **2018**,137, 147–153
 - [101]. Lambert B, Van de Wiele C. *Eur J Nucl Med Mol Imaging*, **2005**, 32, 980–89.
 - [102]. Raoul JL, Boucher E, Rolland Y, et al. *Q J Nucl Med Mol Imaging* **2005**, 53, 348.
 - [103]. Raoul JL, Bourguet P, Bretagne JF, Duvauferrier R, Coorneart S, Darnault P et al. *Radiology* **1988**, 168, 541-5.,
 - [104]. Nakajo M, Kobayashi H, Shimabukuro K, Shirono K, Sakata H, Taquchi M et al. *J Nucl Med* **1988**, 29,1066-77.,
 - [105]. Madsen MT, Park CH, Thakur ML. *J Nucl Med* **1988**, 29,1038-44.
 - [106]. Raoul JL, Boucher E, Roland V, Garin E. *Q. J Nucl Med Mol Imaging.* **2009** Jun, 53(3), 348-55.
 - [107]. Francesco Giammarile, LisaBodei, Carlo Chiesa, GlennFlux, Flavio Forrer, Francoise Kraeber-Bodere, Boudewijn Brans, Bieke Lambert, Mark Konijnenberg, Francoise Borson-Chazot, Jan Tennvall, Markus Luster. *Eur J Nucl Med Mol Imaging*, **2011**, 38,1393-1406
-

- [108]. Raoul JL, Boucher E, Rolland Y, Garin E et al. *Nat. Rev. Gastroenterol. Hepatol* **2010**, 7, 41–9.
- [109]. Ahmadzadehfar H, Sabet A, Wilhelm K, Biersack HJ, Risse J *Methods* **2011**, 55, 246–252
- [110]. Idée JM, Guiu B *Crit Rev Oncol Hematol* 2013, 88, 530–549
- [111]. Lepareur N, Ardisson V, Noiret N, et al. *Appl Radiat Isot* **2011**, 69, 426.
- [112]. De Decker M, Turner JH. *Cancer Biother Radiopharm* **2012**, 27, 72.
- [113]. Madhava B. Mallia, Anupam Mathur, Suresh Subramanian, Sharmila Banerjee, H. D. Sarma, Meera Venkatesh. *Bioorganic & Medicinal Chemistry Letters* **2005**, 15, 3398–3401.
-